ISTANBUL TECHNICAL UNIVERSITY ★ GRADUATE SCHOOL

ACCURACY OF SIMULATED HYSTERESIS ENERGY DISSIPATION BEHAVIOR OF DUCTILE RC COMPONENTS

M.Sc. THESIS

Ahmed ABUAISHEH

Disaster Management Institute

Earthquake Engineering Program

February 2021

ISTANBUL TECHNICAL UNIVERSITY ★ GRADUATE SCHOOL

ACCURACY OF SIMULATED HYSTERESIS ENERGY DISSIPATION BEHAVIOR OF DUCTILE RC COMPONENTS

M.Sc. THESIS

Ahmed ABUAISHEH
(802181201)

Disaster Management Institute

Earthquake Engineering Program

Thesis Advisor: Assoc. Prof. Dr. Ufuk YAZGAN

February 2021

İSTANBUL TEKNİK ÜNİVERSİTESİ ★ LİSANSÜSTÜ EĞİTİM ENSTİTÜSÜ

SÜNEK BETONARME ELEMANLARI İÇİN HESAPLANAN ENERJİ SÖNÜMLEME DAVRANIŞININ DOĞRULUĞU

YÜKSEK LİSANS TEZİ

Ahmed ABUAISHEH
(802181201)

Afet Yönetimi Enstitüsü

Deprem Mühendisliği Programı

Tez Danışmanı: Doç. Dr. Ufuk YAZGAN

Şubat 2021

Ahmed ABUAISHEH, a M.Sc. student of ITU GRADUATE SCHOOL student ID 802181201, successfully defended the thesis entitled "ACCURACY OF SIMULATED HYSTERESIS ENERGY DISSIPATION BEHAVIOR OF DUCTILE RC COMPONENTS", which he prepared after fulfilling the requirements specified in the associated legislations, before the jury whose signatures are below.

Thesis Advisor :	**Assoc. Prof. Dr. Ufuk YAZGAN** Istanbul Technical University	.....
Jury Members :	**Prof. Dr. Ercan YÜKSEL** Istanbul Technical University	.....
	Prof. Dr. Kutay ORAKÇAL Boğaziçi University	.....

Date of Submission : 27 January 2021
Date of Defense : 25 February 2021

To my family,

FOREWORD

Foremost, I would like to express my gratitude to my supervisor, Assoc. Prof. Dr. Ufuk Yazgan, For his continuous support and trusts throughout my studies. His passion and continuous push for excellence has helped me grow in all different aspects of my life, shaping me into who I am today.

My sincere thanks also go to Dr. Ziya Muderrisoglu for his encouragement throughout this project. His door was open to me whenever I ran into a trouble spot or had a question about my research.

I am also grateful to Mr. Saeed Ghaemian, for his endless support and insightful guidance. He boosted my motivation and supported me in the challenging stages of this thesis.

It is an honor for me to have had the opportunity to study at Department of Earthquake Engineering and Disaster Management of Istanbul Technical University and learn from such amazing faculty.

Finally, I must express my very profound gratitude to my family for providing me with unfailing support and continuous encouragement throughout my years of study. My parents, my brothers Majd and Haytham, my beloved sisters Tasneem, Haneen and Sireen you are everything to me, without you I would not be where I am today. I love you all.

Feb 2021 Ahmed ABUAISHEH

TABLE OF CONTENTS

Page

ABBREVIATIONS

BH : Beam with hinges
DB : Displacement-based element model with Bilinear hysteresis
DBE : Displacement based element
DF : Displacement-based element model with Fiber-section
DT : Displacement-based element model with modified Takeda hysteresis
FB : Force-based element model with Bilinear hysteresis
FBE : Forced based element
FE : Finite Element
FF : Force-based element model with Fiber-section
FT : Force-based element model with modified Takeda hysteresis
HB : Double hinges element model with Bilinear hysteresis
HF : Double hinges element model with Fiber-section
HT : Double hinges element model with modified Takeda hysteresis
MLM : Maximum likelihood method
MOM : Method of moment
PGA : Peak Ground Acceleration
PO : Pushover

SYMBOLS

b_{sec} : Section strain hardening ratio
b_{steel} : Steel strain hardening ratio
c : Damping coefficient
C_E : Error correction factor
E_a : Absorbed energy
E_c : Concrete's modulus of elasticity
E_{exp} : Hysteretic energy dissipated by shaking table test
E_H : Hysteretic dissipated energy
E_I : Input energy
$EI_{cracked}$: Cracked stiffness
EI_{eff} : Effective stiffness
E_k : Kinetic energy
E_{mod} : Hysteretic energy dissipated by model
$Error$: Cumulative error
E_s : Elastic strain energy
E_{steel} : Steel's initial modulus of elasticity
E_ζ : Damping energy
f_s : Equivalent static force
f_y : Steel yielding strength
k : Stiffness
L_1 : Length of the hinge
m : Mass
M_u : Fracture moment
M_w : Earthquake magnitude
M_y : Yielding moment
R : Design reduction factor
t : total number of time steps
U : Relative displacement
U_g : Ground displacement
β : unloading stiffness related parameter
ε_{cc} : Confined concrete yielding strain
ε_{cu} : Confined concrete ultimate strain
ε_{ys} : Steel yielding strain
ε_{fs} : Steel fracture strain
σ_{uc} : Unconfined concrete yielding strength
σ_{cc} : Confined concrete yielding strength
θ_y : Yielding rotation
θ_u : Fracture rotation
$\varnothing$: Diameter

LIST OF TABLES

Page

LIST OF FIGURES

Page

ACCURACY OF SIMULATED HYSTERESIS ENERGY DISSIPATION BEHAVIOR OF DUCTILE RC COMPONENTS

SUMMARY

Accurate simulation of seismic response is critical in reliable assessment of the capacity of a structure to resist the expected seismic action. Numerical modeling approaches proposed for seismic response prediction have advanced considerably in the last decades. The accuracy of the responses obtained using the available methods is a critical open issue that is yet to be identified. Earlier investigations on the accuracy of simulated seismic response were mainly focused on the prediction of the force and displacement demands, since these response quantities play a critical role in today's seismic design practice. On the other hand, there has been an ever growing interest in energy-based seismic design approaches where the energy dissipation under seismic action is the decisive design parameter. However, the accuracy of available modeling approaches in simulating the energy dissipation has not been sufficiently investigated. In this study, the accuracies of hysteresis energy dissipation methods are investigated, by means of numerically reproducing shaking table tests of a set of RC components and comparing the results with the actual observed behavior.

A large set of assumptions is introduced while establishing a numerical model for predicting the seismic response. Among these, two assumptions have a strong impact on the simulated energy dissipation response: (1) assumed hysteresis behavior and (2) utilized finite element formulation. The objective of this study is to assess the accuracy of the simulated hysteretic energy dissipation for a given RC component subjected to a specific excitation. For this purpose, shaking table tests of a set of 9 RC components were numerically recreated. The simulated responses were compared against the actual observed behavior.

It was seen that the simulated dissipated energies were on the average underestimating the actual value by approximately 10.5 percent for the Force-based element model with Bilinear hysteresis model, with a dispersion of 14 percent, The errors associated with the results from alternative models were correlated with each other.

Sensitivity analyses were also implemented in this investigation. Particularly, the damping ratio was found to have a significant impact on the predicted hysteretic energy dissipation.

In the end, the investigation revealed a preliminary assessment of the accuracy of available modeling approaches in terms of simulating the energy dissipation behavior of ductile RC components. Results can be considered as an indicative evidence for choosing suitable finite element modeling approaches can predict the energy dissipation with higher accuracy.

SÜNEK BETONARME ELEMANLARI İÇİN HESAPLANAN ENERJİ SÖNÜMLEME DAVRANIŞININ DOĞRULUĞU

ÖZET

Bir yapının beklenen deprem etkisine direnme kapasitesinin doğru şekilde değerlendirilmesinde dinamik davranışın doğru hesaplanmansı çok önemlidir. Dinamik davranışın hesabı için önerilen sayısal modelleme yaklaşımları, son birkaç on yılda önemli ölçüde ilerlemiştir. Ancak mevcut modelleme yöntemleri kullanılarak hesaplanan davranışın gerçek davranışı hangi seviyede başarıyla temsil edebildiği henüz tüm boyutlarıyla belirlenmemiş kritik bir konudur. Zaman tanım alanında hesap yöntemleriyle elde edilen dinamik davranışın doğruluğu ile ilgili daha önceki araştırmalar, esas olarak kuvvet ve yer değiştirme taleplerinin tahminindeki doğruluk düzeyinin belirlenmesine odaklanmış bulunmaktadır. Bunun önemli bir nedeni bu talep parametrelerinin günümüzün sismik tasarım uygulamasında kritik bir rol oynamasıdır. Öte yandan, günümüzde deprem etkisi altındaki enerji sönümleme davranışının esas tasarım parametresi olarak göz önüne alındığı enerji bazlı sismik tasarım yaklaşımlarına olan ilgi giderek artmaktadır. Buna karşılık, enerji sönümleme davranışının mevcut modelleme yöntemleriyle ne derece doğru hesaplanabildiği yeterli seviyede araştırılmamış bir konudur.

Bu çalışmada, mevcut sonlu eleman modelleme yaklaşımıyla elde edilen çevrimsel enerji sönümleme davranışının gerçek davranışı yakalama başarı düzeyleri incelenmiştir. Bu kapsamda, sarsma tablası üzerinde test edilmiş bir dizi betonarme (BA) kolon ve perdenin dinamik testleri sayısal olarak yeniden gerçekleştirilmiştir. Farklı modelleme yöntemleriyle elde edilen enerji sönümleme miktarları, dinamik deneyler sırasında gözlemlenen "gerçek" enerji sönümleme davranışlarıyla karşılaştırılmıştır.

Deprem etkisi altındaki dinamik davranışın doğru tahmini, yapıya etkimesi muhtemel deprem talebinin doğru şekilde değerlendirilebilmesi açısından kritik önem taşımaktadır. Bununla birlikte, yapının elastik ötesi çevrimsel davranışının ve ilgili enerji sönümleme özelliklerinin doğru şekilde modellemek, basit bir görev değildir. Dinamik deprem davranışının simüle edilmesi kapsamında çok sayıda basitleştirme ve varsayımın yapılmasına ihtiyaç duyulur. Sünek BA elemanlar için en kritik varsayımlar histeretik davranış, malzeme gerilme-şekil değiştirme ilişkisi ve sonlu eleman formülasyonu ile ilgili yapılan idealizasyonlardır. Bu ana faktörlere ek olarak, hesaplanan dinamik davranışı etkileyen diğer başka varsayımlar (ör. sınır koşulları, sönümleme modellemesi) da mevcuttur. Simülasyon sonucu elde edilen dinamik davranışı etkileyen bütün bu varsayımlar ve idealleştirmelerin tümü, sonuçların doğruluğu üzerinde önemli seviyede etkiye sahiptir. Bununla birlikte kaçınılmaz olarak, hesaplanan davranışındoğruluğu, büyük ölçüde göz önüne alnan yapının/elemanın özelliklerine ve etkiyen dinamik kuvvetin karakteristiğine bağlıdır. Aynı kuvvetli yer hareketi ivmesi etkisine tabi tutulan iki farklı sünek bileşen için,

aynı modelleme yaklaşım kullanılarak simüle edilen davranış çok farklı seviyelerde hataya sahip olabilir. Benzer şekilde, iki özdeş bileşen, bu sefer farklı frekans, faz ve süre özelliklerine sahip yer ivmelerine tabi tutulduğunda, dinamik hesap sonucu elde edilen yanıt çok farklı düzeylerde hata sergileyebilir. Kısaca, dinamik analiz sonucu elde edilen elastik ötesi davranşın doğruluğu duruma özel bir parametredir. Yine de, yeterince büyük bir dinamik olarak test edimiş deney üntiesi grubu, belirli bir modelleme yaklaşımı kullanılarak modellendiğinde, elde edilen hataların istatistiksel dağılım özellikleri, bu modelleme yaklaşımının beklenen doğruluğunun bir göstergesi olarak düşünülebilir. Böyle bir stratejiyle elde edilen sonuçlar esas alınarak, belirli bir modelleme yaklaşımın sismik davranışı tahmin etme açısından diğerlerine göre "ortalamada" daha doğru olduğu şekilde bir çıkarım yapmak mümkün olabilir. Mevcut tez çalışması, bu temel stratejiye dayanan bir ön inceleme niteliğindedir.

Bu tez çalışmasında, 9 BA elemanın sarsma tablası deneyleri sayısal olarak modellenmiş ve hesaplanan çevrimsel enerji sönümleme davranışının doğruluğu ilgili deneyler sırasında gözlenen gerçek davranış göz önüne alınarak değerlendirilmiştir. Elde edilen sonuçlar, sayısal modellerle hesaplanan enerji sönümleme miktarının, sarsma masası testleri sırasında sönümlenen gerçek histeretik enerjiye kıyasla ortalamada daha az olduğu görüldü. Test edilen 9 sonlu eleman modelleme yaklaşımından hiçbiri ortalamada gerçeğe göre daha fazla sönümleme davranışı göstermedi. Çevrimsel enerji sönümleme davranışlarının doğruluk seviyeleri bütün modeller için yaklaşık aynıydı. Bununla birlikte, az bir far da olsa, çevrimsel enerji sönümleme davranışını en yüksek başarıyla tahmin edebilen model, ortalamada % 10.5'lik hata oranı ile çift doğrusal histeresis modeline sahip kuvvet-esaslı sonlu eleman modeliydi. Buna karşılık, çevrimsel enerji yutma davranışını en düşük başarıyla tahmin edebilen model, %17.0'lik ortalama hata oranıyla Takeda histerezis modeline sahip kuvvet-esaslı sonlu eleman modeliydi.

Bu tez çalışması kapsamında, enerji sönümleme hesaplarıyla ilgili duyarlılık analizleri de yapılmış bulunmaktadır. Bu kapsamda, kritik viskoz sönüm oranının ve eşdeğer plastik mafsal uzunluğunun sayısal modelden elde edilen sonuçlar üzerindeki etkisi göz önüne alınmıştır. Hasasiyet analizi sonucunda, eşdeğer plastik mafsal uzunluğunun simülasyon sonucu elde edilen enerji sönümleme seviyesi üzerinde önemli bir estkiye sahip olmadığı gözlenmiştir. Buna karşılık, modelde göz önüne alınan kritik viskoz sönümleme katsayısının elde edilen elastik ötesi çevrimsel enerji sönümleme davranışı üzerinde büyük bir etkiye sahip olduğu gözlendi.

Çalışma kapsamında, bir de sayısal modellerden elde edilen maksimum yer değiştirme seviyesinin doğruluğu ile çevrimsel davranışla sönümlenen toplam enerji seviyesinin doğruluğu arasındaki ilişki incelendi. Sonuç olarak, bu iki parametrenin doğruluk düzeyleri arasında herhangi bir güçlü ilişki gözlenmedi.

Sonuç olarak, sayısal modellerle elde edilen çevrimsel enerji sönümleme davranışının doğruluk düzeyinin değerlendirildiği bir çalışma ortaya konulmuş bulunmaktadır. Elde edilen sonuçlar, çevrimsel enerji sönümleme davranışı açısından başarılı sonuç veren modelleme yaklaşımlarının belirlenmesi konusunda yol gösterici nikteliktedir.

1. INTRODUCTION

1.1 Problem Statement

Earthquake hazard is known to pose significant risks to civil engineering structures in the seismically active regions of the world. At present, accurate assessment of seismic risk to structures is a field that is subject to significant uncertainty.

Existing seismic design practice is based on making sure that the structure has sufficient strength, displacement capacity and stiffness to fulfill the desired performance objectives. In this context, the demand and capacity are defined in terms of forces (stresses), and displacements (strains). This approach fails to explicitly take into account two important aspects of demand and capacity: 1-duration of the strong ground motion and 2-specific cyclic energy dissipation (hysteretic) characteristics of the structure.

Within the last few decades, a series of innovative approaches were proposed to address these issues in the seismic design of structures that put a special emphasis on considering energy dissipation explicitly in the assessment. These approaches are known as *energy-based approaches*. Compared to the strength and displacement-based approaches, energy-based approaches are still new and further research is needed before they can be implemented into seismic design practice. In 1992, Bertero [2] remarked that further research was needed in three essential topics: 1-definition of input energy, 2-estimation of demand to the structure and 3-assessment of the energy dissipation capacity of the structure. Since then these issues have attracted significant research effort. This study aims at contributing to this efforts by providing a discussion of the important issues related to numerical simulation of hysteresis energy dissipation behavior of RC systems.

In the conventional seismic design practice, finite-element models are utilized for assessing the peak forces and displacements a structure will be subjected to during its service life. For this purpose, most of the existing models have been validated

to predict these response quantities with reasonable accuracy. On the other hand, accurate simulation of energy dissipation behavior is key in designing new structures or assessing existing ones, using energy-based approaches.

It is known that hysteresis energy dissipation behavior of a structure is a highly case dependent phenomenon. Various properties of the structural system (e.g. framing layout, material characteristics, section detailing) influence the energy dissipation behavior. Furthermore, the specific characteristics of the strong ground motion (e.g. phasing of different frequencies, duration, polarization) that excites the structure also have a strong influence on the resulting energy dissipation behavior. Accordingly, the error associated with the simulated energy behavior is expected to be a highly case sensitive parameter that depends on the specific structural system and ground motion combination that is being considered in the analysis. Even if the actual error is highly uncertain, the probability distribution characteristics (i.e. expected value and dispersion) of this error can still be assessed given that its value is "observed" for a sufficiently wide range of alternative cases.

One option for identifying the error associated with the simulated hysteresis energy dissipation is to compare the simulations against the actual responses for the systems that are tested dynamically. In order to identify the specific factors that have a critical influence on the energy dissipation error, the best strategy is to consider simple components (e.g. individual columns, beams, walls) in which the energy is dissipated only in a few locations (i.e. flexural plastic hinges) and in a controlled way (i.e. preventing other failures like shear, axial etc. failure) . After the issues related to simulation of energy dissipation behavior are well understood component-level, the related issues can be further investigated at the structural system level.

1.2 Objective and Scope

The objective of this thesis is to investigate the accuracy of hysteretic energy dissipation behavior simulated for slender RC components subjected to strong ground motions. Both the probability distribution characteristics of the expected error associated with the simulated energy demand as well as its sensitivity to the major modeling assumptions are assessed in this study.

The scope of this investigation is limited to a set of 9 slender ductile RC components and the conventional beam-column finite-element modeling approaches. The errors associated with the hysteresis energy dissipation estimates are identified by comparing the simulations against the actual behaviors of these components "observed" during their dynamic testing. In the dynamic tests considered here, all test units were subjected to shaking table excitations that were comparable to their design level motions.

In terms of numerical modeling, a wide range of component level modeling approaches are considered in this study. Three different beam-column element formulations and three different section behavior models (e.g. fiber section, rule-based hysteresis) are considered in the analyzes. The objective in covering such a wide range of modeling approaches was to identify the relative influences of a range of idealizations/simplifications that have major impact on the simulated energy dissipation behavior.

Additionally, the sensitivity of results to the values assumed for some of the modeling parameters (e.g. plastic hinge length and critical viscous damping ratio) was investigated as well. The purpose of this investigation was to identify the sensitivity of the expected error to the specific values assumed in the modeling.

Moreover, a series of conventional response measures (e.g. backbone top displacement-base shear curves and maximum displacements) simulated using alternative modeling approaches were also compared as well. The objective in this comparison was to assess the relationship between the deviation of the dissipated energy from the actual value as compared to deviations exhibited in more conventional response measures (e.g. strength, maximum displacement).

1.3 Limitations

- The set of 9 shaking table test units considered in this study falls short in terms of covering the infinite range of possible combinations of structural component and strong ground motion properties. Utilization of such a limited sample set inevitably introduces some statistical sampling uncertainty (and maybe bias) that should be

kept in mind. The results reported here should be considered as preliminary findings.

- The amount energy dissipated by means of hysteretic behavior can be computed at various levels of detail. Evidently, different results can be obtained by using different approaches. One possible approach is to integrate the area below cyclic top displacement versus total base shear hysteresis response plot. This integral provides a global measure of energy dissipation. On the other hand, energy dissipated by individual material particles may be evaluated by integrating the area below their cyclic stress-strain response plots. In this study, the global system level energy dissipation behavior was considered.

- In dynamic testing, the malfunctioning of the sensors sometimes results in some part of the data becoming useless. Such an issue was exhibited for one of the units (i.e. CAMUS3 wall) considered in this thesis. The displacement sensor attached to the top (i.e. 5th) story was not functioning well during the test. As a result, the displacement data for the 4th story was considered in the analysis. However, it is expected that this has a small effect on the accuracy of the results associated with the specific unit.

- The amount of dissipated hysteresis energy is directly related to the total number and the sizes of inelastic displacement cycles of the system. The results reported here are related to components that are subjected to design level shaking intensities which deform the components to displacement ductility levels ranging from 2 to 5. Direct adoption of the reported results to other shaking levels may not be appropriate. Particularly, in the case of low shaking amplitudes that results in very limited yielding, relative accuracy of the simulated energy dissipation may be considerably lower. This is due to sharp nonlinear increase in the energy dissipated at around the yield displacement.

1.4 Overview

This thesis is organized as follows:

In the next chapter, the state of the art presents two subjects 1- Energy-based approaches 2- Investigation of the performance of analytical models in terms of

predicting the dynamic response. First, it starts with the energy equation for a singe-degree-of-freedom (SDOF) system. The types of energies are defined for the systems subjected to dynamic actions. Subsequently the definition of hysteretic energy is introduced. After that, the state-of-the-art in assessment of analytical modeling approaches in terms of predicting the inelastic dynamic response of structures are reviewed.

In the third chapter, the considered test units are presented and the utilized finite-element modeling approaches are explained. The procedures followed while modeling the test units are presented.

In the fourth chapter the analysis, modeling process of the test units and the statistical analyzers made for finding accuracy are presented.

In the fifth chapter, the dissipated energies identified from the simulation results are compared with the actual values observed during the shaking table tests. The correlation of the simulation results with the actual values are evaluated. The imperfections of each numerical model are pointed out. Additionally, the sensitivity of the results to major modeling parameters (e.g. plastic hinge length and viscous damping ratio) are investigated. Lastly, the top displacement versus base shear plots (i.e. pushover curves) obtained using quasi-static analyzes are compared against the backbone curves of force-displacement responses of the tests units during the dynamic tests.

In the last chapter, the summary and conclusion of the study are provided.

2. STATE OF THE ART

Capabilities and limitations of the existing dynamic response simulation methods and tools in terms of predicting hysteretic energy dissipation behavior is an important topic that has not been investigated sufficiently.

In this chapter, the key topics and important milestones in energy-based seismic performance assessment approaches are presented alongside an investigation of the analytical models and their validity in predicting the dynamic response.

First, the fundamental concepts in energy-based seismic assessment and design are discussed. Second, a series of fundamental questions are addressed: what is the difference between the dissipated energy and recoverable energy?, what is hysteretic energy? and why it is important?

At the end, some of the earlier publications that discuss the capabilities and limitations of analytical models in predicting the nonlinear dynamic response of RC structures and components, are reviewed.

2.1 Energy Based Approach

The main premise in energy-based approach is that the level of damage to a structure that had been exposed to seismic loading is not only determined by the maximum deformation, but it is related to the cumulative dissipated energy, as well Park and *et. al*. [3]. Accordingly, it is suggested that the energy-based assessment would be advantageous over a strength-based one since it is based on a more reliable measure of damage and seismic performance.

Equation of motion: for a linear elastic single degree of freedom (SDOF) system the equation of motion is defined as in Equation 2.1 below:

$$m\ddot{U}(t) + c\dot{U}(t) + kU(t) = m\ddot{U}_g(t) \tag{2.1}$$

Where m refers to mass, c refers to damping coefficient, k refers to stiffness, U refers to relative displacement and U_g refers to ground displacement.

Energy concept: Energy is equal to force multiplied by displacement and to move from the equation of motion to the energy concept, Equation (2.2) above is integrated with respect to displacement, which leads to the following (Equation 2.2).

$$\int m\ddot{U}\,\delta U + \int c\dot{U}\,\delta U + \int kU\,\delta U = \int m\ddot{U}_g\delta U \tag{2.2}$$

In a more general way, total energy can also be expressed as a sum of various types of energy components as given below in Equation (2.3):

$$E_k + E_\zeta + E_a = E_I \tag{2.3}$$

.

where E_k is kinetic energy, E_ζ is damping energy, E_a is absorbed energy and E_I is input energy. Specific energy components present in the expression above, are equal to the following integral expressions defined below:

$$E_k = \int m\ddot{U}\,\delta U \tag{2.4a}$$

$$E_\zeta = \int c\dot{U}\,\delta U \tag{2.4b}$$

$$E_a = \int kU\,\delta U \tag{2.4c}$$

$$E_a = E_s + E_H \tag{2.4d}$$

$$E_I = \int m\ddot{U}_g\delta U \tag{2.4e}$$

For an inelastic structure, absorbed energy E_a consists of elastic strain energy E_s and the hysteretic dissipated energy E_H. As a result, the most generic form of energy balance equation that is applicable for elastic and inelastic systems is obtained as in Equation (2.5) below:

$$E_k + E_\zeta + E_s + E_H = E_I \tag{2.5}$$

.

As shown in Figure 2.1, the total energy input to a structure subjected to dynamic loading can be categorized into two main types: 1) *Recoverable energy* and 2) *Dissipated energy*.

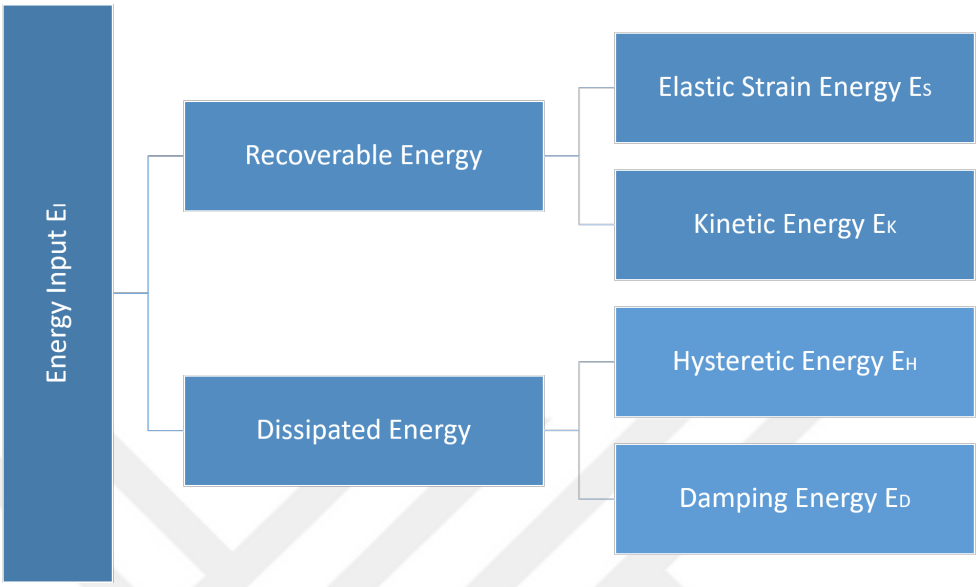

Figure 2.1 : Recoverable and Dissipated energy types.

For a structure subjected to seismic action, the *dissipated energy* is equal to the total input energy that enters the structure during the entire duration of shaking. When designing a structure, it is important to estimate the total energy that will be dissipated by the system in order to assess if it has sufficient energy dissipation capacity to survive the event without collapsing.

The *recoverable energy* on the other hand, is the one that is stored temporarily in the structure during the seismic action, and it consists of kinetic energy E_k (i.e. related to the moment of inertia) that is generated due to the movement of the masses, and the strain energy E_s, which is the energy stored in the structure element throughout the elastic deformation.

Based on the premise of energy-based seismic design, Bertero et al. [2] identified the following topics to be the critical ones that should be addressed: 1-Earthquake input, 2-Demands on the structure, and 3-Supplied capacities of the structure.

In this study, the accuracy of a set of models, in terms of simulating the "energy demand" or in another words, the hysteretic energy dissipation behavior during seismic action, is investigated and clarified.

2.2 Hysteretic Energy Demand

During the design seismic action, structures are expected to undergo inleastic response. Where after the strain energy stored in the structure exceeds its elastic strain energy storage capacity, the system starts to dissipate the excess energy through inelastic deformation or the hysteretic energy dissipation, in another words. Therefore, the structure should be able to provide enough ductility or hysteretic energy capacity to limit the damage and to avoid any failure.

In the energy-based seismic design and assessment, determining the hysteretic energy dissipation during the seismic activity is a critical issue. Many studies have been done on that subject, and the hysteretic to input energy ratio E_H/E_I is identified to be a convenient parameter for determining the dissipated energy, and here are some of these major studies that discussed the E_H/E_I parameter.

Zahrah and Hall [4] investigated the damage potential of seismic action on a structure. They found that the amount of input energy, hysteretic energy and damping energy are the most critical factors that affect the amount of damage. Zahrah and Hall found that as the damping ratio increases the amount of damped energy increases, which leads to a decrease of the E_H/E_I ratio.

Fajfar *et al.* [5] investigated the demand energy and the hysteretic energy to input energy ratio for a set of inelastic single-degree-of-freedom systems subjected to strong ground motion. It was found that E_H/E_I is the most stable parameter in terms of representing the energy demand. This ratio was found to be insensitive to the structural and ground motion parameters, except for the damping ratio.

Akiyama [6] performed an investigation based on the approach by Zahrah and Hall [4]. Akiyama proposed an expression to evaluate E_H/E_I based on the viscous damping ratio and the strength of a system. Subsequently, he made a series of approximations and developed an expression for estimating E_H/E_I as a function of damping only.

2.3 Analytical Prediction of Experimental Response

Accuracy of analytical predictions of seismic response has been an active research topic since the earliest attempts for analyzing response of structures subjected to

earthquakes. In the following, some of the key contributions that investigate validity of numerically simulated seismic response of RC structures and components are reviewed.

Negro and Colombo [7] considered a full scale RC frame building subjected to pseudo-dynamic testing, to investigate the accuracy of seismic response simulated by means of conventional modeling strategies. In their investigation, a four-story RC building had been constructed as a full scale test structure. The building was designed considering a design seismic action that is equivalent to a peak ground acceleration of 0.3g according to Eurocode 8 [8]. During the test, the building had been subjected to a motion that is 1.5 times stronger earthquake shaking than what it had been designed for during the test. The reason for this test was to check the validity of the commonly utilized nonlinear analytical models and to investigate their accuracy in predicting the actual results.

Negro and Colombo observed that predicting dynamic response using the Takeda hysteresis model is the best modeling choice due to the fact that it does not require a large computational effort but still provides an acceptable representation of stiffness degradation behavior. Accordingly, they utilized the modified Takeda model by Kunnath [9] in their simulations. In their finite-element, Negro and Colombo discretized each column into three finite-elements, one at the base, one at the middle section and one at the top section. They used the cracked stiffness instead of the uncracked stiffness for the base segment.

The results that Negro and Colombo found in their investigation can be summarized as follows:

- The initial stiffness choice was found to have a significant effect on the simulated behavior.
- Considering the cracked section stiffness was found to be more suitable than uncracked stiffness
- The reason for choosing the cracked stiffness as initial stiffness even though it did not face any seismic activity, is due to the axial load and other static loads.

- Slippage of reinforcement was observed to an important factor related to shape of hysteretic loops.
- It was observed that the first cycles of the response could be matched rather easily by the numerical model when the strength is properly respresented.
- Results indicated that post-yield strengths assumed for the members did not a significant impact on the overall results.

Lee and Kang investigated the correlation between the analytical and experimental responses of a 10 story building. The building model was constructed at a scale of 1:12 and it was designed non-seismically according to 1998 version of the Korean design code. The building was tested under a simulated earthquake. The analytically simulated responses where compared with the experimental ones. The numerical modeling approach used by Lee and Kang [10] was the one that was initially proposed by Prakash [11]. This model consists of a rigid zone at the end of the side, a plastic hinge, and an elastic section at the middle.

Lee and Kang drew the following conclusions:

- The beam with hinges model, proposed by Prakash [11] was simple and it was easy to apply.
- Analytically predicted ultimate strength and the vertical drift profile along the structure were reliable even though it may had some errors in inputs.
- As for the plastic deformation distribution, the models' distribution were found to be very much the same as the experiment
- The analytical results were found to be inaccurate in terms of predicting the actual shape of hysteresis response: it was smooth in the experimental results while it behaved bilinearly in the numerical results.
- The model was representing the flexural behavior only, that is why the shear failures at the joints were not considered.

Accuracies of the responses obtained using two alternative analytical modeling approaches for RC structures were investigated by Mazars et al. [12]. In their investigation, they considered the five-story test structure known as *CAMUS 2000* which was constructed on a scale of 1:3 [13].

The *CAMUS 2000* test unit consisted of 2 parallel walls connected with six rigid masses. The unit was tasted on a shaking table, with a multiple types of excitation being applied on it (ie. both one-directional and bidirectional loading). The test unit has been modeled analytically using two models: 1)Fiber model and 2) Beam model. Based on their results, Mazars *et al.*, concluded the following:

- Both models performed well in capturing the maximum values and the frequency characteristics of the response.
- Numerically simulated reinforcement elongation and the concentration of damage agreed well with the experimental observation.

Two full scale four story buildings were tested dynamically on a shaking table by Nagae and Wallace [14], to compare the analytically simulated response with the experimental response. The units were subjected to set of seismic actions with increasing intensity. The numerical model considered in this investigation was developed using the commonly used program: Perform 3D ().

As a result of their investigation, Nagae and Wallace stated the following conclusions:

- The analytical models were capable of capturing roof drifts and lateral loads in a reliable way under the service loading.
- For some features such as the elongation of the reinforcement, strength degradation, and shear behavior of the foundation, the analytical models were found to be doing better at the collapse level loading.

Yazgan and Dazio [1] investigated the capability of analytical models to predict maximum and residual displacements of RC components. In their investigation, a

set of 12 RC columns that had been tested on shaking tables, were numerically recreated. Also the same set of test units are considered in this thesis study. Yazgan and Dazio repeated the simulation by considering six models in order to investigate the reliability of alternative models in predicting maximum and residual displacements and to identify which model is better, and which modeling parameters have the strongest impact. As a part of their investigation, Yazgan and Dazio considered three alternative section flexural hysteretic behavior models: 1) Bilinear model, 2) Modified Takeda model (i.e. by Saiidi and Sozen [15]) and 3) Fiber model. Also in this thesis, this set of section hysteresis models are considered. For the component level finite-element formulation, Yazgan and Dazio investigated two models. 1-Displacement based element model, which is based on the Euler Bernoulli beam theory and 2-Forced based element defined by Neuenhofer and Filippou [16].

Based on their investigation, Yazgan and Dazio reported the following observations:

- Section flexural hysteretic model was found to have a higher impact compared that due to utilized finite-element model formulation.
- Models that take into consideration stiffness degradation were significantly more accurate compared to those that utilize Bilinear model.
- The considered analytical models were found to be more accurate in estimating the maximum drift than estimating the actual residual displacement.

As it can be seen from the state-of-the-art review provided above there has been considerable effort in developing seismic assessment strategies that are based on an energy-approach. Meanwhile, there has been an ongoing interest in validating analytical response simulation approaches for predicting the inelastic response of structures based on dynamic testing data. On the other hand, there has been very limited research that address the intersection of these two research topics that is: an investigation of the accuracy of numerical response simulation approaches in terms of estimating the energy dissipation behaviors of RC structures. This thesis aims at providing a preliminary discussion of this topic by discussing the results obtained for a set of ductile RC components.

3. ANALYSIS

3.1 Analysis Framework

Accurate prediction of the inelastic structural response under seismic actions is critical for reliable assessment of the demand. However, this is not a straightforward task to estimate the level of accuracy of the simulated response. A large set of assumptions needs to be introduced while establishing numerical models for simulating the seismic response. For the case of ductile RC components, the most critical assumptions are the ones related to hysteretic behavior, material stress-strain relationship, and finite element formulation. In addition to those major factors, there are several other assumptions (e.g. boundary conditions, damping modeling) that influence the simulated response. All of these assumptions and idealizations that influence the simulated response also have a direct influence on the accuracy of the results. Moreover, the accuracy of the simulated response is highly case dependent on the specific structure and component that is being considered. For two different ductile components subjected to the same excitation, the responses simulated by using the same approach may exhibit very different errors. Similarly, when two identical components are subjected to excitations with different frequency and duration characteristics again the simulated response may exhibit very different errors. In brief, the accuracy of the simulated response is a very case specific parameter. Still however, when a sufficiently large set of test cases are modeled using a specific modeling approach the statistical distribution characteristics of the exhibited errors can be considered as an indicator of the expected accuracy of that modeling approach. Based on such a strategy, the modeling approaches that are "on the average" more accurate in terms of predicting seismic response than the others, can be identified. This study is a contribution based on this strategy.

In this study, shaking table tests of a set of 9 RC components were numerically recreated, and the simulated responses were compared against the actual observed behavior in order to assess the accuracy of the simulated hysteretic energy dissipation

behavior, The schematic representation of the overall strategy adopted in this study is presented in Figure 3.1.

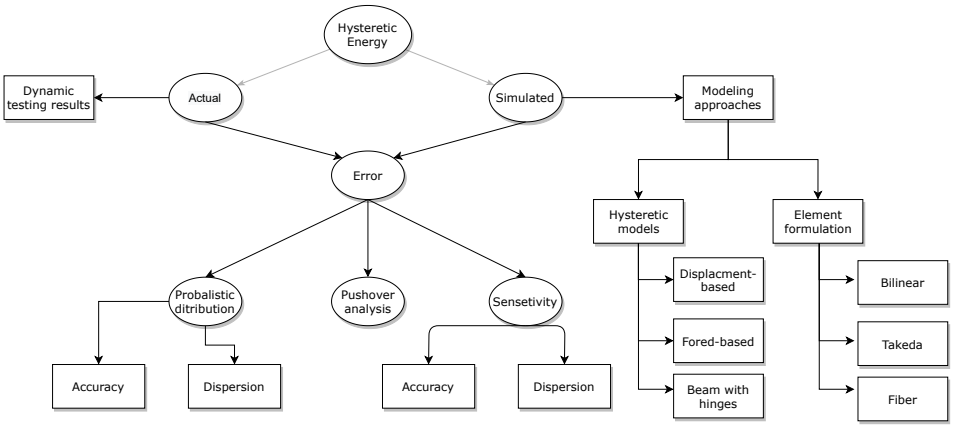

Figure 3.1 : Process followed in the study.

3.1.1 Energy dissipation

The hysteretic energy is defined as the energy dissipated by the structure through inelastic excursions during the seismic excitation. According to Equation 2.4d, the hysteretic energy, E_H can be obtained as follows:

$$E_H = E_a - E_s \tag{3.1}$$

This expression leads to the following:

$$E_H = \int f_s.dU - E_s \tag{3.2}$$

where f_s refers to equivalent static force for the structural component and dU refers to incremental displacement. And as far as the elastic energy E_s is a recoverable energy, its cumulative amount at the end of motion is equal to zero.

The numerical value of the integral expression in Equation 3.2 at the end of excitation (i.e. E_s=0) can be approximated using trapezoidal integral as follows:

$$E_H = \int_{U(0)}^{U(t)} f_s.dU = \sum_{i=1}^{N} \frac{(f_s)_{i-1} + (f_s)_i}{2} \Delta U_i \tag{3.3}$$

.

In the equation above, N is the total number of time steps, $(f_s)_{i-1}$ and $(f_s)_i$ are the amplitude of equivalent static force at the start and the end of i^{th} time step, ΔU_i is the change of relative displacement within i^{th} time step $(U_i - U_{i-1})$.

An example of this is integral for a single force-deformation cycle is presented in Figure 3.2. The area inside the force-displacement relationship is equal to the dissipated hysteresis energy within a single cycle. During the entire duration of excitation, ductile structural components typically undergo several cycles of such inelastic excursions. The total dissipated energy is equal to the sum of these integrals for all cycles during the entire response history. The main objective of this thesis is to identify how accurately this total integral can be predicted using some of the common modeling strategies.

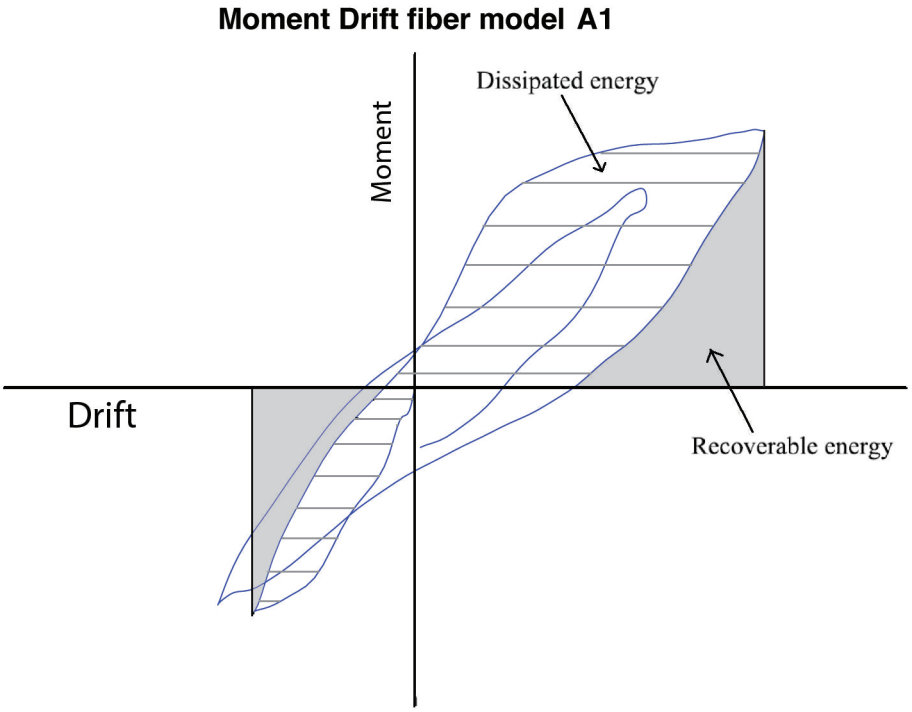

Figure 3.2 : Hysteretic energy dissipated within a single cycle of motion.

3.1.2 Error and correction factor

In order to identify the accuracy of the simulated energy dissipation behavior, an error parameter needs to be defined. In this thesis, the amount of energy dissipated, E_{exp} by the test unit during the shaking table experiment minus the amount of energy dissipation, E_{mod} simulated by using a specific modeling strategy, is defined as the error $Error$:

$$Error = E_{exp} - E_{mod} \tag{3.4}$$

Another useful parameter that can be utilized for quantifying the accuracy of results is the ratio of E_{exp} to the E_{mod}. This ratio is referred to as the correction factor C_E and it

is evaluated as follows:

$$C_E = E_{exp}/E_{mod} \tag{3.5}$$

According to this definition, a correction factor that is close to one means that simulated response is accurate while a value greater than one would indicate that numerical prediction is underestimating the actual energy dissipation behavior.

3.2 Finite Element Modeling Approaches

The accuracies of the simulated energy dissipation behaviors are investigated for a range of modeling approaches in this study. For this purpose, the set of considered test units are modeled using various alternative strategies. The common characteristic of all considered modeling approaches is that they are all frequently adopted strategies for simulating the response of ductile slender RC components subjected to design level excitations.

All finite element models considered in this study were developed using the "Open System for Earthquake Engineering Simulation (OpenSees)" platform [17].

OpenSees is an open-source software framework, that is used mainly for simulating structural and geotechnical system response under earthquakes. It has been launched by the Pacific Earthquake Engineering Research Center (PEER) [17], for educational and research reasons, OpenSees is being developed using C++ language and it is run by using TCL and Python languages.

In order to automatize the analysis process, a suite of TCL scripts were prepared. In the code developed as a part of this thesis study, there are three main parts, which are 1-modeling code, 2-analysis code and 3-output code. Modeling code is the first step where the model is meshed into finite elements and nodes. Afterward, the materials and geometrical transformations are defined. After that analysis code defines everything about the analysis process (loads, time integration, constraint equations enforced in the analysis, etc.). Finally, the output code, is the code that is used to get the output of the program.

Set of considered modeling approaches were developed by utilizing various combinations of:

1. Hysteretsis behavior models

2. Finite element formulations.

Hysteresis behavior models have a critical impact on the simulated response since they have a direct impact on the simulated stiffness and strength degradation behavior. Finite element formulation influences the analytical relationship between local and global response parameters. It directly affects the localization or spread of plastic deformations over the members. As a result, these two factors listed above are considered in this study to be the essential characteristics that define a modeling strategy. Categorization of the considered modeling approaches in terms of their major characteristic properties is shown in Figure 3.3.

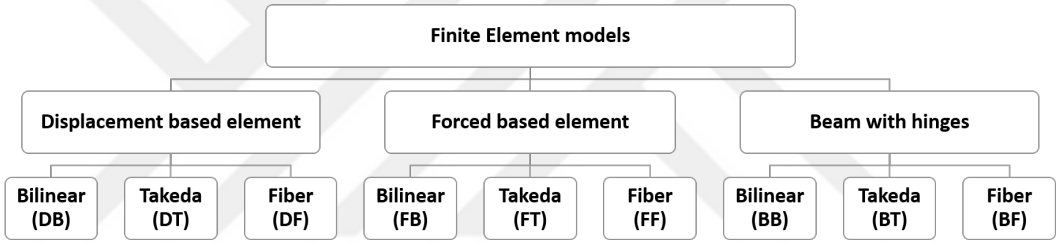

Figure 3.3 : Categorization of the considered finite element modeling approaches.

A total of 9 alternative modeling approaches were obtained by combining 3 alternative cyclic behavior models with 3 different finite element formulations. The open forms of the specific abbreviations noted in Figure 3.3 are as follows:

1. DB: Displacement-based element model with bilinear hysteresis

2. DT: Displacement-based element model with modified Takeda hysteresis

3. DF: Displacement-based element model with fiber-section

4. FB: Force-based element model with bilinear hysteresis

5. FT: Force-based element model with modified Takeda hysteresis

6. FF: Force-based element model with fiber-section

7. HB: Beam with hinges element model with bilinear hysteresis

8. HT: Beam with hinges element model with modified Takeda hysteresis

9. HF: Beam with hinges element model with Fiber-section

3.2.1 Section hysteresis models

The force-deformation relationship is a very essential aspect in predicting the nonlinear performance of a component in the earthquake simulation. Based on this fact, many hysteretic models have been proposed with the aim of representing that relation, putting into consideration section's stiffness degradation, energy dissipation, and strength deterioration. Since this study is about the prediction of energy dissipation, hysteresis modeling has a fundamental impact on it.

In this study: (1) Bilinear model, (2) Modified Takeda model and (3) Fiber model, which are the most commonly used hysteresis models, were considered to represent the flexural response of the RC component sections.

3.2.1.1 Bilinear hysteresis model

Bilinear hysteretic model is the oldest and most widely used model in practical engineering design applications. This is simply due to the fact that it is the least complicated model among all nonlinear hysteresis models. Bilinear model consists of three characteristics only: (1) cracked stiffness $EI_{cracked}$, (2) post-yield stiffness b, and (3) yield curvature ϕ_y. As presented in Figure 3.4, Bilinear model behaves linearly with a constant cracked section stiffness, $EI_{cracked}$ (i.e. lower than the gross section stiffness) until it reaches the yield deformation ϕ_y. After that, the model starts to act again linearly but with a much lower stiffness (i.e. post-yield stiffness) that is equal to b times the initial one. When the loading is released, model unloads with initial stiffness. The *Steel01* model available in OpenSees was used to construct the Bilinear model in this study.

Even though the Bilinear model is a commonly used model, it is known to be relatively inaccurate when it comes to simulating the response of RC structures. This is due to the fact that it does not take into account the stiffness degradation effect caused by

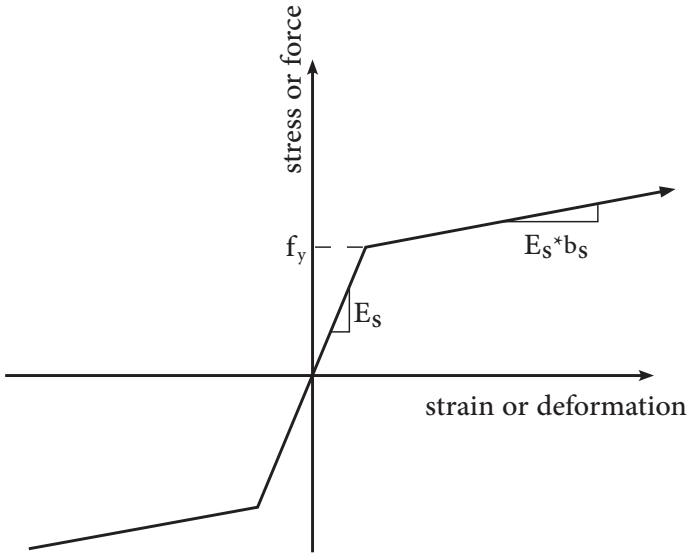

Figure 3.4 : Monotonic moment-curvature relationship definition for the Bilinear model.

softening of component's stiffness under cyclic loading due to cracking and yielding. This difference can be seen clearly in Figure 3.5.

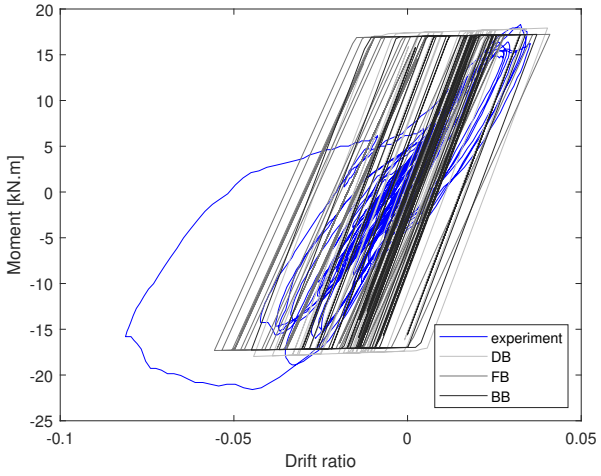

Figure 3.5 : Cyclic behavior obtained using Bilinear model plotted against the actual behavior of an RC column observed during a representative dynamic experiment.

3.2.1.2 Modified Takeda hysteresis model

Takeda hysteresis model was developed by Takeda and Sözen [18] based on observed response of RC components subjected to dynamic testing. Unlike the bilinear model, Takeda model takes into consideration the stiffness degradation. The original Takeda model was complicated and had a lot of rules, and that is why many researchers

attempted to simplify this model [15, 19, 20]. In this study, the simplified version that is commonly known as the *Q-hyst model* proposed by Saiidi and Sozen [15], has been utilized. Saiidi and Sozen has demonstrated that the response simulated using this simplified version is practically the same as the original Takeda hysteresis model.

The *Hysteretic* model available in OpenSees was used to construct this section model (Figure 3.6). This model is defined using 5 main parameters: (1) Yielding moment, M_y (2) yield curvature ϕ_y, (3) ultimate moment M_u, (4) Ultimate curvature ϕ_u and (5) unloading stiffness related parameter, β. The *Hysteretic* model in OpenSees is defined in a more generic way and it that additional parameters, *pinch factor*, and *damage factor*, that control the pinching behavior. In order to achieve the desired Takeda hysteresis behavior these two factors are taken as 1 and 0 in a row to eliminate their effects.

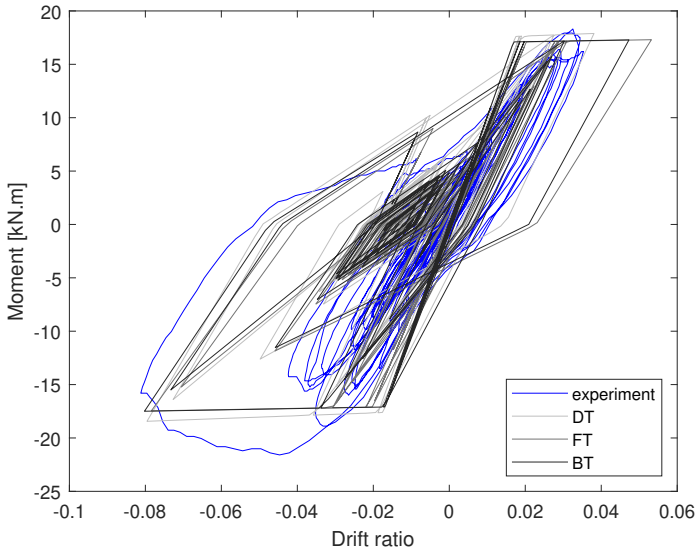

Figure 3.6 : Cyclic behavior obtained using modified Takeda hystersis model plotted against the actual behavior of an RC column observed during a representative dynamic experiment.

3.2.1.3 Fiber-section model

Fiber section model is based on the strategy of discretizing the cross-sections slender RC members into small pieces called fibers [21].

A uniaxial stress-strain behavior is assigned to each of these fibers. During nonlinear cyclic response simulation, moment-curvature behavior of the cross-section is computed by assuming a planar strain profile over the section and integrating the

stresses obtained for each fiber. This way, it also allows for capturing the interaction between axial load and the flexural response. Several studies have shown that the fiber model has a reliable precision in terms of capturing the cyclic behavior of slender RC components [1, 22].

As a result, it may be also considered as the most promising model in capturing the energy dissipation behavior. In Figure 3.7, the cyclic behavior simulated using fiber section model is compared against the actual response for the case of a slender ductile RC column. It can be seen that -similar to Takeda hysteresis model- fiber section model accounts for stiffness degradation, as well. Moreover, unloading and reloading paths are much smoother compared to those simulated using Takeada hysteresis.

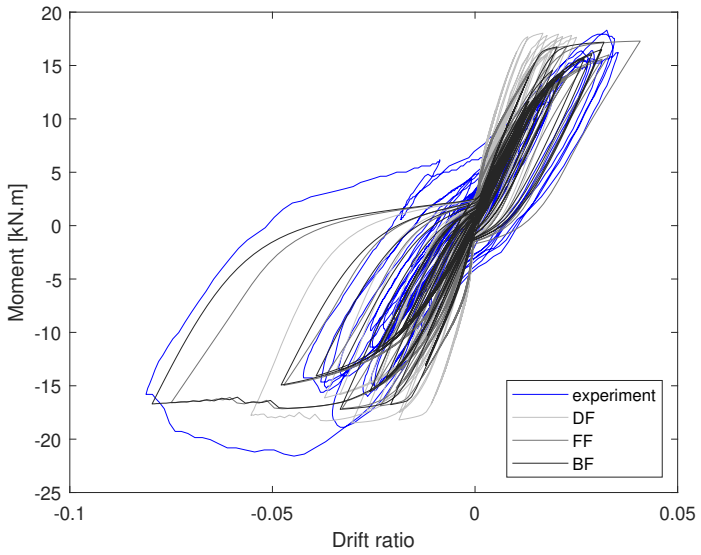

Figure 3.7 : Cyclic behavior obtained using fiber section model plotted against the actual behavior of an RC column observed during a representative dynamic experiment.

The section discretization is a critical step in modeling the fiber section modeling. If a highly dense discretization scheme is adopted it leads to extra computational effort. On the other hand, a very coarse meshing of the section into fibers may lead to errors in the results. This makes the discretizing process a critical step for achieving the best possible results in Fiber section model.

The uniaxial stress-strain models assumed for the fibers representing concrete and the reinforcement steel, have significant influence on the results. In this study, the

most popular approaches that are utilized for representing the uniaxial stress-strain responses are considered.

Confined concrete

The effects of confinement were estimated using the approach known as *Manders model* as presented in Priestly et. al. [23].

The confined concrete uniaxial stress-strain relationship in this study was modeled using the *Concrete04* material model available in OpenSees [17]. The backbone of this stress-strain relationship is based on the work by Popovics [24]. Cyclic stress-strain behavior simulated for a confined concrete fiber is shown in Figure 3.8.

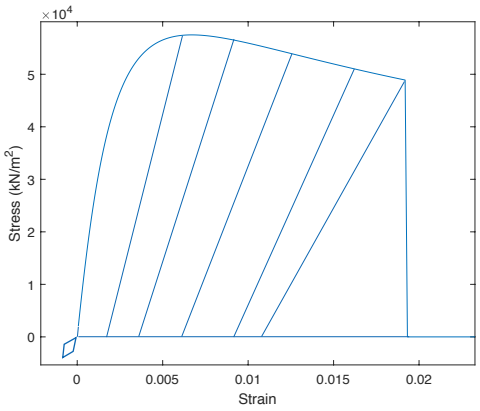

Figure 3.8 : Uniaxial stress-strain relationship assumed for the confined concrete fibers in the fiber-section model.

Unconfined concrete

The uniaxial stress-strain behavior of the unconfined concrete fibers in this study, is defined using the *Concrete01* model available in OpenSees. This model is based on the constitutive model by Kent and Park [25]. The monotonic stress-strain response simulated using this model is presented in Figure 3.9.

Reinforcement steel

In the fiber-section models considered in this study, the reinforcement steel hysteresis model by Menegotto and Pinto [26]. which accounts for the Bauschinger effect.

For this purpose, *Steel02* material model available in OpenSees was utilized for modeling the uniaxial stress-strain response of steel fibers. The characteristics of this model is defined using six parameters: (1) Steel initial modulus of elasticity $E_{initial}$,

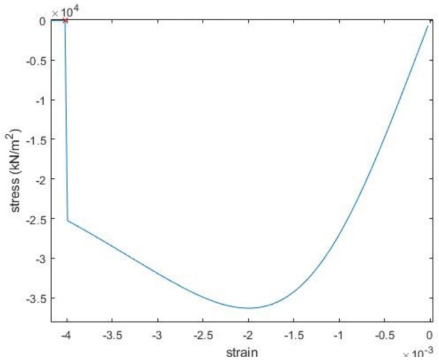

Figure 3.9 : Uniaxial stress-strain relationship assumed for the unconfined concrete fibers in the fiber-section model.

(2) Yielding strength f_y, (3) Post-yield strain hardening ratio b_{steel}, (4) Initial elastic to post-yield stiffness transition radius, R_0, and (5, 6) Pair of parameters controlling the evolution of transition stiffness, c_{R1} and c_{R2}. In this study, Bauschinger effect related parameters were been taken as R_0=20, c_{R1} =0.925 and c_{R2} =0.15. An example of the stress-strain relation obtained using is *Steel02* shown in Figure 3.10.

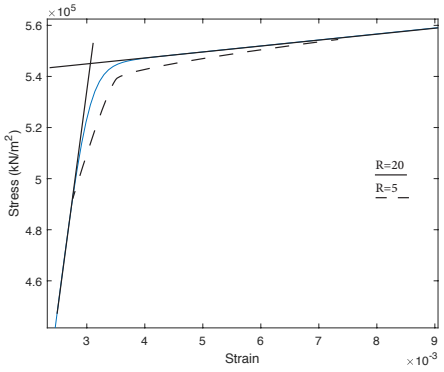

Figure 3.10 : Steel stress-strain relationship.

3.2.2 Beam-column element models

The accurate prediction of nonlinear response is a critical issue in predicting the energy dissipation . The finite element modeling assumptions are a fundamental aspect in computing the nonlinear behavior. This makes the element model assumptions a critical factor in this study.

The element model formulation is a complicated subject, where many assumptions can be considered. Among these, the most important assumption is the plasticity distribution over the element. Many experimental studies had been done to develop plastic hinge length models for estimating the expected spread of plasticity over critical

regions in reinforced concrete members [27]. Meanwhile, several finite-element modeling strategies have been proposed to capture the spread of plasticity in the numerical models of concrete members [28]

In this investigation, the equivalent plastic hinge length, L_p expression proposed by Priestley et al. [27] was taken into consideration for determining the estimated length of plastic hinge. Accordingly, the ultimate displacement capacity estimated based on this approach was considered as the benchmark value for displacement capacity at which finite-element models should reach their ultimate limit state deformations. For all the finite-element formulations considered here, this principle was utilized in developing appropriate meshing schemes, etc..

Another critical assumption related to element modeling is the element formulation type. Here, element formulation type represents the numerical analysis strategy adopted for computing the element end forces and displacements that both achieve force equilibrium and displacement compatibility within the structure as well as inside each finite-element. In this study three element formulation types were considered: (1) BH "Beam with hinges" (2) DBE "Displacement-based element" and (3) FBE "Forced-based element" formulations.

3.2.2.1 Displacement-based element formulation

Displacement-based element, or "stiffness-based approach" as some prefer to call it, is the most commonly used element formulation. It is implemented into almost all finite element analysis programs. Displacement-based element model is based on the Euler Bernoulli beam theory in defining the behavior of the element. A linear curvature profile is enforced over each element since cubic displacement interpolation functions are utilized. In this study, *dispBeamColumn* element model available in OpenSees [17] was used to construct models with displacement-based finite elements. In each finite-element, two-point Gauss-Legendre integration was utilized.

A key assumption in the displacement-based element is the linear curvature profile enforced along the element length. The element state definition and stiffness evaluation are directly impacted by this linear variation of the curvature profile. Since the actual curvature profiles in RC members may be highly nonlinear, this assumption leads to errors if RC members are not properly discretized into multiple finite-elements.

Particularly, the meshing of concrete members at critical locations with steep curvature gradients has a strong impact on the accuracy of results. The discretization scheme recommended by Yazgan [29] was adopted here to obtain a proper inelastic behavior.

3.2.2.2 Forced-based element formulation

Forced-based element formulation, or the "flexibility based approach" as some prefer to call, was first proposed by Kaba and Mahin [30]. Later, it was further improved Neuenhofer and Filippou [16]. In the flexibility-based approach, the internal forces are determined based on member end-force interpolation functions. As a result, the section forces at all integration points are directly in equilibrium with external forces at all times. Since section deformations are identified directly by considering section flexibility, there are no constraints introduced regarding the curvature variation along with the element. This leads to an improved representation of spread of plasticity along with the element. Still however, discretization of RC members into force-based finite-elements is a critical issues particularly at the regions of plastic hinging. The quadrature rule-based integration of displacements and flexibilities leads to regions and amplitudes of plastic deformations, being sensitive to the adopted meshing scheme. In this study, the recommendations by Yazgan [29] were followed in discretizing RC members into force-based finite elements.

In this study *forceBeamColumn* model available in OpenSees [17] was used to construct models with force-based element formulation. In each force-based element, two Gauss-Lobatto integration points were utilized.

3.2.2.3 Beam with hinges

Beam with hinges (BH) model was developed by Scott and Fenves [28] and it is considered as one of the best suited models that take into consideration the nonlinear behavior of slender RC components, In the BH model, consists of two plastic hinge segments at both ends, and an elastic segment in between. The behavior of the end segments are analyzed according to force-based approach and modified Gauss-Radau quadrature rule is adopted for the integration. The utilized integration rule is specifically tailored to capture potential sharp curvature gradients that may be exhibited in RC members.

In this study, *beamWithHinges* element model available in OpenSees [17] was used for established the models with BH elements. When the components considered had a free end, length of the plastic hinge at that end was set equal to zero. Otherwise, the expected plastic hinge length was set equal to L_p estimated using the expressions by Priestley [27].

3.3 Simulation Approaches

3.3.1 Pushover analysis

The first step in understanding the similarities and differences between the simulated responses and the actual behaviors of the components, is to compare the pushover (PO) analysis results. In this context, PO curves obtained by means of nonlinear static analysis are compared against the actual force-displacement responses of the test units.

The response during the largest cycle for each component during the experiment were identified, in order to compare the simulated PO behavior against the actual response. Inevitably, such an approach does not provide a very clear picture of the comparison since the actual unit is subjected to a cyclic motion whereas the simulated one is subjected to quasi-static monotonic loading. Still however, it provides a sufficiently good indication of the strength capacity of the unit and the post yield stiffness.

Another issue that should be kept in mind is that there are damping/friction etc. effects included in the experimental backbone curve derived from the shaking table test since it is related to the dynamic response of the actual unit. On the other hand, these effects are missing in the simulated pushover. Still however, the results provide some indication of the general trends. In all cases, the results were plotted over the experimental full cyclic hysteresis curve to be able to present the effects of the stiffness degradation throughout the cycles.

3.3.2 Time history analysis

After comparing the results from pushover analysis, the dynamic response of the test units were simulated by performing time history analyses.

Damping was assigned to the model using Rayleigh method. In Reference models of the WDH1, WDH3, WDH4, WDH5 and WDH6 walls components, a ζ=2% viscous

damping ratio was considered, ζ=3.34% for CAMUS3, ζ=1.96% for A1, ζ=2.4% for B1 and ζ=2.00% for EBII07. The last-committed (tangent) stiffness and mass proportional damping was applied to the instantaneous stiffness matrix using Rayleigh damping model. The Transient type analysis was set for the dynamic ground motion analysis. For the numerical evaluation of components dynamic response, the Newmark time integration method Newmark [31], with the parameters (γ =1/2, β=1/4) was adopted in analyses.

Time integration step size are Δt = 0.02 for WDH1 test unite, Δt = 0.0133 second for WDH3, WDH4, WDH5 and WDH6 tests units and Δt = 0.01 second for CAMUS3, A1, B1 and EBII07 tests units. The analysis increment was set the same as the ground motion step size. Thus all the steps in ground motion set were considered in the analysis. The Newton algorithm was chosen in the analysis.

3.4 Properties of Test Units

The expected level of accuracy of the energy dissipation behavior simulated using the presented finite element modeling approaches, was investigated by considering the responses of 9 test units tested on shaking table in earlier studies. All units were slender ductile RC units that were subjected to shaking intensities close to their design level seismic actions. The test units were tested on 3 different shaking table test facilities by different groups of researchers.

The sectional geometries and the geometries of the tested components are provided in Figures 3.11 and 3.12. For all test units, the excitation was applied along the x-axis.

In the following, each test unit is introduced briefly. Further details can be found in the specific test report cited for each unit.

3.4.1 A1-B1 test units

Test units A1-B1 are RC columns components are two cylindrical RC columns tested by Hachem et al. [32]. The units were designed according to CALTRANS Bridge Design Specifications (1993) [33]. They were constructed at a scale of 1 to 4.5. Units were constructed with the aim of representing concrete bridge piers. They had rigid

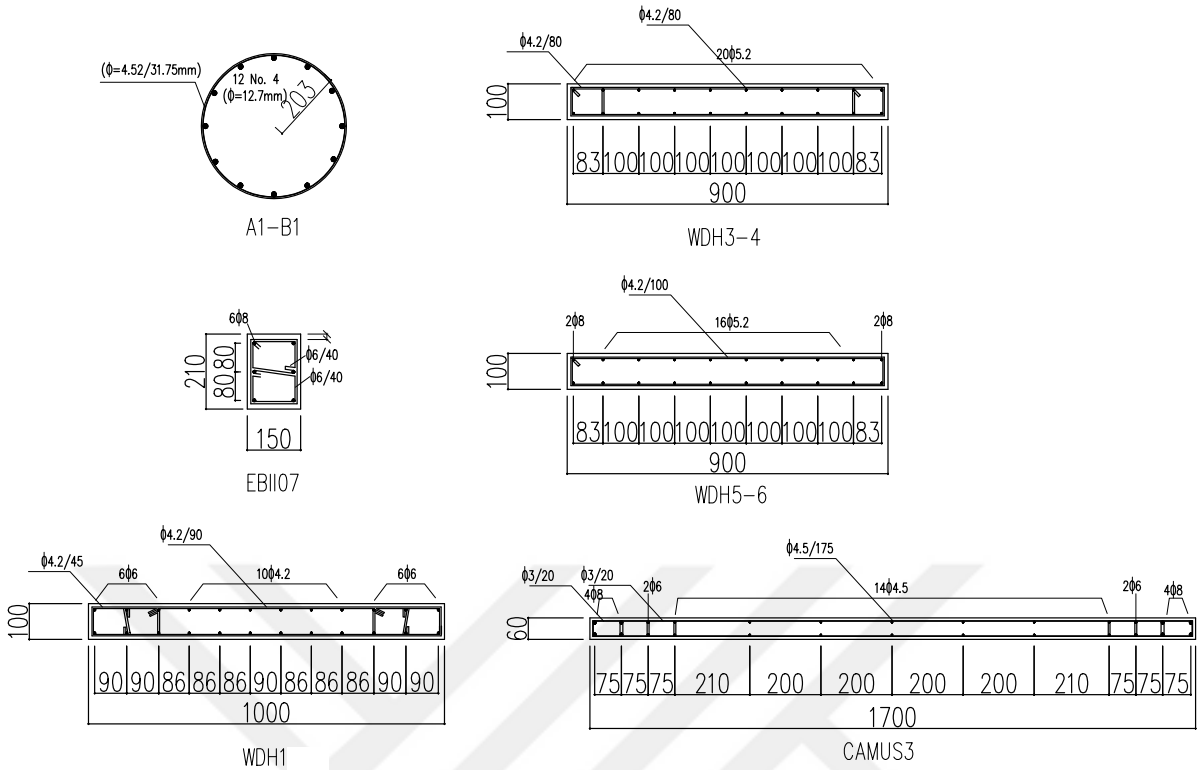

Figure 3.11 : Cross section geometries and reinforcement detailing of the test units.

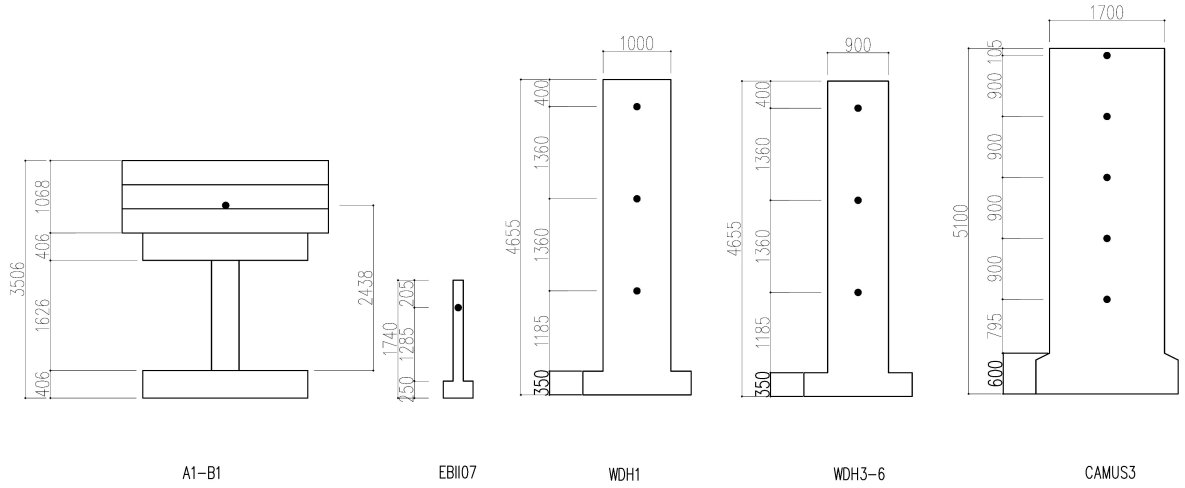

Figure 3.12 : Geometries of the 9 test units.

mass blocks located above to represent the inertial forces related to the mass of the girder.

Units A1 and B1 were identical components that have been built to investigate the influence of various strong ground motion characteristics [32]. A1 component was subjected to the strike normal ground motion component recorded at *Olive View* station during 1994 Northridge M_w 6.7 earthquake. This station was located at a distance of 6.4 km from the rupture plane and had near-fault characteristics. B1 component was tested under the *Llolleo* station record from the 1985 Chile M_w 7.8 earthquake. This record has a longer duration and was taken from 64 km away from the epicenter.

For A1 and B1 units, two tests were considered for each, A1 Run-2 test (110% of the design load intensity), and B1 Run-5 test (150% of the design load intensity) were considered to be suitable for the main objective of this study which is investigating the sensitivity of the estimated hysteretic energy dissipated to major finite element modeling assumptions. On the other hand, A1 Run-1 (30% of the design load intensity) and B1 Run-4 tests (52% of the design load intensity) were considered to check the results' validity when low load intensity earthquake is applied.

3.4.2 EBII07 test unit

EBII07 component is a rectangular RC column, which has been designed to fail in flexure and behave in a ductile manner under earthquake loading [29]. The unit was excited using the *Caleta de Campos* station ground motion that was recorded during the 1985 Michoacan M_w 8.1 earthquake. The unit was subjected to a set of excitations with different intensities during the testing sequence. In this study, the third test with the 100% design load intensity was considered.

3.4.3 CAMUS3 test unit

CAMUS3 component is an RC wall that was constructed on a scale of 1 to 3 and was tested on a shaking table by Combescure and Chaudat [13]. This unit is a model for 5 story shear-wall structure. It consists of 2 RC walls connected by five body masses plus one in the footing. The CAMUS3 component was designed according to Eurocode 8 (1998) [8] provisions.

The unit was subjected to excitations that cover a range of intensities. In this study, the specific test designated as *MR2* was considered. During this test, the unit was subjected to *Melendy Ranch* station ground motion that was recorded near the epicenter

of the 1972 Stone Canyon earthquake. MR2 test was the first test to reach the yielding deformation, which makes it the most suitable one for this study. Before the MR2 test the wall unit had minor damage. Combescure and Chaudat [13] reported that there were cracks observed in the first three stories after the *MR2* test.

For CAMUS3 component, Combescure and Chaudat (2000) [13] reported that the displacement for the top story was not recorded correctly. Accordingly, in this study, fourth story's displacement record will be considered as the top story's displacement.

Nice r2 test (i.e. 30% of the design load intensity) was also considered in this study as a tests with excitation lower than the design level. The purpose behind considering this second case is to check the results' validity when low load intensity earthquake is applied.

3.4.4 WDH1, WDH3, WDH4, WDH5 and WDH6 test units

WDH1, WDH3, WDH4, WDH5 and WDH6 components are six reinforced concrete walls that had been built by Lestuzzi et al. [34]. Responses of these walls were investigated further by Lestuzzi and Bachmann [35]. These components are models of an RC walled structure constructed on a scale of 1 to 3. WDH1 as well as WDH3 and WDH4 have identical geometries, to simplify the comparison of the behavior between them. These walls were designed according to the capacity design method for a displacement ductility capacity of 3. However WDH5 were designed according to SIA 162 (1993) with a displacement ductility capacity of 2, WDH6 component is very close in design to WDH5 component, with a 40% less transverse reinforcement.

For the WDH1 component, even though the applied load intensity was only 70% of the designed level load, the 3rd test was the most suitable test to consider in this study. For the cases of WDH3, the first test were considered in this study since 100% design load intensity was applied during this test. For the last three components: WDH4 WDH5 and WDH6, again the first tests with 80% of the designing level intensities were identified to be suitable to be used in this study.

3.5 Modeling of the Test Units

Using OpenSees software, the test units' flexure response and the section flexural models were established. Using these models their responses were simulated numerically. The level of accuracy in capturing the hysteretic energy dissipation was identified by comparing the numerical results with that observed during the shaking table testing. In the following, major properties of the constructed models are presented.

3.5.1 Section flexural response

Components' sectional flexural response characteristics are modeled based on their moment-curvature relationships. In order to identify the characteristic properties of the flexural response of the columns, a fiber modeled was created as shown in Figure 3.13. Cross-sections of the test units A1, B1, were discretized into 30 segments in the radial direction and 15 segments in the circumferential direction. Section of EBII07 test unit was discretized into 80 segments in the confined region and 2 segments per centimeter in the unconfined part. For the wall units, the confined sections were discretized into 5 segments per cm. The unconfined regions in the cross-section were discretized into 3 segments per cm in the core and 1 segments per cm in the edges. The resulting section discretizations are presented in Figure 3.13.

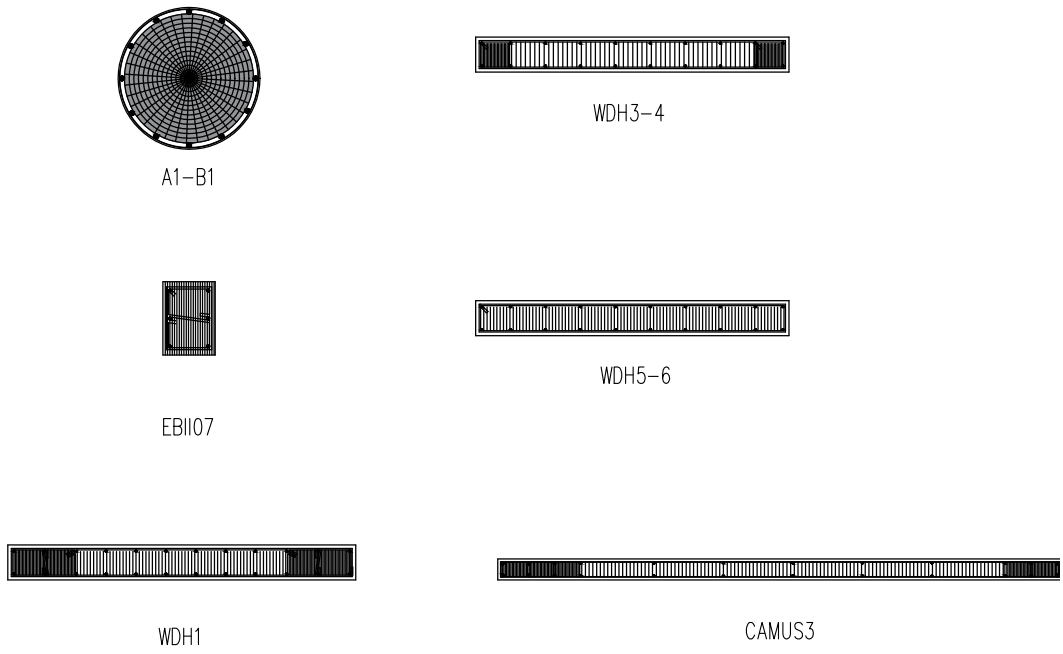

Figure 3.13 : Cross-section discretization of the fiber model.

The reinforcement steel characteristic material properties were taken from Yazgan [1] who recommended the parameter values in Table 3.1. The reduction of ultimate strain capacity due to cyclic loading as recommended by Priestley et al. [27] has been considered, as well. As shown in Figure 3.14, the ultimate strain is equal to 60 percent of the strain corresponding to the ultimate strength of the reinforcement.

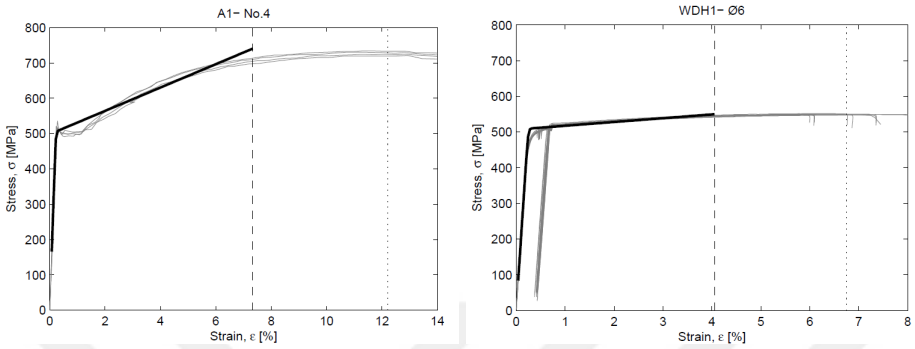

Figure 3.14 : Sample stress strain plots obtained for: (a) the No.4 (12.7∅) reinforcement bar used in unit A1 and (b) the 6∅ bar used in WDH1 (Adaped from: [1].

Table 3.1 : Reinforcement steel modeling parameters.

Unit	size	f_y [MPa]	E_s [GPa]	b_s [%]	ε_{ys} [%]	ε_{fs} [%]
WDH1	∅ 4.2	565	202	0.7	0.28	3.0
	∅ 6	509	206	0.5	0.25	4.1
WDH3	∅ 5.2	479	215	1.2	0.2	4.3
WDH4	∅ 5.2	486	219	1.0	0.22	5.2
WDH5	∅ 5.2	489	222	1.0	0.22	4.4
	∅ 8	580	216	1.1	0.27	3.5
WDH6	∅ 5.2	497	219	0.9	0.23	5.0
	∅ 8	581	218	1.1	0.27	4.0
CAMUS3	∅ 4.5	561	197	1.5	0.29	1.0
	∅ 6	595	192	0.7	0.31	1.9
	∅ 8	483	196	0.5	0.25	9.4
A1,B1	∅ 12.7	506	226	1.5	0.22	7.3
EBII07	∅ 8	545	180	1.3	0.30	7.1

The unconfined concrete strength and elasticity modulus of concrete were taken from the tests reports. Confined concrete strength, strain and maximum compressive stress, and ultimate strain were all calculated according to the model by Mander et. al. [23]. Unconfined and confined concrete parameters are listed in Table 3.2. For all units strain at peak compressive stress and the ultimate strain for unconfined concrete were assumed to be equal to 0.2% and 0.4%, respectively.

Table 3.2 : Concrete modeling parameters.

Unit	E_c [GPa]	σ_{uc} [MPa]	σ_{cc} [MPa]	ε_{cc} [%]	ε_{cu} [%]
WDH1	31.5	39.7	53.0	0.54	1.55
WDH3	30.2	36.5	44.4	0.42	1.17
WDH4	30.1	36.3	44.2	0.42	1.18
WDH5	30.2	36.5	40.1	0.28	0.78
WDH6	32.6	42.6	46.2	0.25	0.73
CAMUS3	31.5	39.6	77.1	1.15	2.28
A1,B1	31.3	39.2	57.5	0.67	1.92
EBII07	31.6	40.0	67.6	0.89	3.76

When modeling the flexural behavior, axial load acting on the system has a critical influence on the results. For EBII07 column and walls from WDH1 until WDH6 the axial loads were applied through a tension cable and dynamic masses were free to move only in the lateral direction on the rails. This setup separates the dynamic masses and the axial load acting on the system. In the other tests, axial loads were mainly due to gravity load, and partly due to the vertical acceleration. This caused a ΔP effect on the system. This ΔP was considered in the analysis. In this study, the axial force applied at the models were taken from related test reports.

For both Bilinear and Takeda models, idealized moment-curvature envelopes are needed to be constructed. The idealization of the flexural response of the established models was done according to the method proposed by Priestley et al. [36]. Cracked stiffness $EI_{cracked}$, the post yielding stiffness hardening ratio b_{EI}, the yield curvature ϕ_y, the ultimate curvature ϕ_u, the yielding moment M_y and the ultimate moment M_u parameters are presented in Table 3.3., For the case of Takeda hystersis model, there is an extra parameter β defined by Saiidi and Sozen [15]. This parameter controls the unloading stiffness of the model and it was assumed to equal to 0.5. Two sample idealization processes related to units EBII07 and WDH3 are presented in Figures 3.15 and 3.16. For the rest of the components the details of the idealization process are presented in Appendix A.

3.5.2 Finite element discretization

As mentioned in Section 3.2.2, three different finite element formulations were tested in this study. Determining element discretization for each model is a critical step that

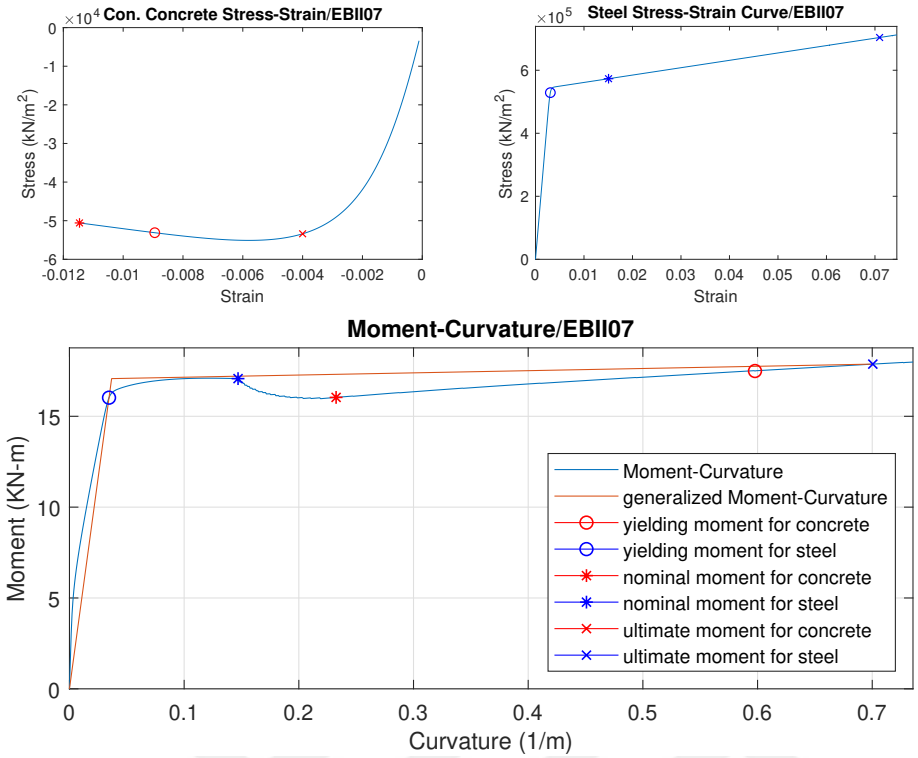

Figure 3.15 : Bilinear idealization established for the EBII07 test unit.

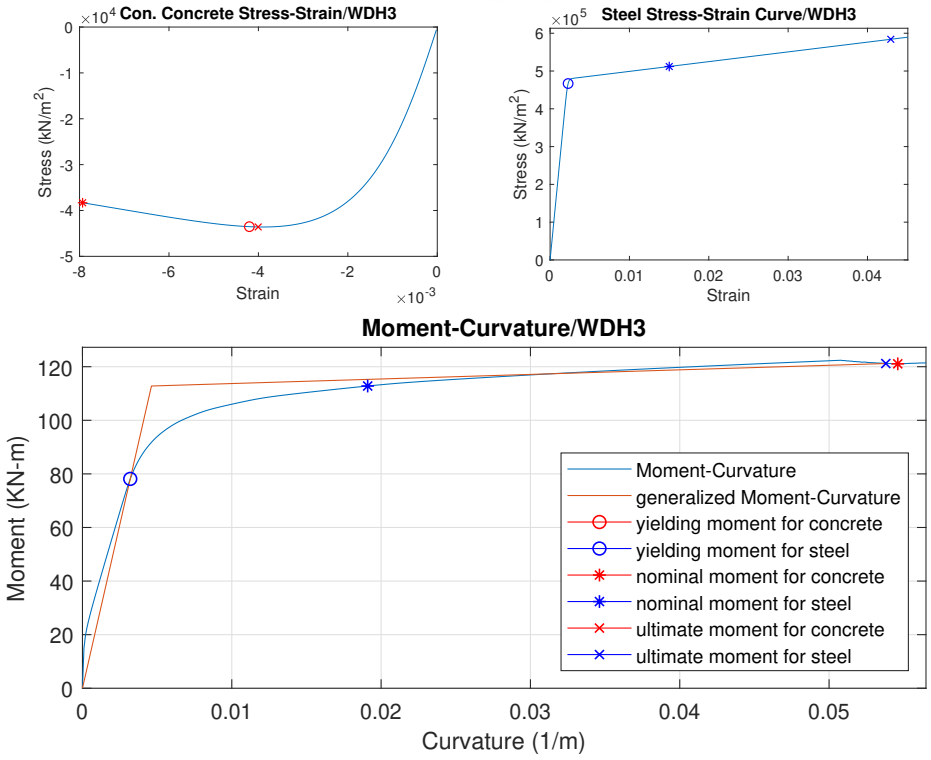

Figure 3.16 : Bilinear idealization established for WDH3 test unit.

Table 3.3 : Moment curvature idealization parameters.

Unit	EI_{eff} $[MNm^2]$	b_{sec} $[\%]$	θ_y $[km^{-1}]$	θ_u $[km^{-1}]$	M_y $[kNm]$	M_u $[kNm]$
WDH1	40.3	0.37	4.1	45.6	146.6	166.3
WDH3	24.4	0.71	4.6	53.8	112.8	121.35
WDH4	24.7	0.59	4.6	65.2	113.3	122.2
WDH5	29.7	0.89	5.0	43.6	146.5	156.5
WDH6	30.1	0.88	4.9	49.4	148.7	160.4
CAMUS3	169.7	1.00	2.3	48.6	393.1	472.5
A1,B1	11.8	1.02	1.36	189.0	160.1	181.2
EBII07	0.46	0.26	36.8	700.5	17.1	17.9

needs to be done finely. In this study, equivalent plastic hinge lengths obtained using Priestley et al. [27] are utilized. Accordingly, the discretizations of the models were done according to the recommended method Yazgan [29].

Displacement-based Element Finite element discretization of the members into displacement-based elements are presented in Figure 3.17. For walls from WDH1 until WDH6 and CAMUS3, were discretized as a two displacement-based elements in the first story. In these models, length of the first element located at the critical region (i.e. referred to as L_1) was set equal to the estimated plastic hinge length. For the upper stories one displacement-based element was considered per story. For the EBII07 test unit, only two displacement-based elements were utilized and L_1 was set equal to the estimated plastic hinge length. For A1 B1 units, an extra element was defined at the top of the model with a 20 times higher stiffness than other elements in order to capture the rigid body movement of the mass at the top.

Force-Based Element Force-based element model discretization considered in this study, is shown in Figure 3.18. Here a different discretization is utilized as compared to displacement-based element models. This discretization was also made according to the recommendations by Yazgan [1] related to force-based elements. The length for the first element (L_1) with two integration points is set equal to two times the length of the hinge.

For all the units except CAMUS3, L_1 in force-based formulation is equal to double the amount in displacement-based models. This difference is related to assumption of linear curvature profile imposed in displacement-based element formulation. For

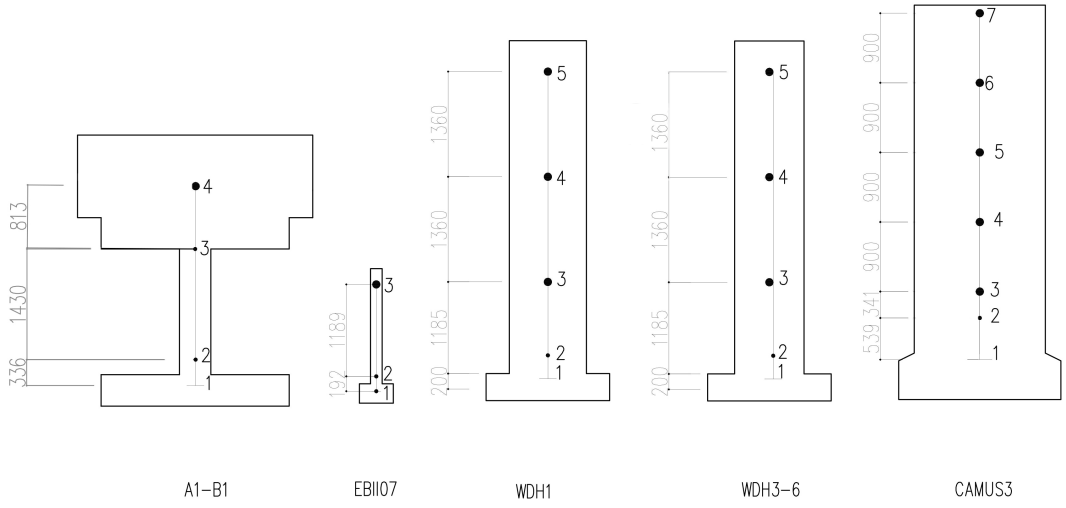

Figure 3.17 : Discretization for: DB, DT, DF, BB, BT and BF models.

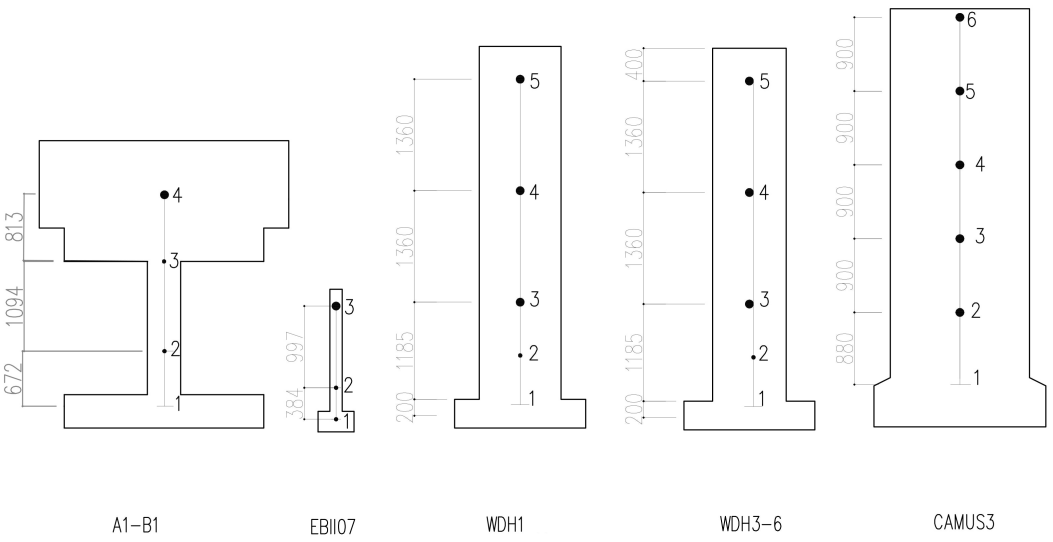

Figure 3.18 : Discretization for: FB, FT and FF models.

CAMUS3 unit, setting L_1 equal to twice L_p is not possible since the story height puts a constrain. Because of that L_1 has been taken equal to the first story height in the force-based element model of CAMUS3 unit.

Beam With Hinges Beam with hinges discretization procedure was much simpler compared to other element formulations. One beam with one hinge element was assigned to the stories. Each hinge region had a length set equal to the estimated equivalent hinge lengths.

4. DISCUSSION OF THE RESULTS

4.1 Introduction

In this chapter the results obtained from the analysis of the tests units are discussed. Models of the test units are established using the modeling approaches introduced in the previous chapter. Using these models the following analyzes are performed:

1. Pushover analysis
2. Time history analysis
    2..1 Design level excitation
    2..2 Low level excitation
3. Parameter sensitivity analysis
    3..1 Damping ratio variation
    3..2 Plastic hinge length variation

Each analysis aims to identify the impact of a specific factor on the accuracy of the simulated energy dissipation behavior.

4.2 Pushover analysis

As a first step in validating the performances of the finite element models in terms of fundamental characteristics, pushover analysis were performed. One thing that has to be kept in mind, is the fact that there are damping/friction etc. effects included in the experimental backbone curve derived from the shaking table test since it is directly related to the dynamic response of the actual unit. On the other hand, these effects are missing in the simulated pushover curves since this is related to quasi-static loading. However, a comparison of the pushover analysis results with the observed dynamic cyclic response is still informative in terms of strength and initial stiffness.

Pushover curves obtained from nonlinear static analyzes of the models are presented in **Figures 4.1-4.5**. In each figure, the moment versus average drift ratio response of the test unit measured during the test is plotted. Here, average drift ratio refers to the lateral displacement of the uppermost mass divided by the height of the mass from the top of the foundation block. Only in the case of CAMUS3 unit, where the measured displacement of the story mass was erroneous and the 4th story displacement measurement was considered instead. In the figures, "Experiment" is the actual cyclic response of the test unit exhibited on the shaking table. Pushover analysis results obtained using 3 alternative finite element formulations are provided in each figure: (1) "DF": Displacement-based model with fiber sections, (2) "FF": Force-based model with fiber sections and (3) "BF": Beam with hinges model with fiber sections.

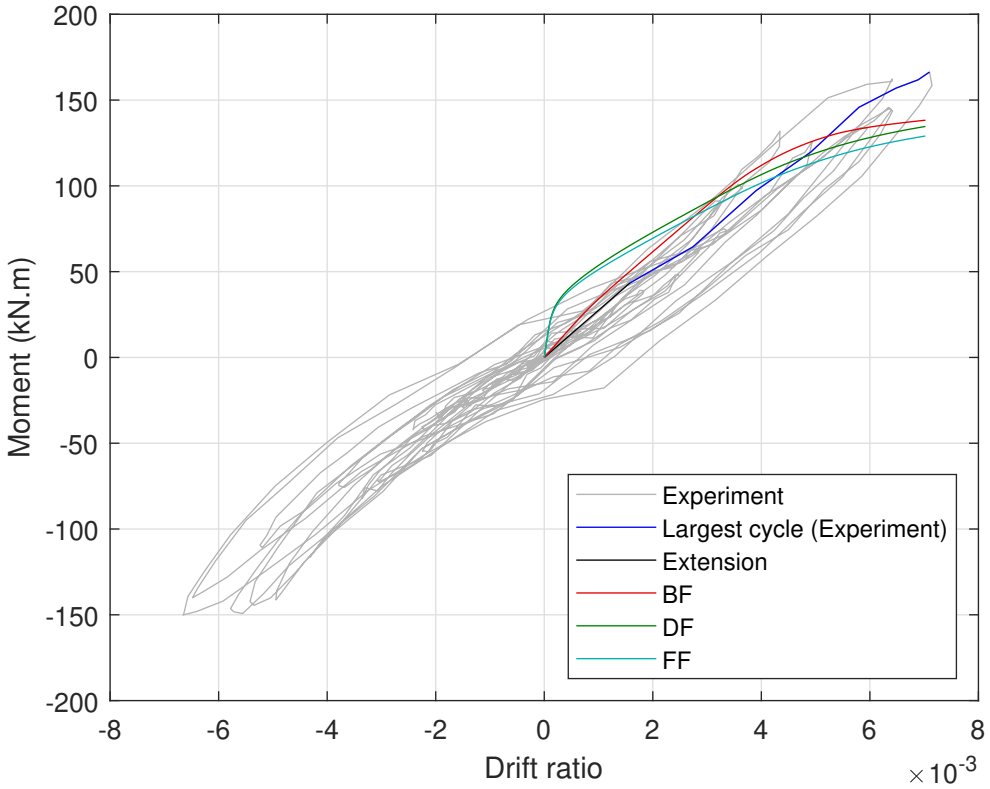

Figure 4.1 : Pushover results obtained for test unit WDH1 obtained using the fiber section model.

It can be seen that for 5 of the units WDH3-WDH6 and EBII07, the actual initial stiffness of the walls is underestimated by all numerical models (**Figures 4.1-4.5**). On the other hand, for the A1, B1 and CAMUS3 initial stiffness is captured very well. It should be noted that the units were subjected to shaking intensities reaching to 30% to 50% of their yield limit during the tests prior to the design-level shaking considered

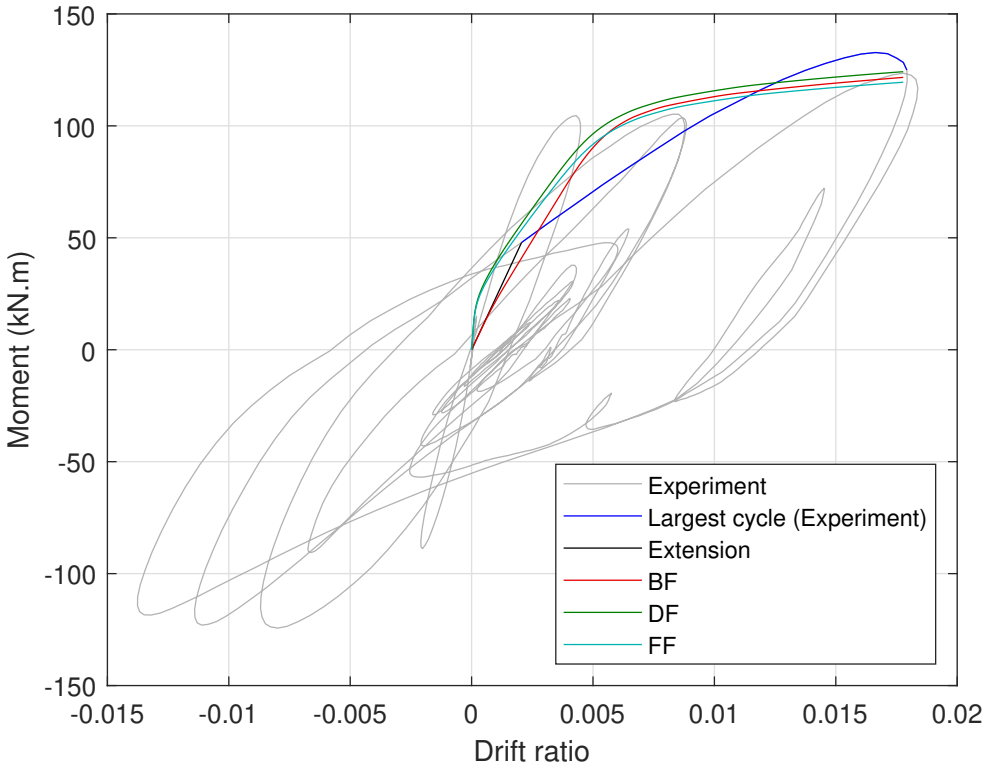

(a)

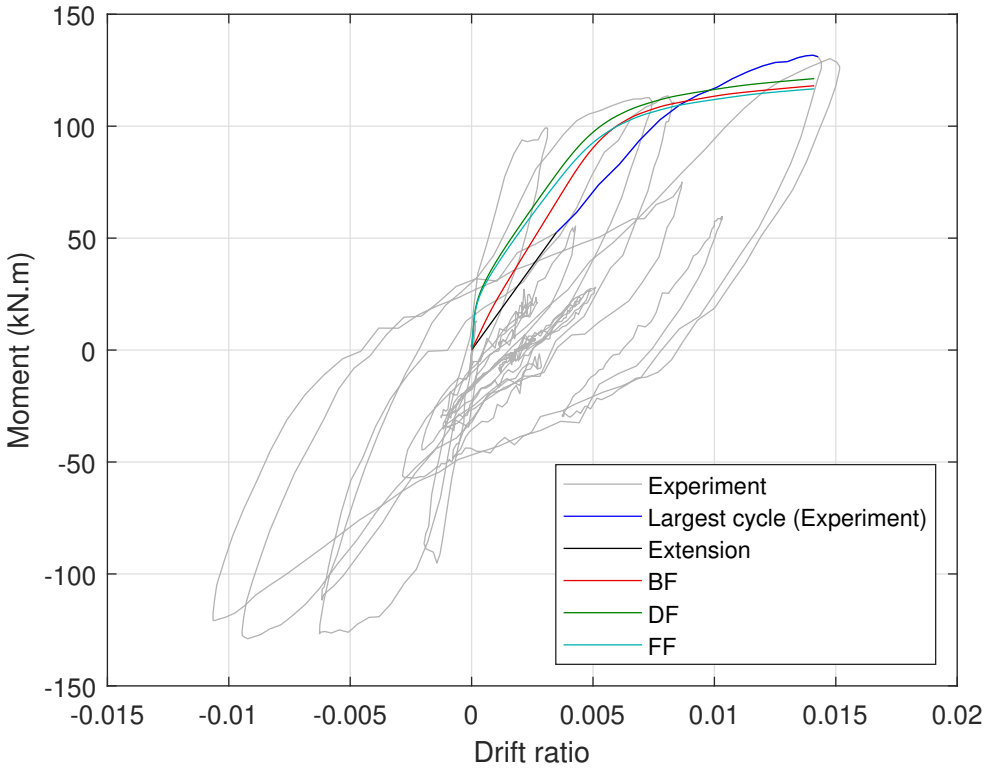

(b)

Figure 4.2 : Pushover results obtained using the fiber section model for the test units: (a) WDH3 and (b) WDH4.

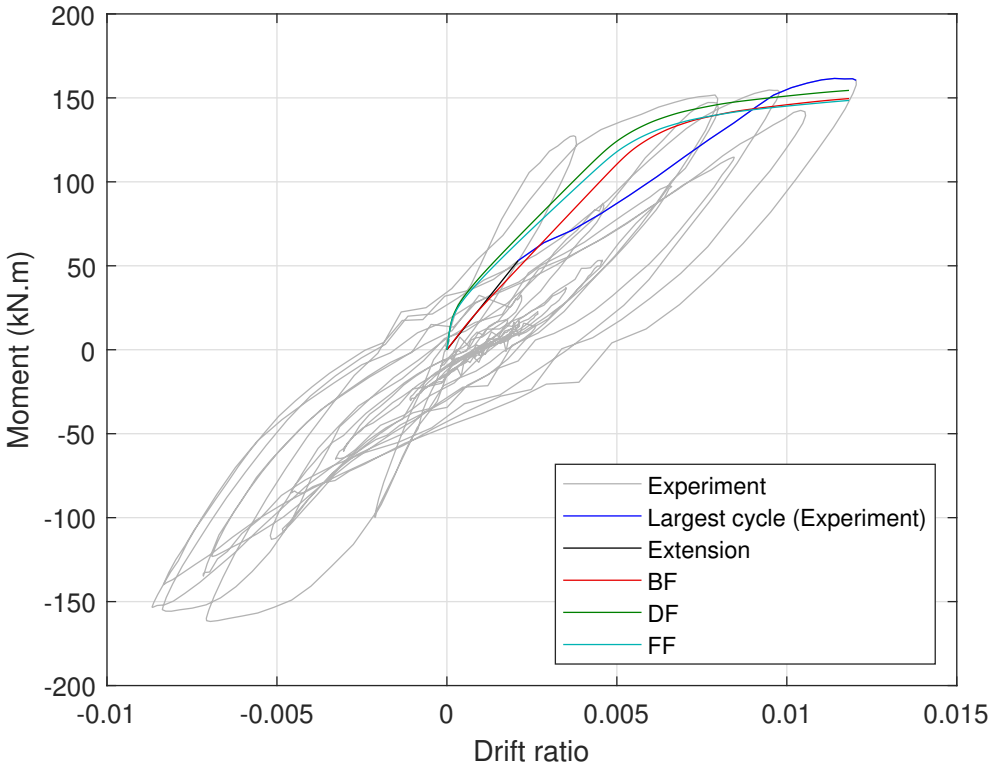

(a)

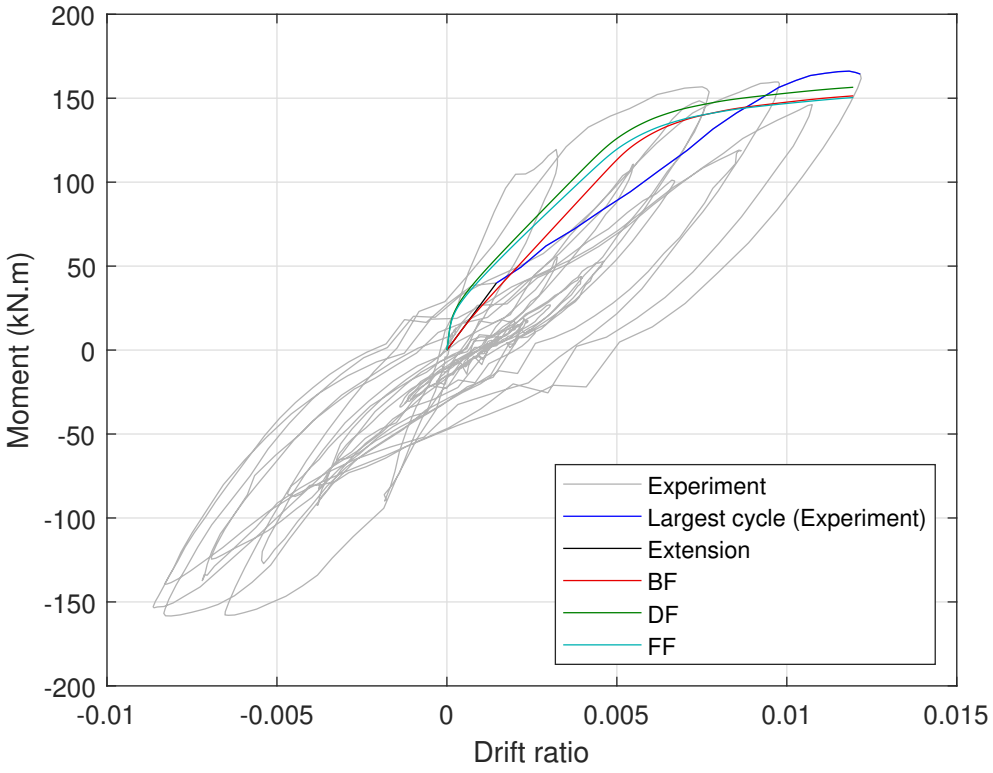

(b)

Figure 4.3 : Pushover results obtained using the fiber section model for the test units: (a) WDH5 and (b) WDH6.

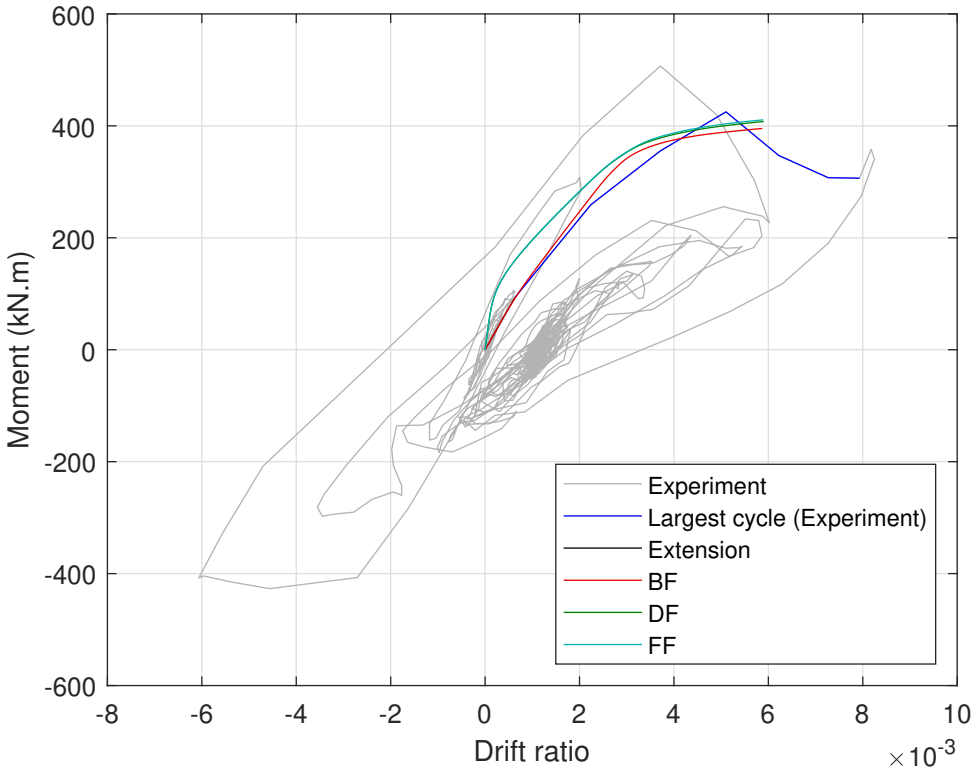

(a)

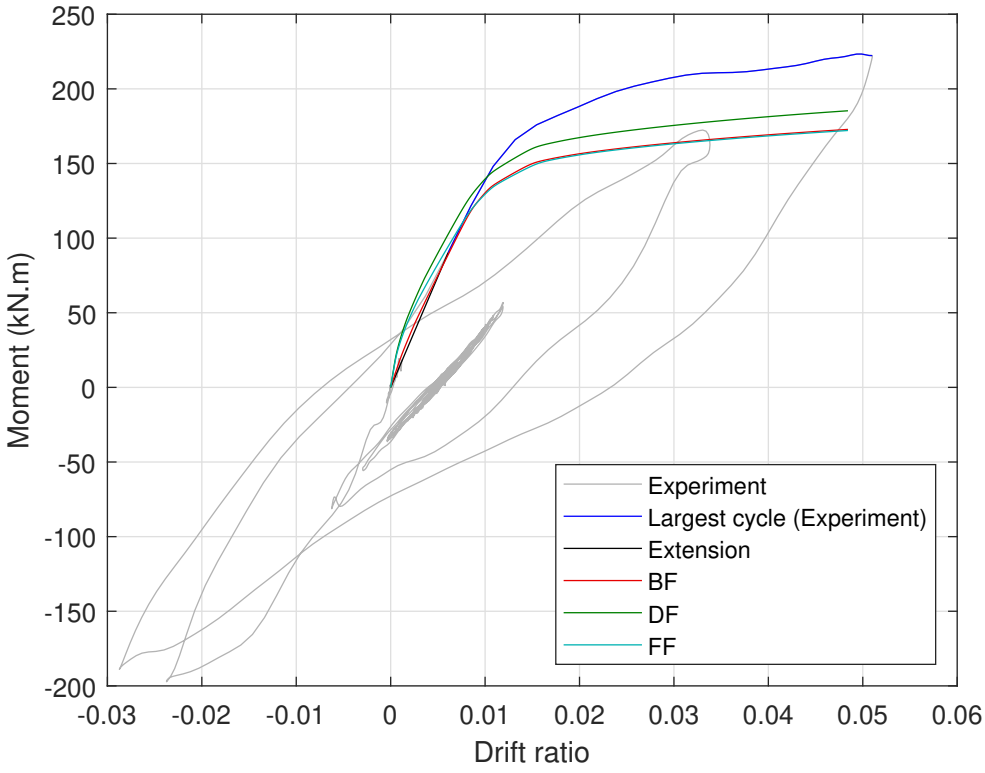

(b)

Figure 4.4 : Pushover results obtained using the fiber section model for the test units: (a) CAMUS3 and (b) A1.

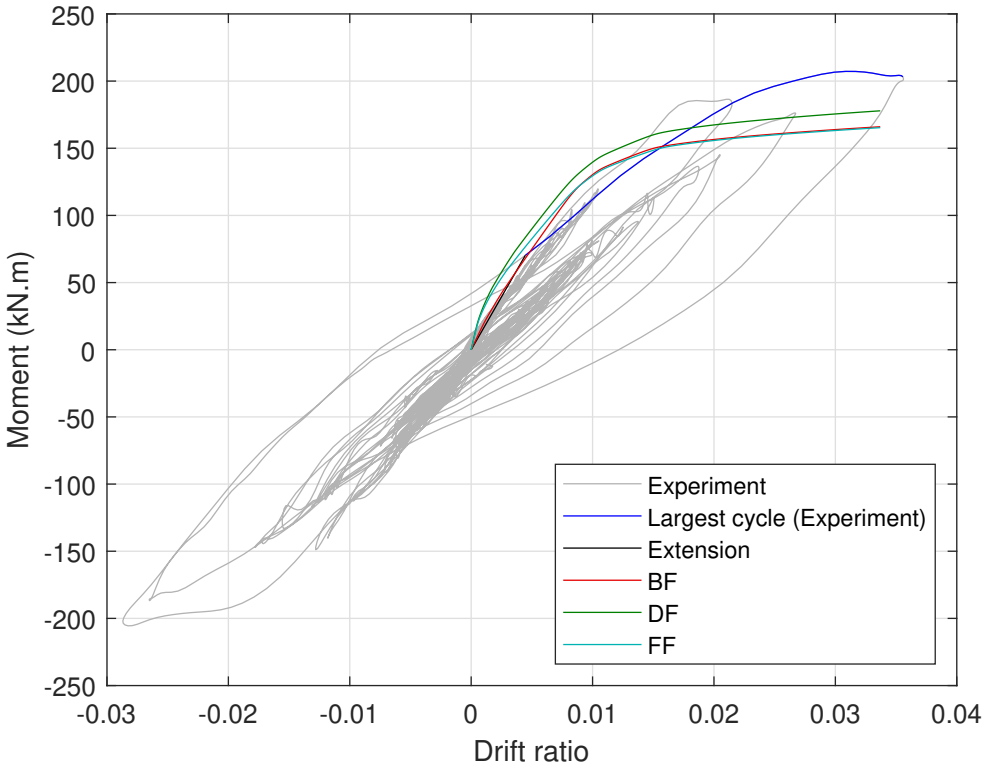

(a)

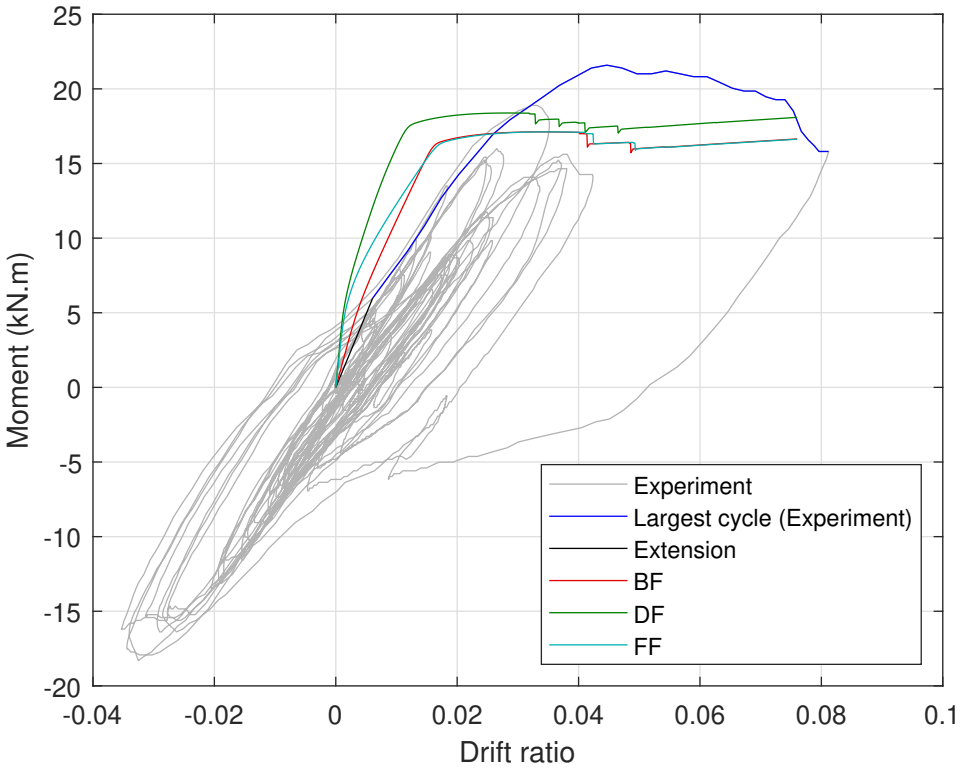

(b)

Figure 4.5 : Pushover results obtained using the fiber section model for the test units: (a) B1 and (b) EBII07.

here. Therefore, it is not possible to directly observe the uncracked stiffness in the case of "Experiment". Still however, all units yield for the first time in the considered set of tests. Therefore, they attain their effective stiffness.

It is also apparent that the simulated initial stiffness is sensitive to the utilized element formulation (**Figures 4.1-4.5**). This is expected since the locations of integration sections and the simulated curvature profiles are different for each modeling approach. For BF model, it was found that this model behaves with lower stiffness than other models below yielding moment. This is due to fact that cracked stiffness was assumed in the elastic segment of the beam with hinges model. In this model, a flexural stiffness needs to be assumed for the middle segment that is expected to remain elastic [28].

When the member deforms up to its inelastic capacity this segment is expected to attain an equivalent stiffness, close to cracked flexural sectional stiffness. On the other hand, at small deformations, this segment would be uncracked. In the analysis, cracked section stiffness was assigned to the elastic segment since the response of the unit subjected to design-level excitation is simulated. However, this assumption leads to stiffness at low force levels being underestimated in the first phase of the response. Such an elastic segment is not assumed in the forced-based and displacement-based models. In these models, the same fiber section is considered over the entire element.

From the resulting pushover curves (**Figures 4.1-4.5**), it is possible to observe that simulated moment strength capacity on the average matches well with the actual capacity. Moreover, it is possible to see that FF models tend to exhibit yielding at moments that are slightly lower than that of DF. This is mostly because of differences in the adopted integration schemes, which results in critical integration sections being located at different positions. DB uses *Gauss-Legendre* and FB utilizes *Gauss-Lobatto* integration method with 2 integration points per element, for computing element stiffness matrices. This difference leads to the observed differences in the simulated strength capacities.

Pushover curves obtained by assuming a bilinear idealization of the flexural response of the plastic hinges are presented in **Figure 4.6** for the test units A1 and EBII07. Effectively, these results are applicable both for Takeda and bilinear hysteresis models since they both exhibit the same monotonic behavior. It is seen that when the hysteresis

model is bilinear, the difference between beam-with-hinges model and other models in terms of the initial stiffness vanishes. This proves the impact of assuming cracked stiffness for the elastic segment in beam-with-hinges model. Pushover results obtained using the bilinear flexural model for the other units are not reported since the essence of the results are quite similar to those reported above.

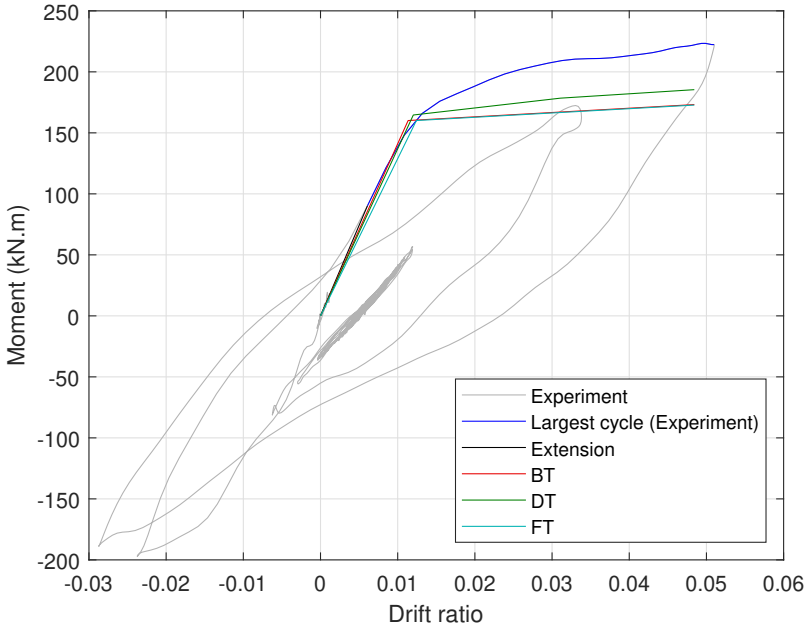

(a)

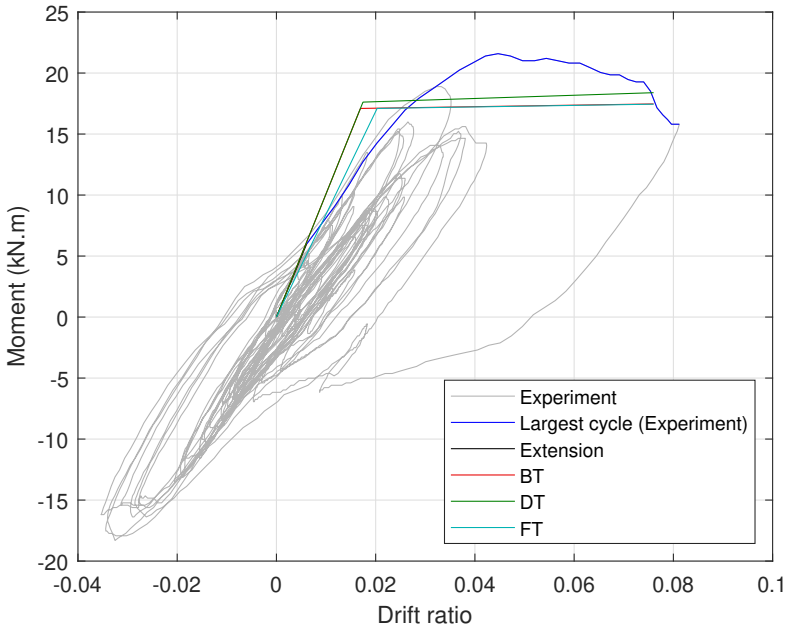

(b)

Figure 4.6 : Comparison of behavior between Takeda models and experiment in a PO simulation for Units: (a) A1 and (b) EBII07.

4.3 Time History Analysis

Set of components considered in this investigation were subjected to multiple excitations with various intensities during the shake table testing. As expected, the energy dissipation behavior and the shaking intensity have a very nonlinear relationship. Levels of hysteresis energy dissipated by the units subjected to excitations below the yield capacity are very low. On the other hand at excitation levels above yield capacity, a sharp increase is exhibited in the dissipated energy. Based on this fact, the accuracy of simulated energy dissipation is investigated at two different excitation levels in this study: (1) Design-level and (2) Low-level. During the design-level excitation, units yield and dissipate significant hysteresis energy while during the low-level excitation they undergo only very limited inelastic response. In the following, the results obtained for these two intensity levels are discusses in separate sections.

For the case of WDH1 unit, identification of a design loading intensity test was not possible. The closest test was *Test 3* during which the unit was subjected to an excitation with an intensity close to 70% of design excitation. Analysis results indicated that the response exhibited during this test could not be considered as representative of the design loading due to above mentioned nonlienear relationship between energy dissipation and shaking intensity. As a result, unit WDH1 was excluded from the design-level excitation analysis and was only considered in low-level excitation.

4.3.1 Design-level excitation

Results of the time history analysis obtained using alternative models indicated that assumed section flexural hysteresis behavior has a strong influence on the simulated energy dissipation behavior. The impact of the assumed finite element formulation was observed to be relatively limited. Therefore, it has been decided to group the results in three groups based on the assumed flexural cyclic behavior model: (1) Bilinear, (2) Takeda and (3) Fiber section.

4.3.1.1 Section hysteresis model

Bilinear

The bilinear model is the simplest nonlinear model and it does not take into consideration the influence of the stiffness degradation under cyclic loading. This is a major limitation in the case of RC members. The hysteresis responses simulated using the bilinear model are presented in **Figures 4.7 to 4.10**.

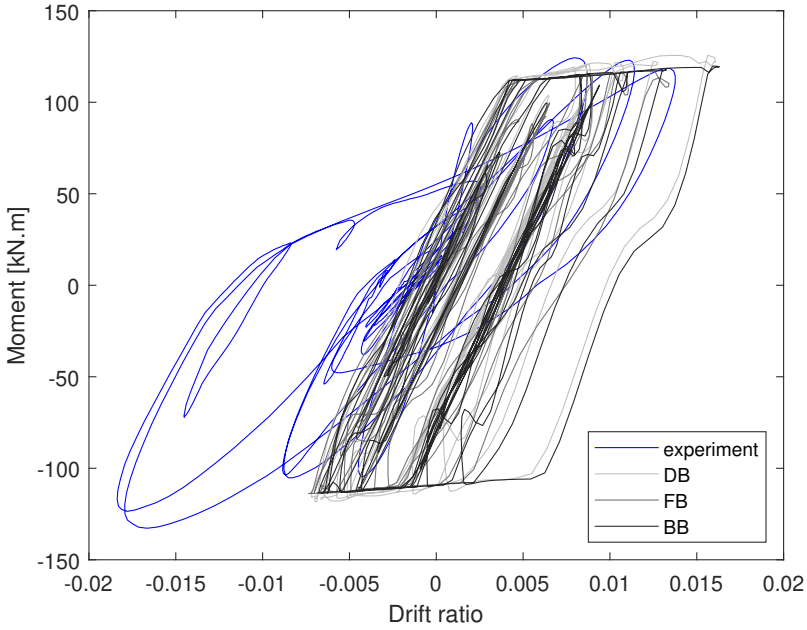

(a)

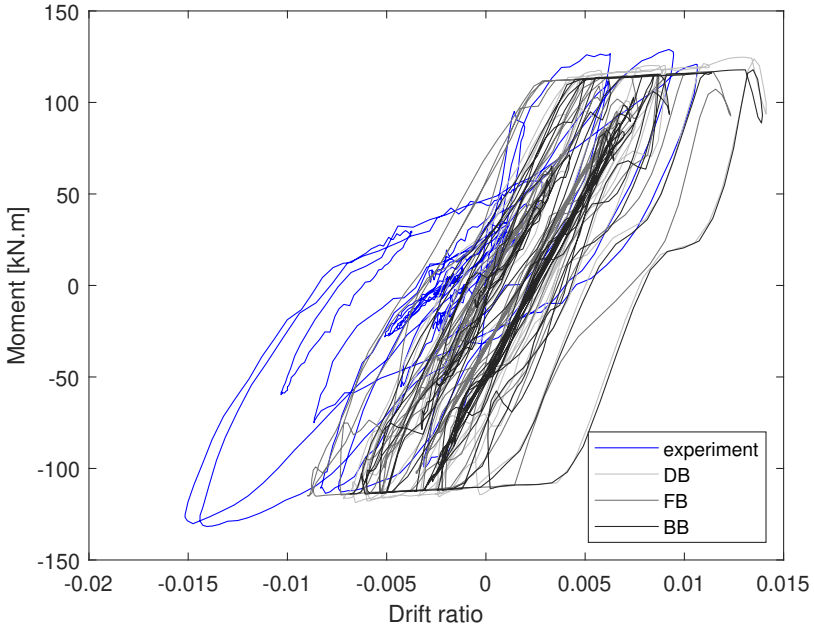

(b)

Figure 4.7 : Comparison of the actual hysteresis behavior and the responses simulated using bilinear models (DB, FB and BB): (a) WDH3 and (b) WDH4.

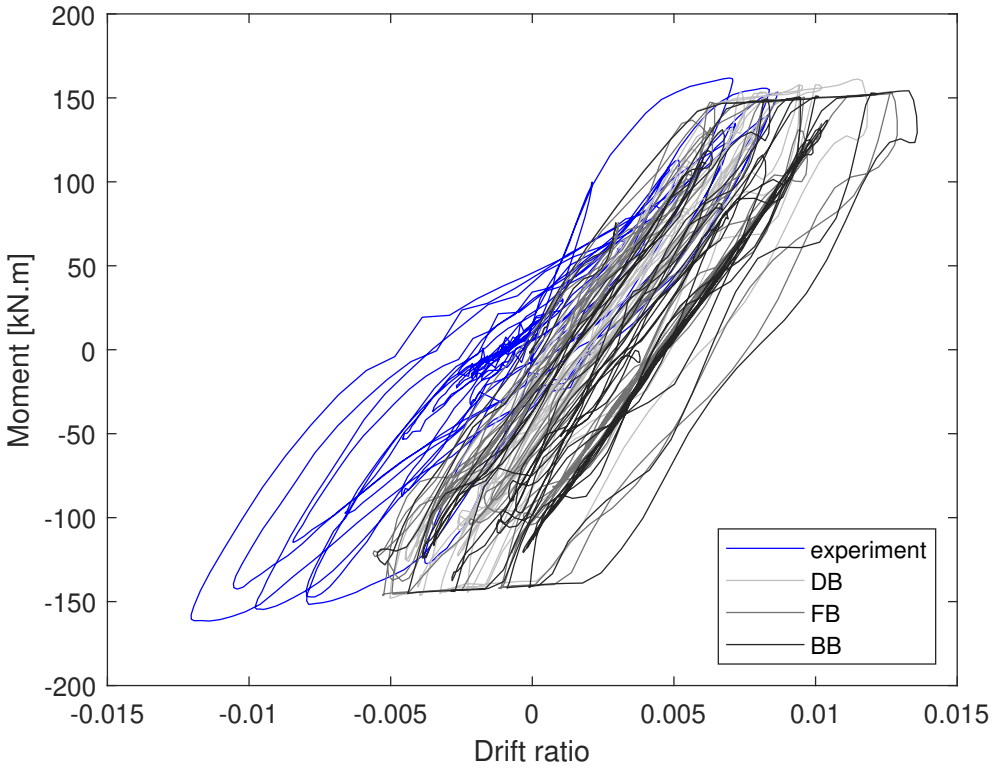

(a)

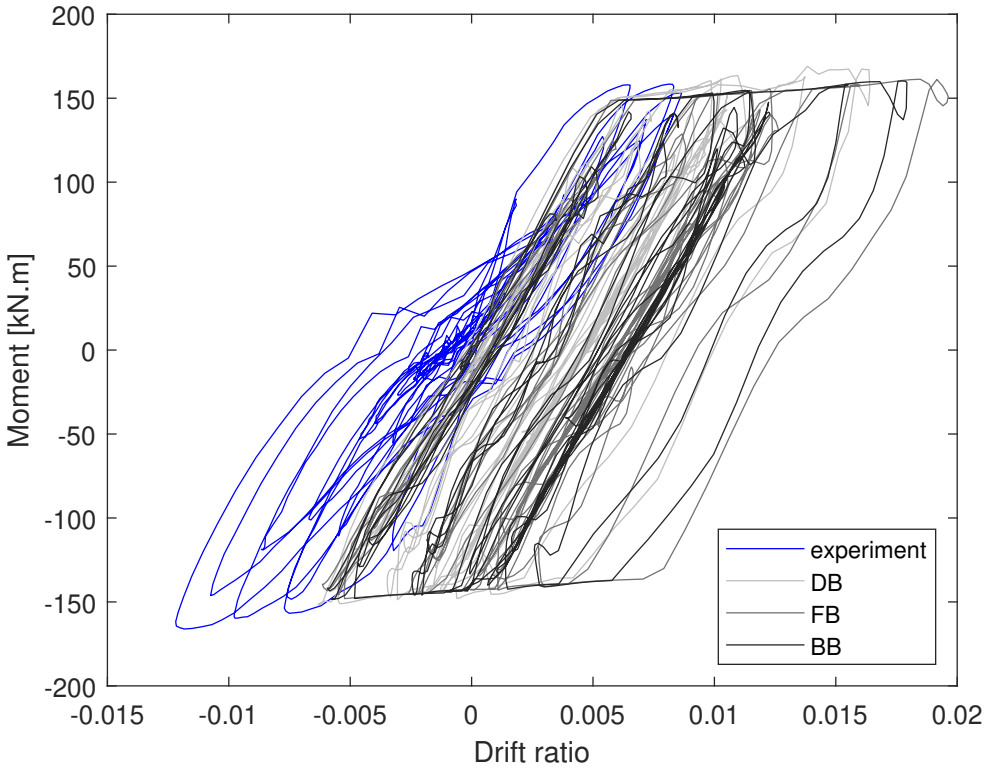

(b)

Figure 4.8 : Comparison of the actual hysteresis behavior and the responses simulated using bilinear models (DB, FB and BB): (a) WDH5 and (b) WDH6.

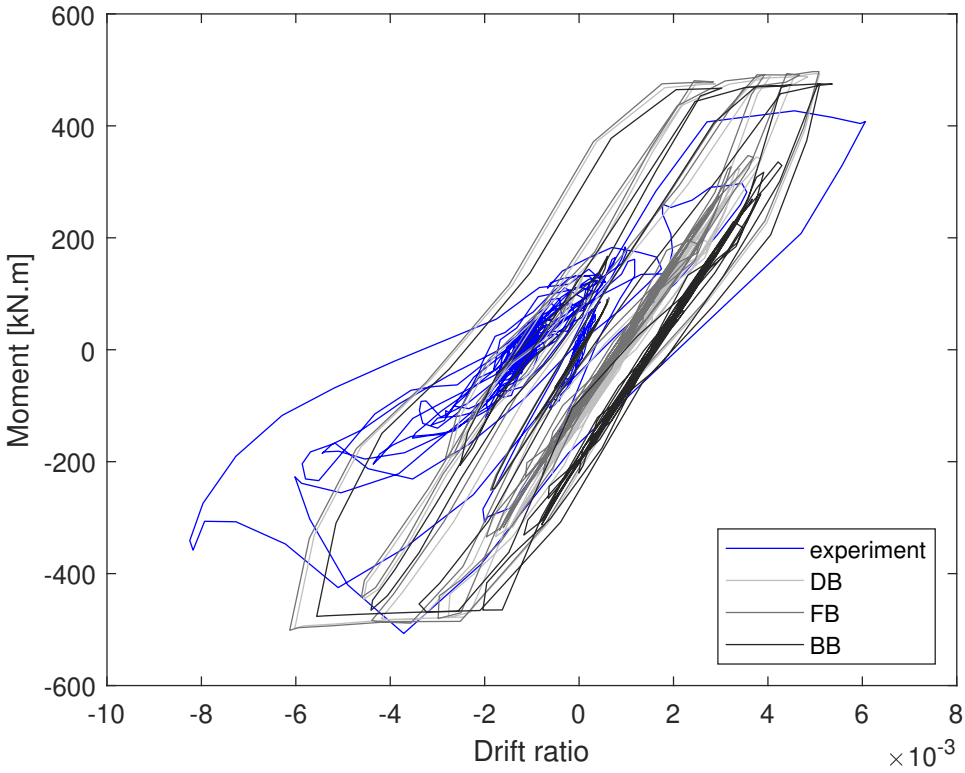

(a)

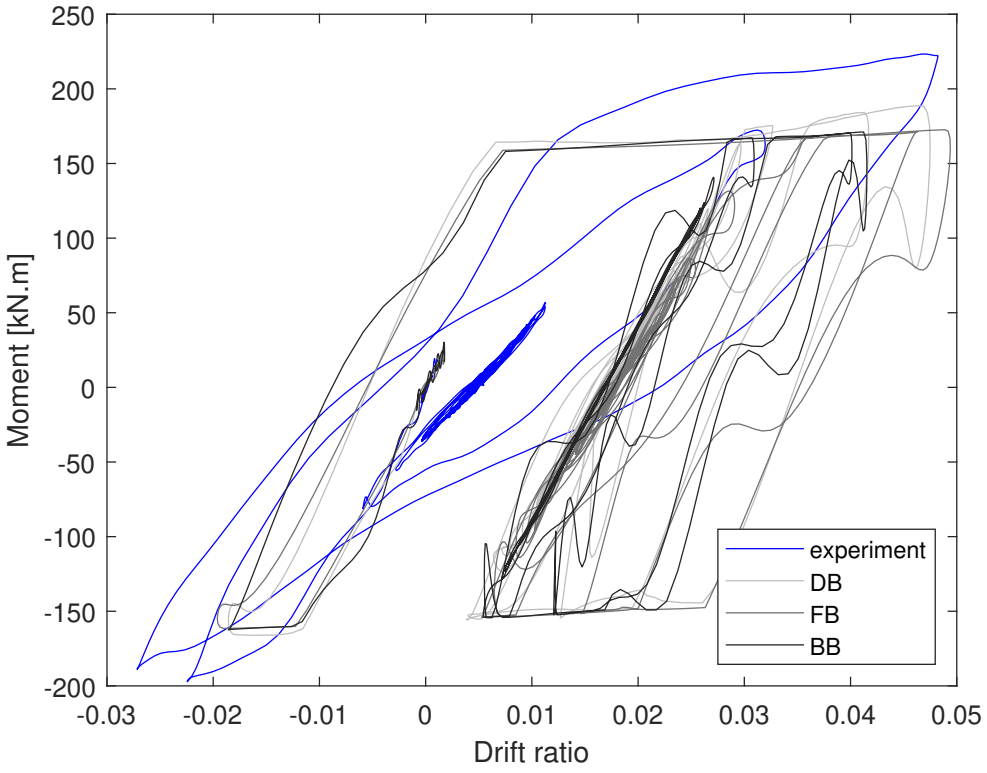

(b)

Figure 4.9 : Comparison of the actual hysteresis behavior and the responses simulated using bilinear models (DB, FB and BB): (a) CAMUS3 and (b) A1.

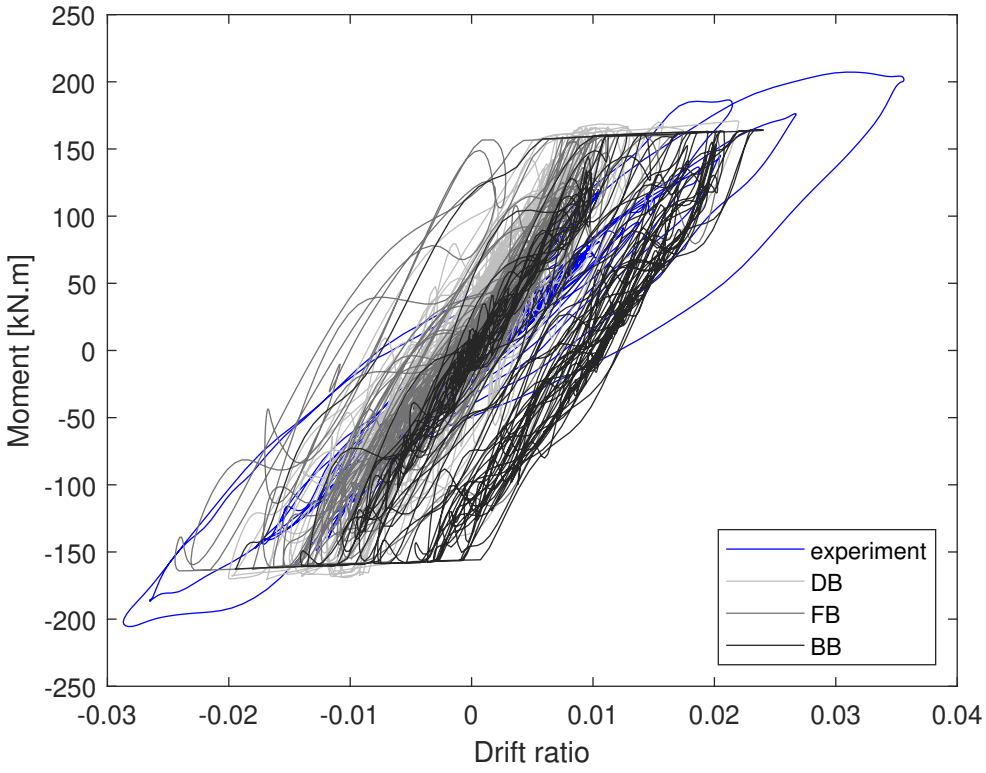

(a)

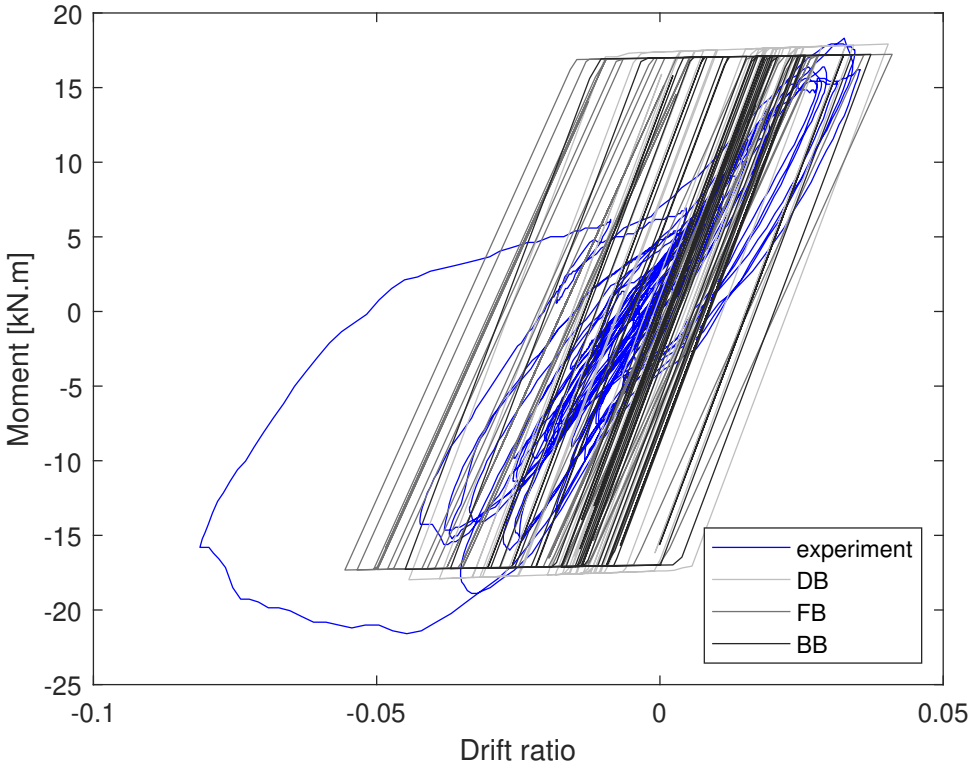

(b)

Figure 4.10 : Comparison of the actual hysteresis behavior and the responses simulated using bilinear models (DB, FB and BB): (a) B1 and (b) EBII07.

It is possible to see that responses simulated using the bilinear models is very different than the actual behavior, as expected. Bilinear model exhibits much smaller peak displacements and misses out a large portion of the area within the actual hysteresis curves cycled by the test units. At the same time, the cycles simulated by the bilinear model are much wider as compared to the actual response. This is a direct result of the stiffness degradation being neglected in the model. Simulated response only shows agreement with the actual behavior in terms of strength capacity.

For each test unit and modeling approach, the dissipated hysteresis energy was evaluated using Equation 3.3. Table 4.1 shows the hysteresis energy dissipation observed during the experiment, E_{exp} and those simulated using the models E_{mod}. It can be seen even though hysteresis plots provided in **Figures 4.7-4.10** indicate a mismatch between the simulation and the actual response, the cumulative energy dissipation estimates are not showing large deviations from the actual values. Particularly for the case of WDH3 the predictions are highly accurate and the largest error (i.e. related to FB model) is less than 2%. On the other hand, the lowest accuracy is observed in the case of WDH5. For this unit, the error in the prediction reaches up to 60% (i.e. DB model). Correction factors, C_E (i.e. defined in Equation 3.5) obtained for each test unit are plotted in **Figure 4.11**.

Table 4.1 : Simulated hysteresis energy dissipation, E_{mod} obtained using DB, FB and BB models and the actual energy dissipation, E_{exp}.

Test	E_{exp} kJ	E_{mod} DB model kJ	E_{mod} FB model kJ	E_{mod} BB model kJ
WDH3	7.12	7.10	6.99	7.15
WDH4	5.72	5.13	5.26	5.20
WDH5	6.29	3.92	4.17	4.03
WDH6	6.36	6.61	6.76	6.67
CAMUS3	7.81	5.88	5.88	6.54
A1	13.95	14.36	14.55	13.20
B1	15.99	17.43	16.07	16.26
EBII07	5.58	4.01	4.35	4.02

In order to assess the impact of finite element formulation, on the accuracy of the simulated energy dissipation, the median, and plus-and-minus standard deviation values of the correction factors, C_E were identified (**Figure 4.12**).

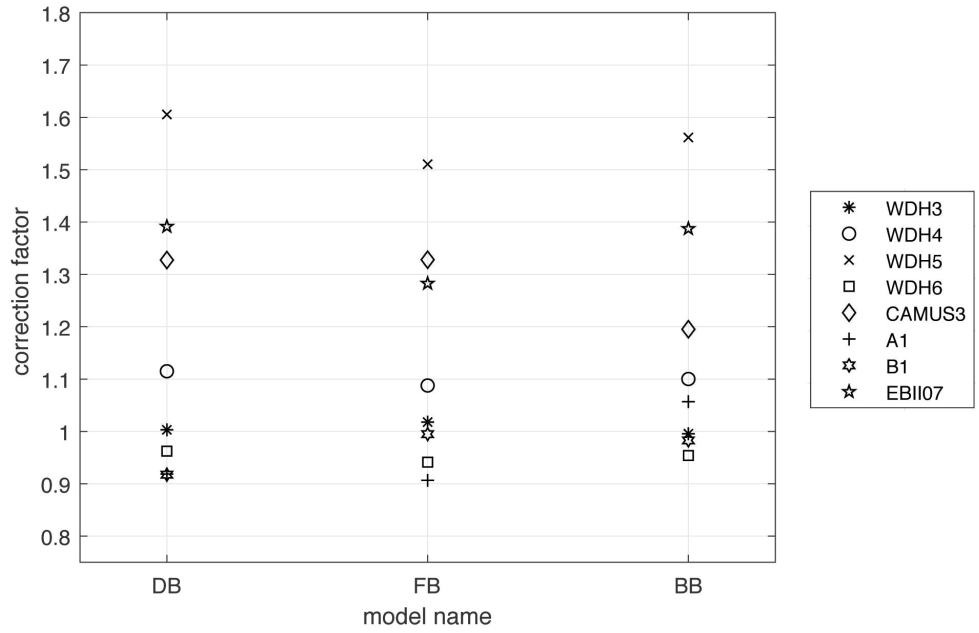

Figure 4.11 : Correction factors, C_E for the energies simulated using bilinear models (DB, FB and BB).

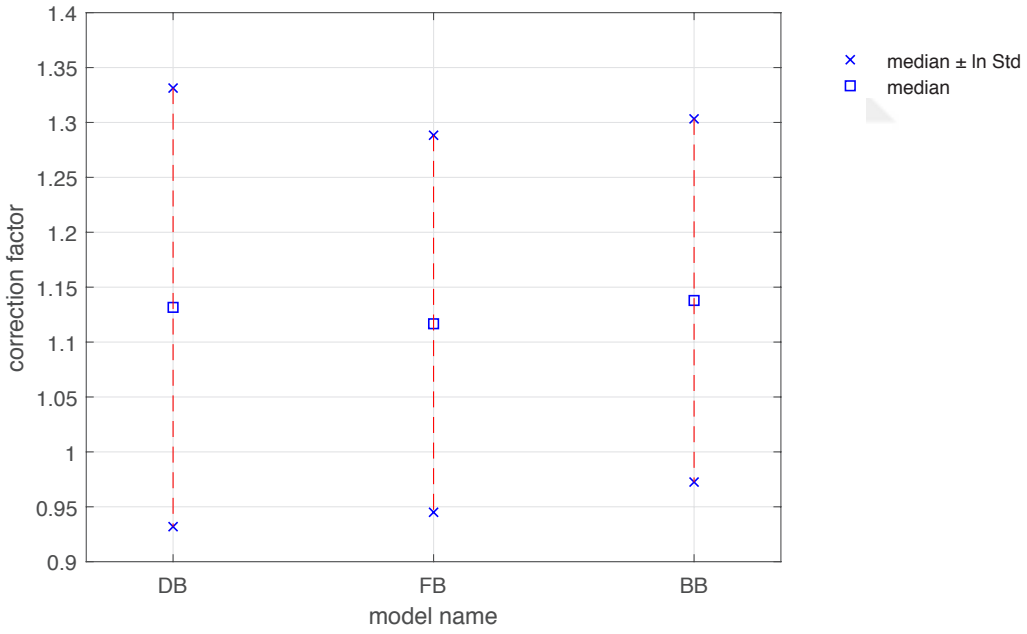

Figure 4.12 : Accuracy and precision of dissipated hysteresis energies simulated using alternative bilinear models (DB, FB and BB).

In order to identify the major factors contributing to the errors in simulated energy dissipation behavior, time variation of the total cumulative dissipation was computed. Resulting plots are provided in **figures from 4.13 to 4.16**

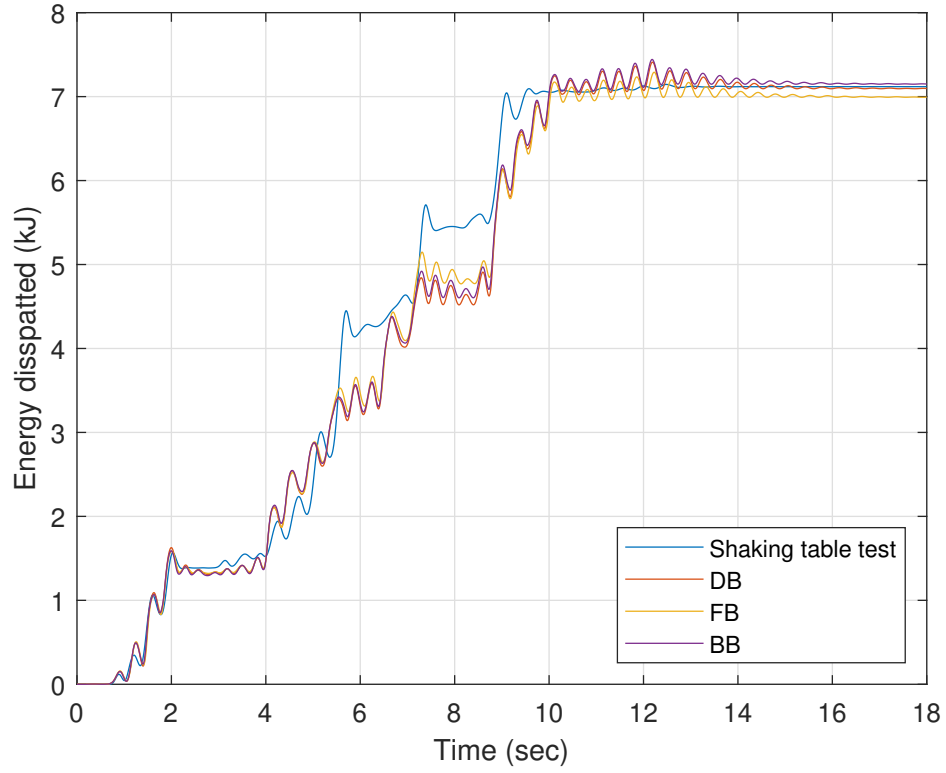

(a)

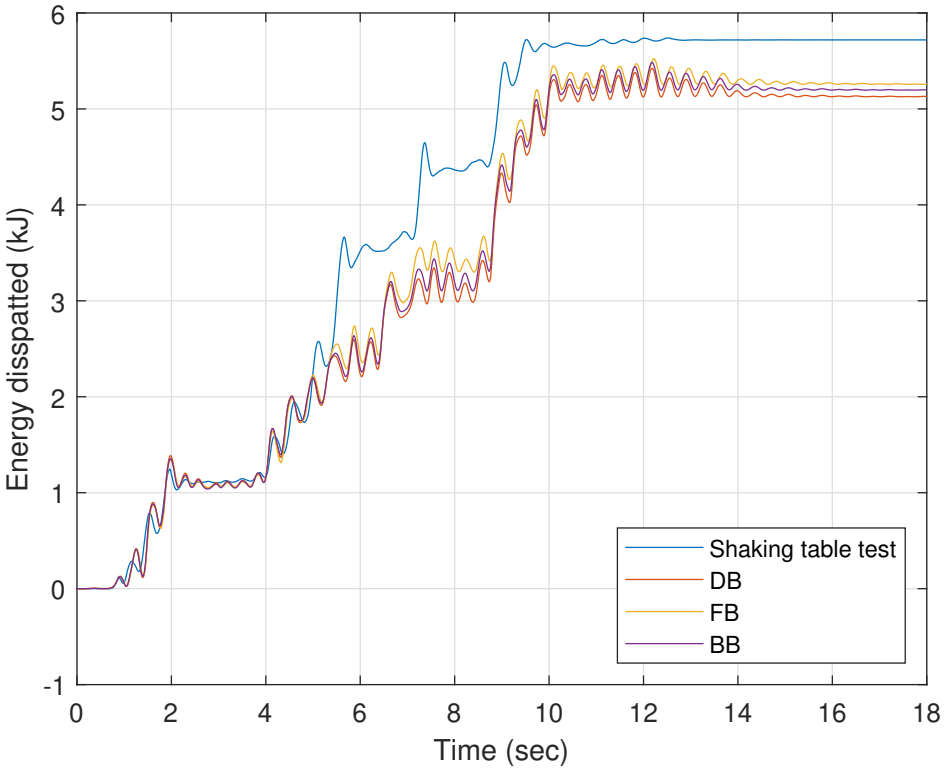

(b)

Figure 4.13 : Comparison of the actual hysteretic energy dissipation and the simulated hysteretic energy using bilinear models (DB, FB and BB): (a) WDH3 and (b) WDH4.

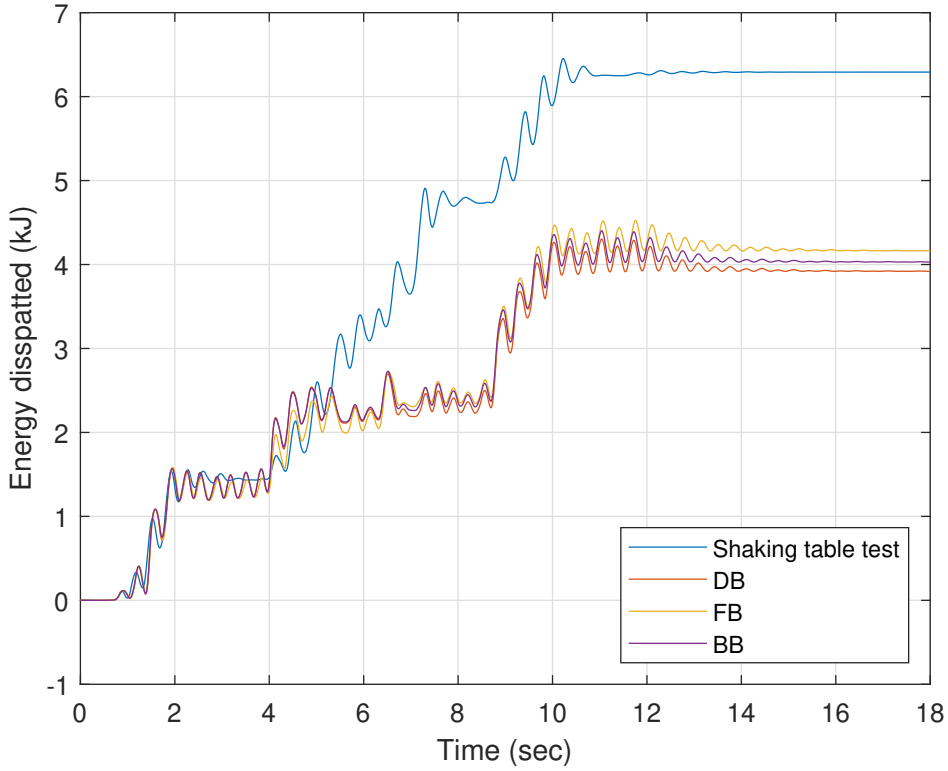

(a)

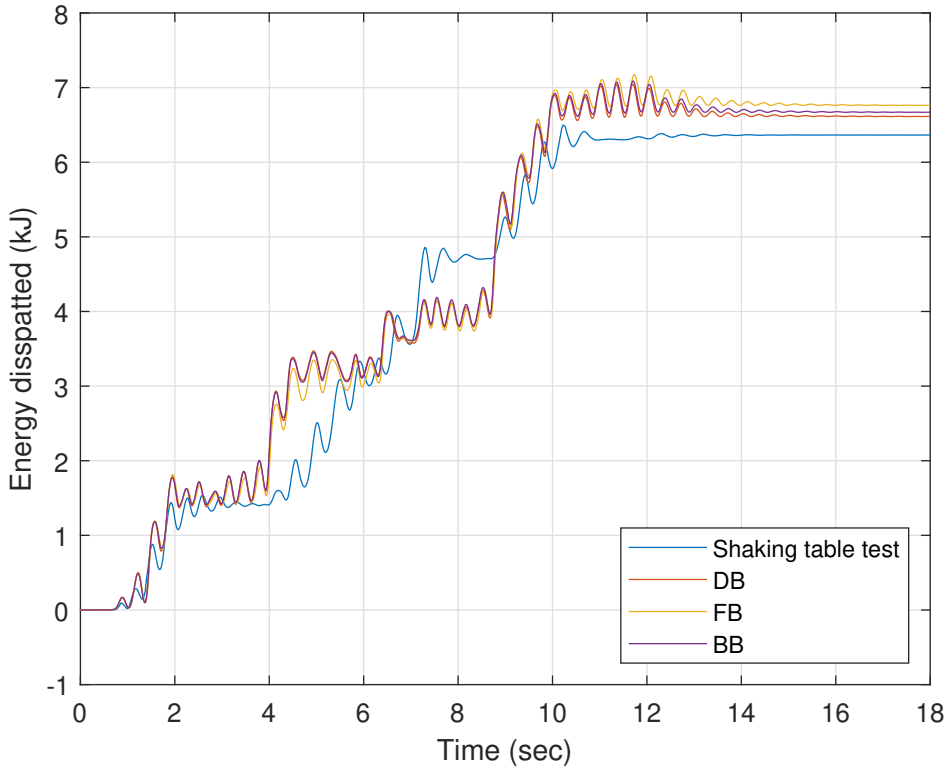

(b)

Figure 4.14 : Comparison of the actual hysteretic energy dissipation and the simulated hysteretic energy using bilinear models (DB, FB and BB): (a) WDH5 and (b) WDH6.

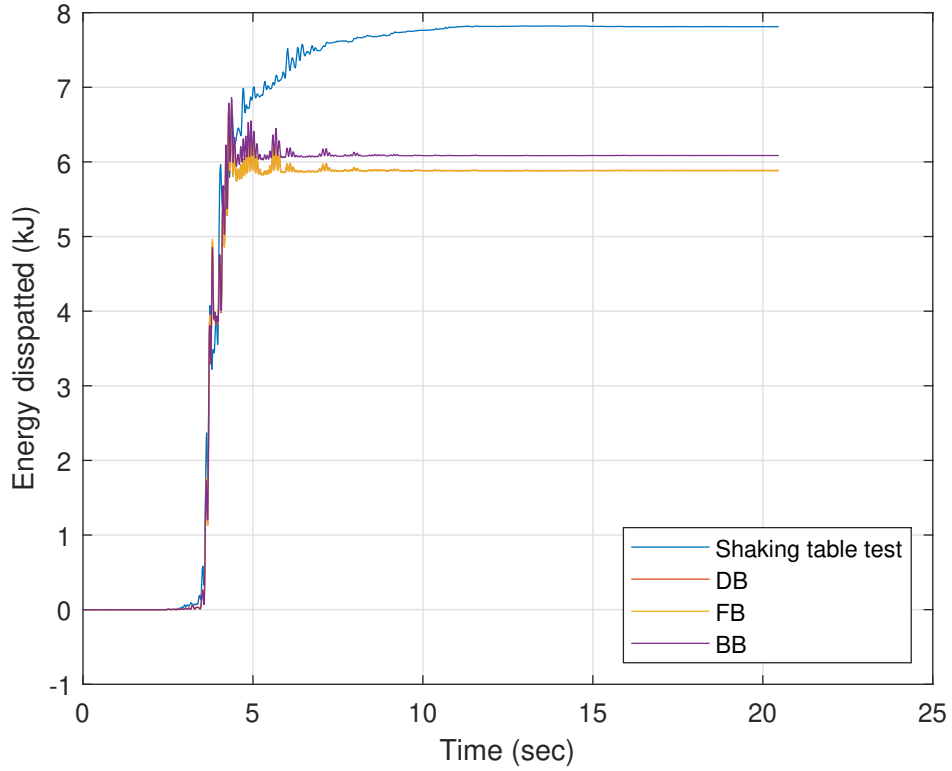

(a)

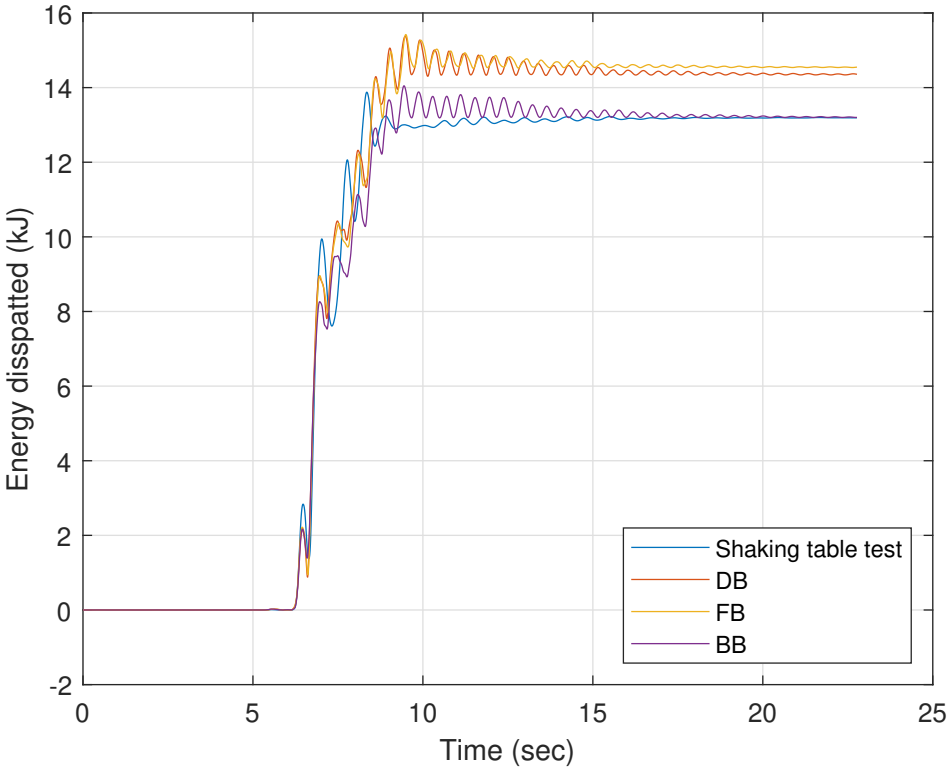

(b)

Figure 4.15 : Comparison of the actual hysteretic energy dissipation and the simulated hysteretic energy using bilinear models (DB, FB and BB): (a) CAMUS3 and (b) A1.

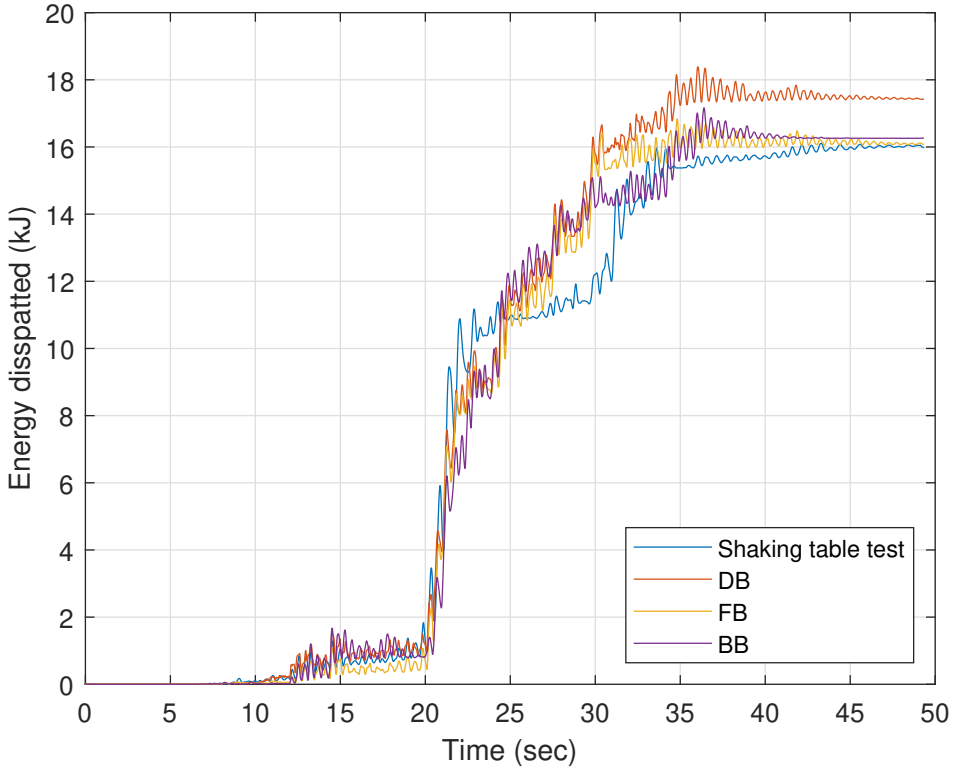

(a)

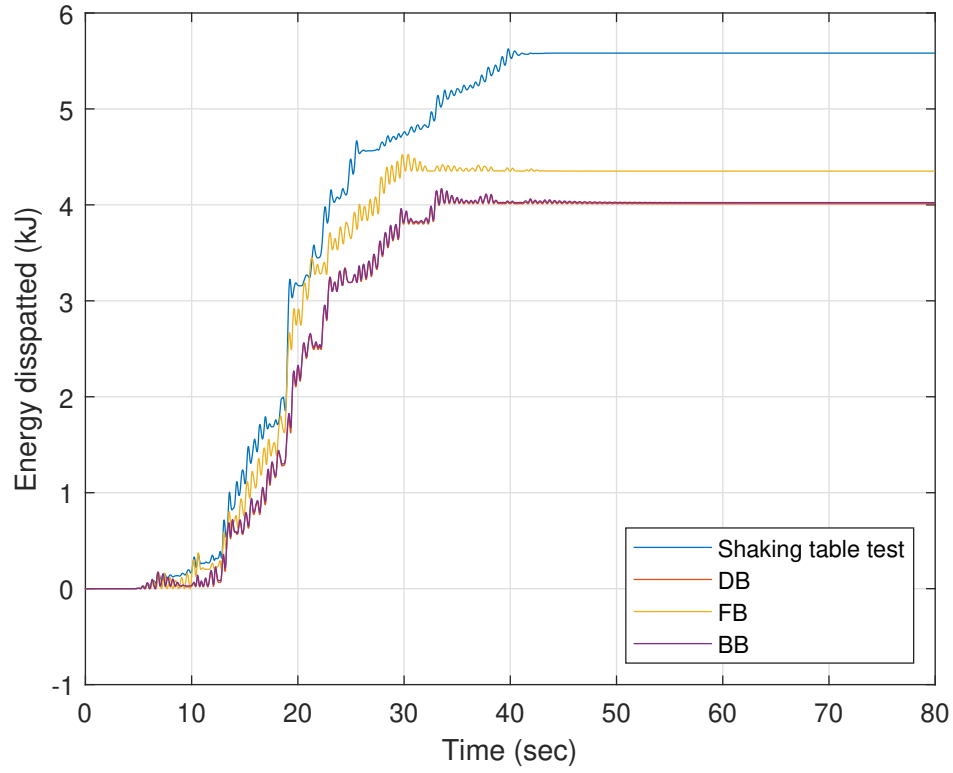

(b)

Figure 4.16 : Comparison of the actual hysteretic energy dissipation and the simulated hysteretic energy using bilinear models (DB, FB and BB): (a) B1 and (b) EBII07.

From those results, it was observed that the major portion of the error occurs when the moment at the base of the component is equal to or just slightly smaller than the yielding moment M_y. Bilinear model does not dissipate any energy in such cycles (i.e. since the yield moment is not exceeded). However, the actual units themselves do not behave that way. They still dissipate some energy even when moment capacity does not reach the yielding moment. This difference is shown in **Figure 4.17** for the case of unit EBII07 between 8 to 11 and between 35 to 40 secondsF. It can be seen that the actual response of the test unit (shown as "exp") exhibits cyclic behavior with relatively thin loops that are repeated over multiple cycles. On the other hand, simulated "model" response simply loads and unloads without any hysteresis energy dissipation. Such differences exhibited in the small cycle responses of the units lead to accumulation of errors in the simulated energy distribution when they are repeated over many cycles.

Based on the fact that Bilinear model does not consider stiffness degradation, it might have been considered to provide very inaccurate hysteresis energy dissipation level. However, the results obtained in this study contradicts such expectations. On the average, the accuracy of the total cumulative energy dissipation obtained using bilinear model was not particularly lower as compared to the other models as presented below. This was due to the fact that fat hysteresis loops simulated by bilinear model during large cycle response is effectively cancelling out the lack of dissipation during small cycle response. In the end, overestimation in large cycle dissipation and underestimation in small cycle dissipation effectively cancels out each other. As a result, simulated energy dissipation -on the average- turns out to provide reasonably accurate estimate of the actual value. Still however, the standard deviation of C_E was observed to be rather high, which makes it accurate but not precise, and that is not the best scenario we are looking for.

Takeda

Takeda model is similar to the bilinear model in the sense that it is based on the same bilinear idealization of the flexural behavior. In this study, this idealization is constructed based on recommendations by Priestley et al. [27]. The main difference between bilinear and Takeda models is in the resulting cyclic behavior. Takeda model takes into consideration the stiffness degradation under cyclic loading. As a result,

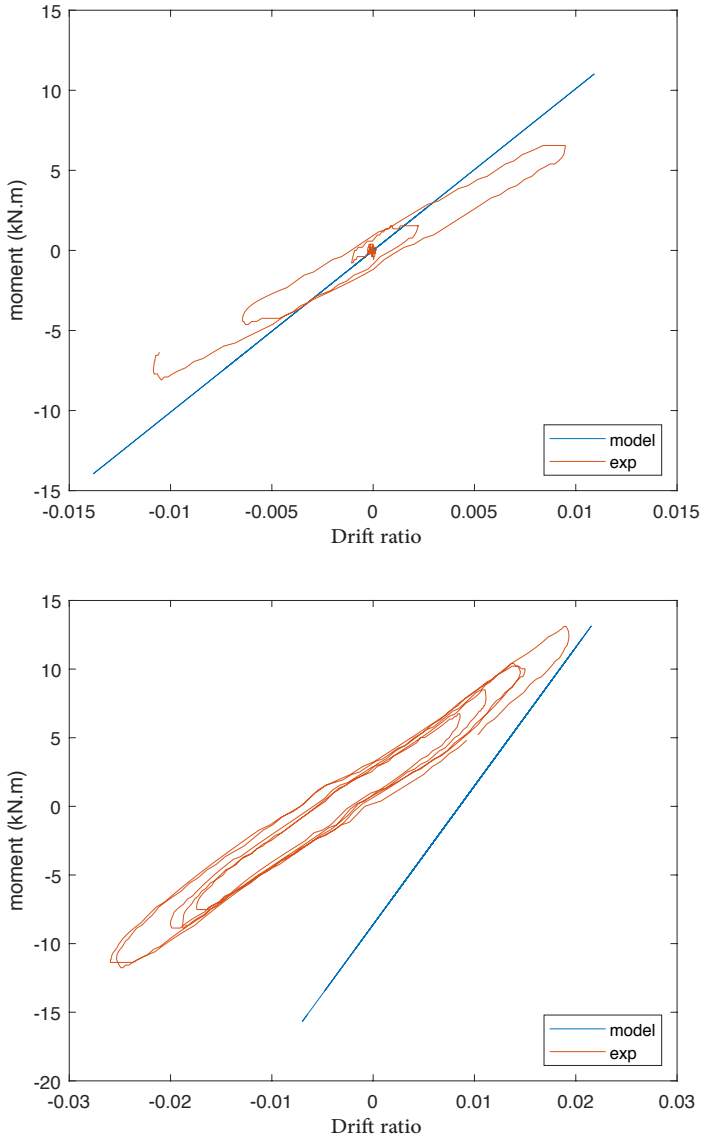

Figure 4.17 : Comparison of the hysteresis behavior of the actual test unit during small vibration cycles and the response simulated using displacement based bilinear model.

comparison of the results obtained using bilinear and Takeda models clearly show the impact of stiffness degradation.

Displacement time histories simulated using the models with Takeda hysteresis: Takeda displacement-based (DT), Takeda forced-based (FT) and Takeda beam-with-hinges (BT) are compared with the experimental time history displacement response in **Figures 4.18-4.21**. It can be seen that simulated displacement time histories show a good match with the actual response.

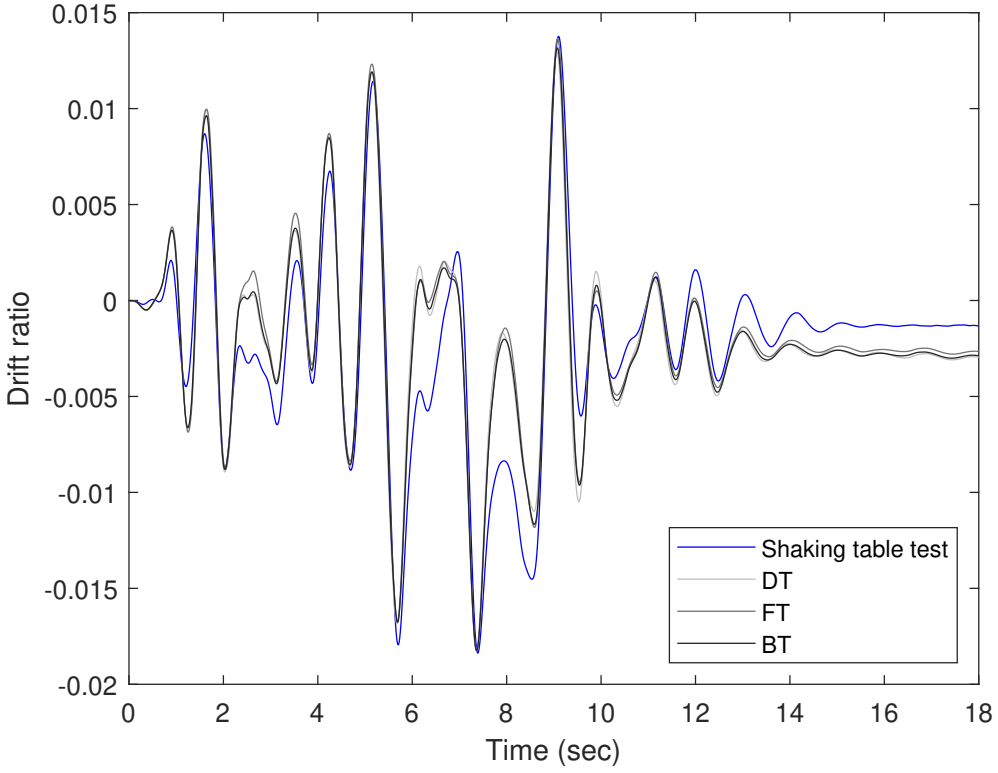

(a)

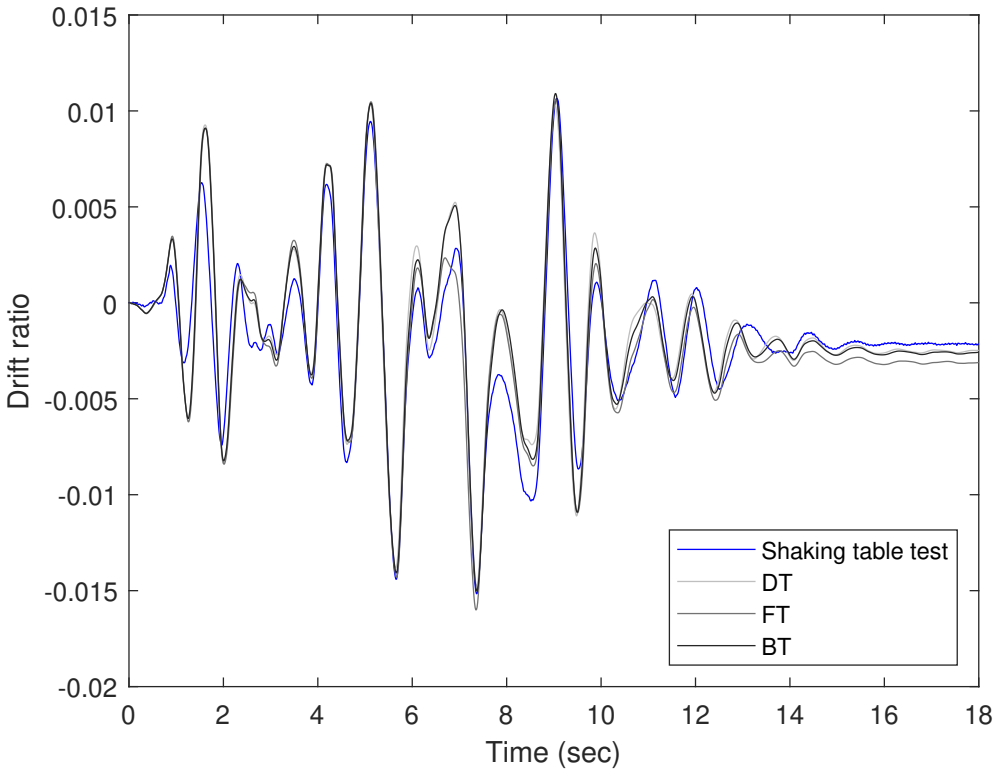

(b)

Figure 4.18 : Comparison of displacement time history simulated using Takeda hysteresis models (DT, FT and BT) and the actual response: (a) WDH3 and (b) WDH4.

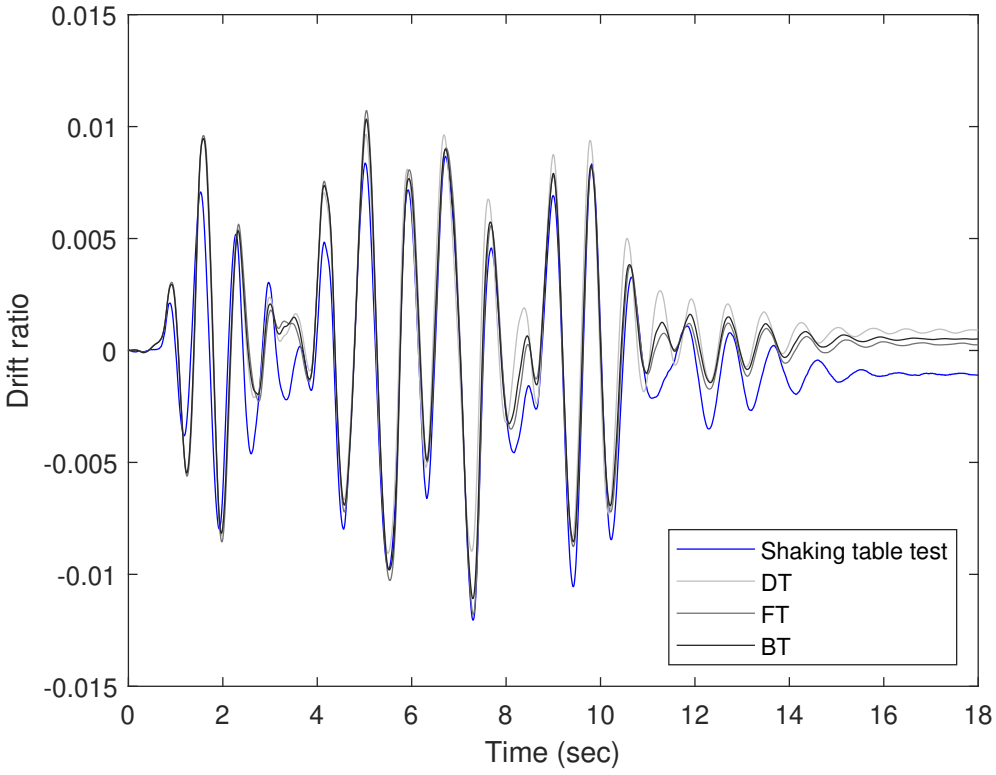

(a)

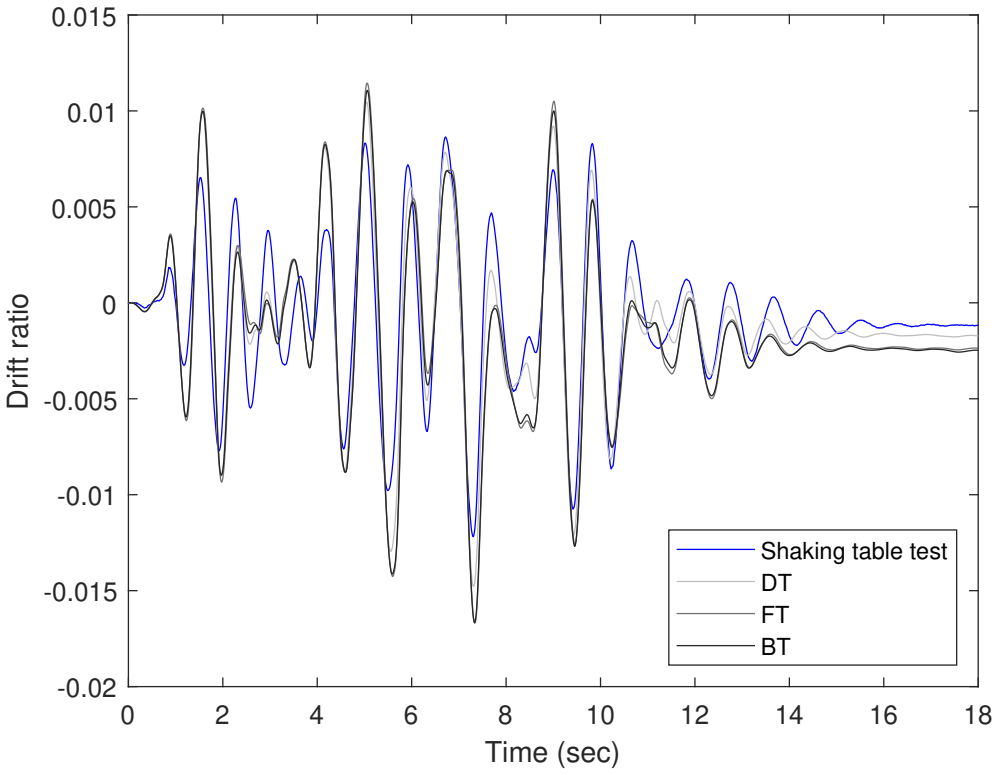

(b)

Figure 4.19 : Comparison of displacement time history simulated using Takeda hysteresis models (DT, FT and BT) and the actual response: (a) WDH5 and (b) WDH6.

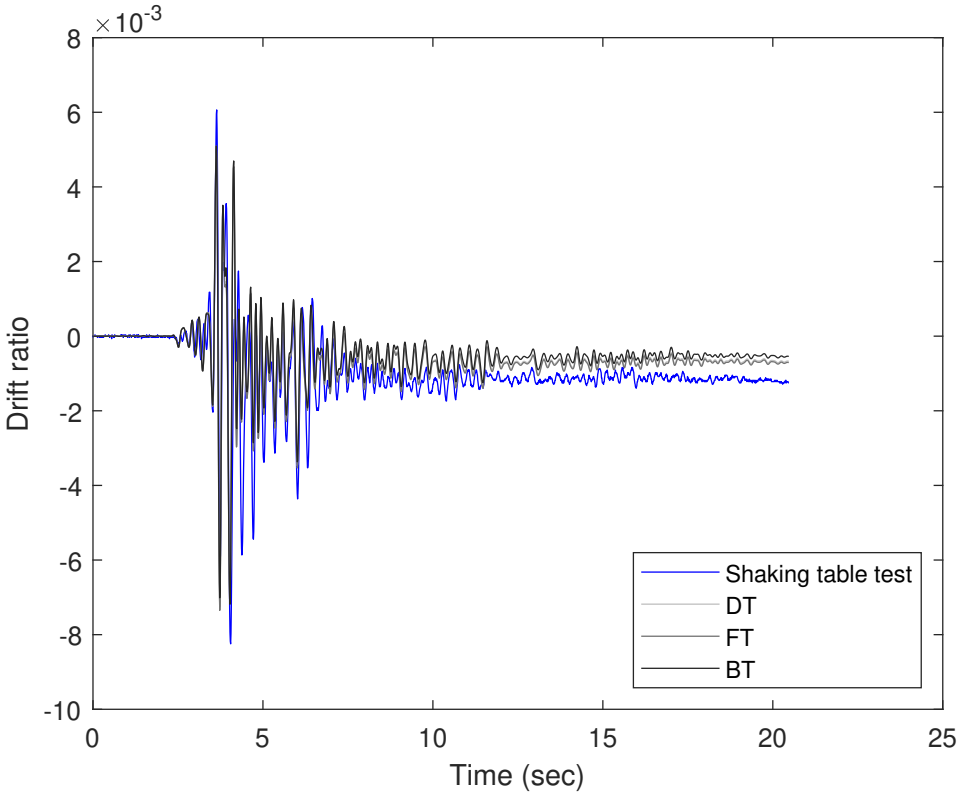

(a)

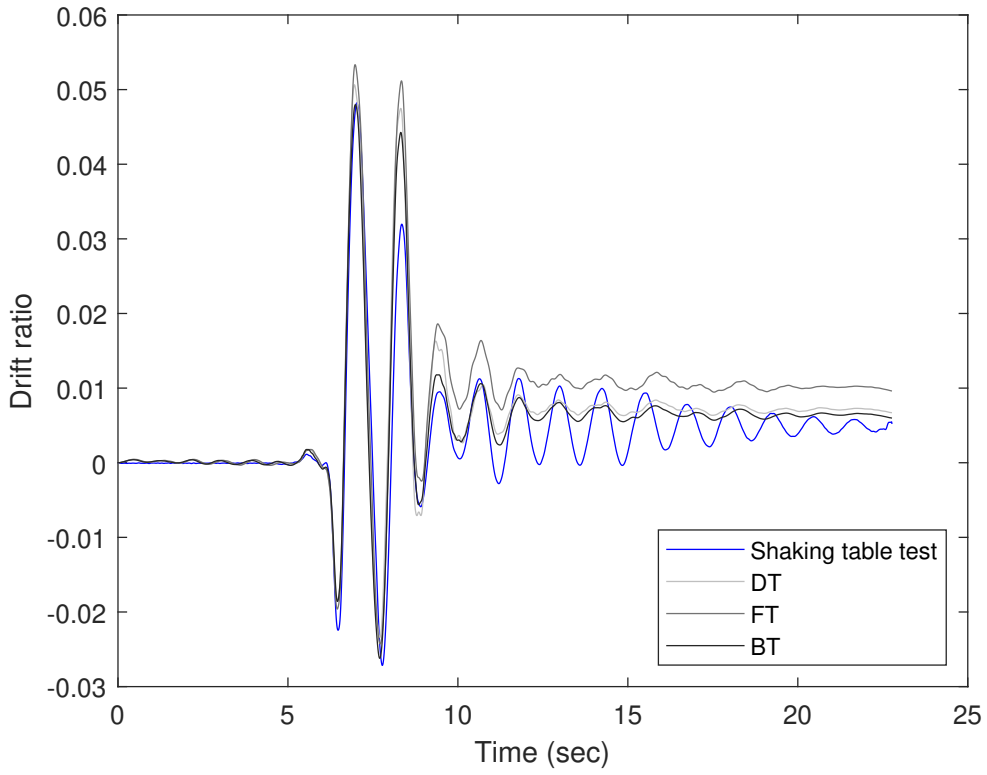

(b)

Figure 4.20 : Comparison of displacement time history simulated using Takeda hysteresis models (DT, FT and BT) and the actual response: (a) CAMUS3 and (b) A1.

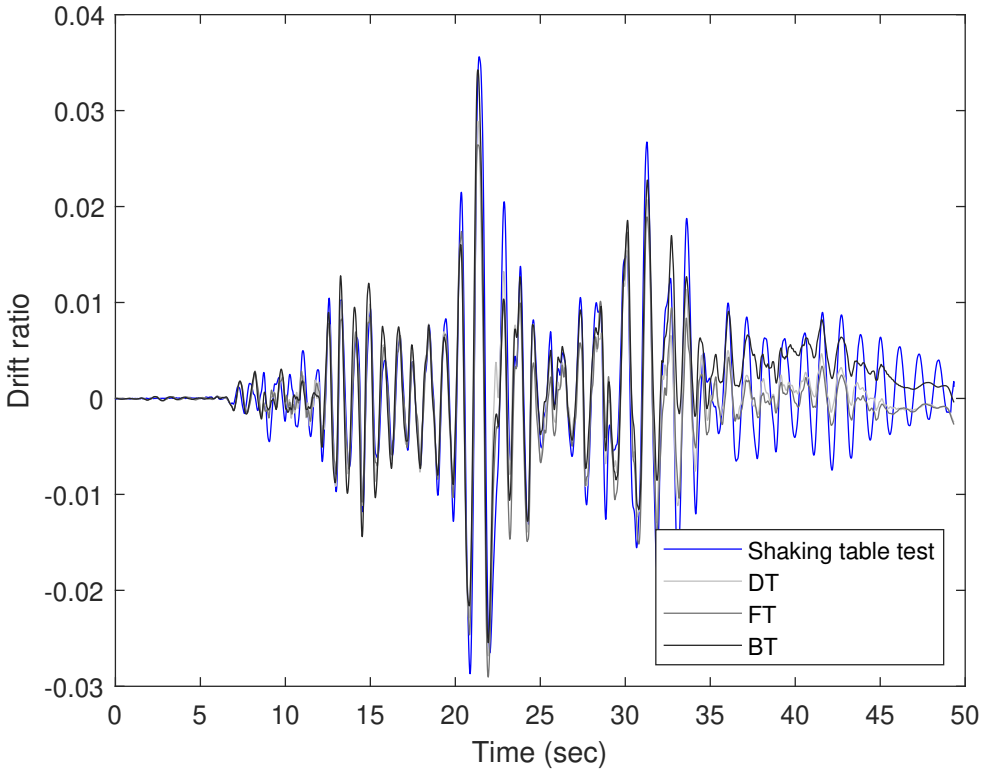

(a)

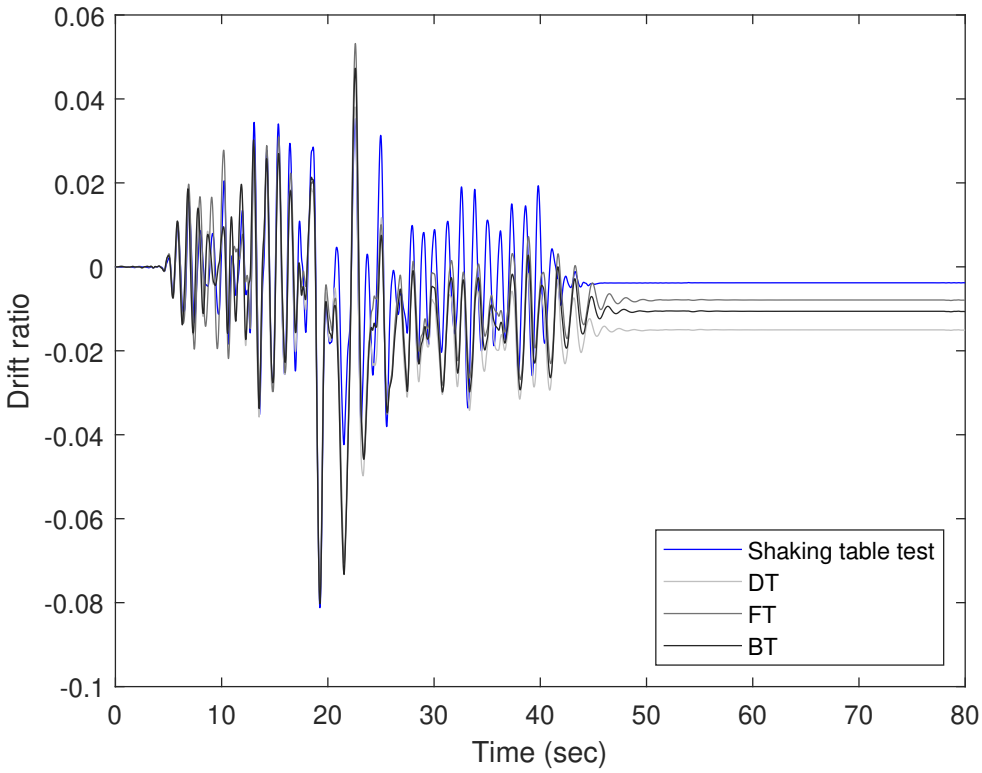

(b)

Figure 4.21 : Comparison of displacement time history simulated using Takeda hysteresis models (DT, FT and BT) and the actual response: (a) B1 and (b) EBII07.

The hysteresis responses simulated using models with Takeda hysteresis are compared against the actual responses observed during shaking table tests are presented in **Figures 4.22-4.25**.

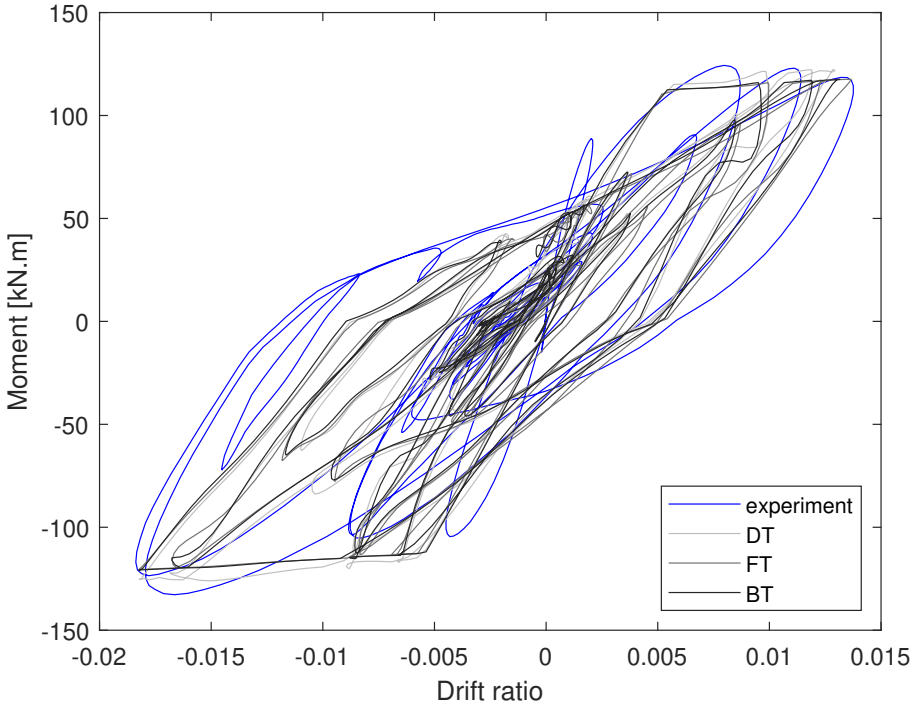

(a)

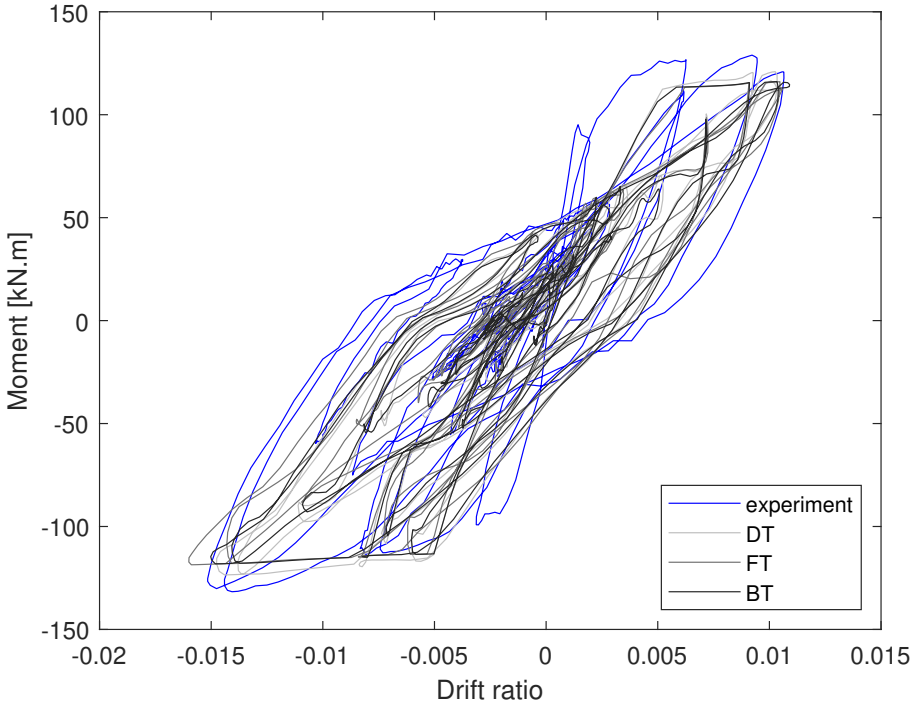

(b)

Figure 4.22 : Comparison of responses simulated using models (DT, FT and BT) with Takeda hysteresis and the actual response: (a) WDH3 and (b) WDH4.

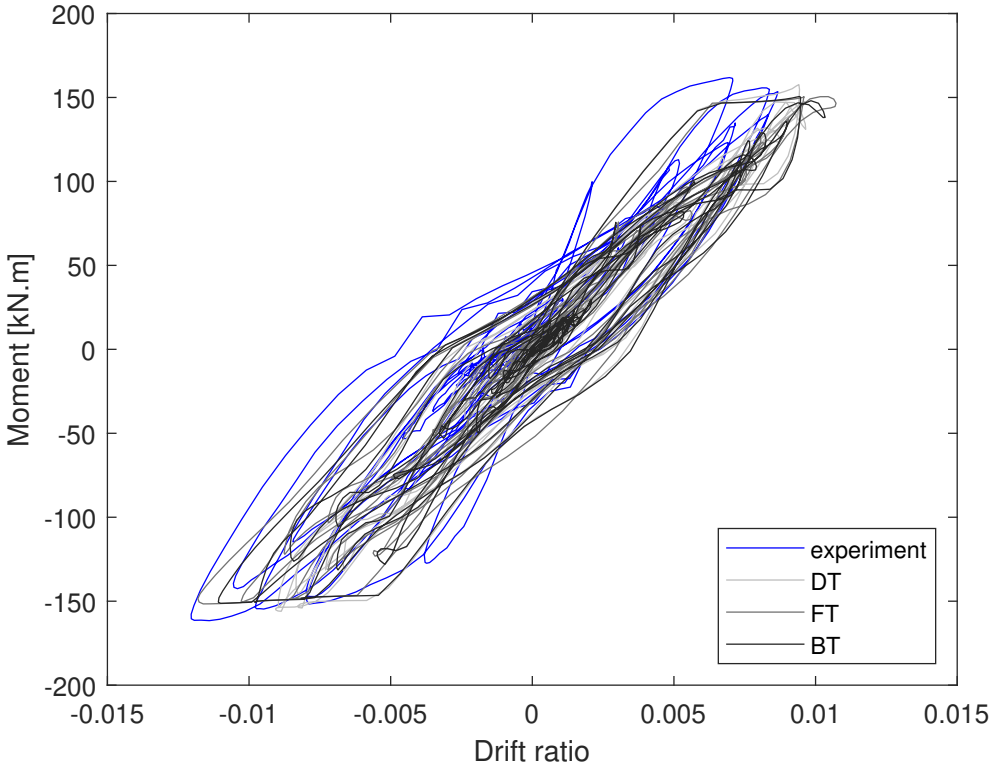

(a)

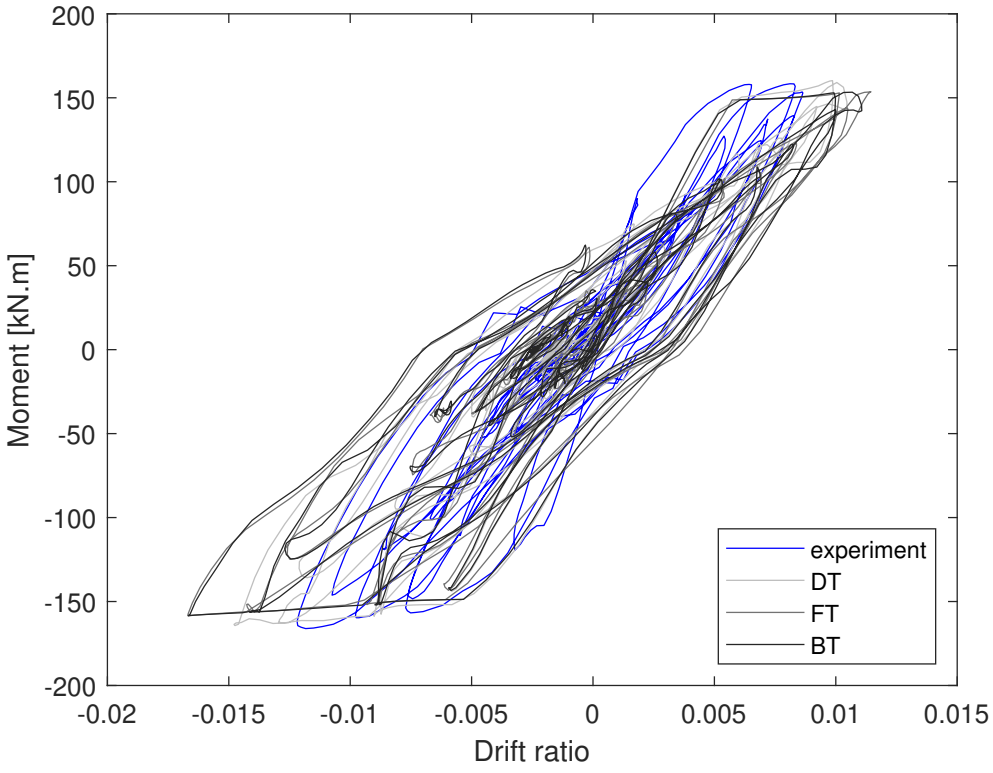

(b)

Figure 4.23 : Comparison of responses simulated using models (DT, FT and BT) with Takeda hysteresis and the actual response: (a) WDH5 and (b) WDH6.

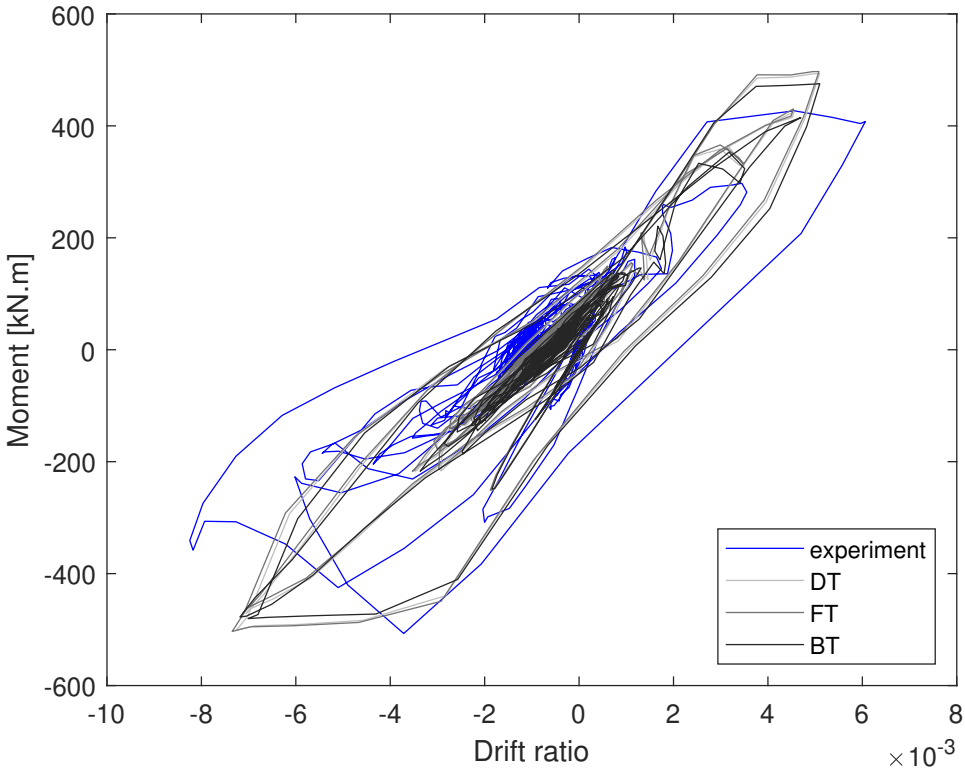

(a)

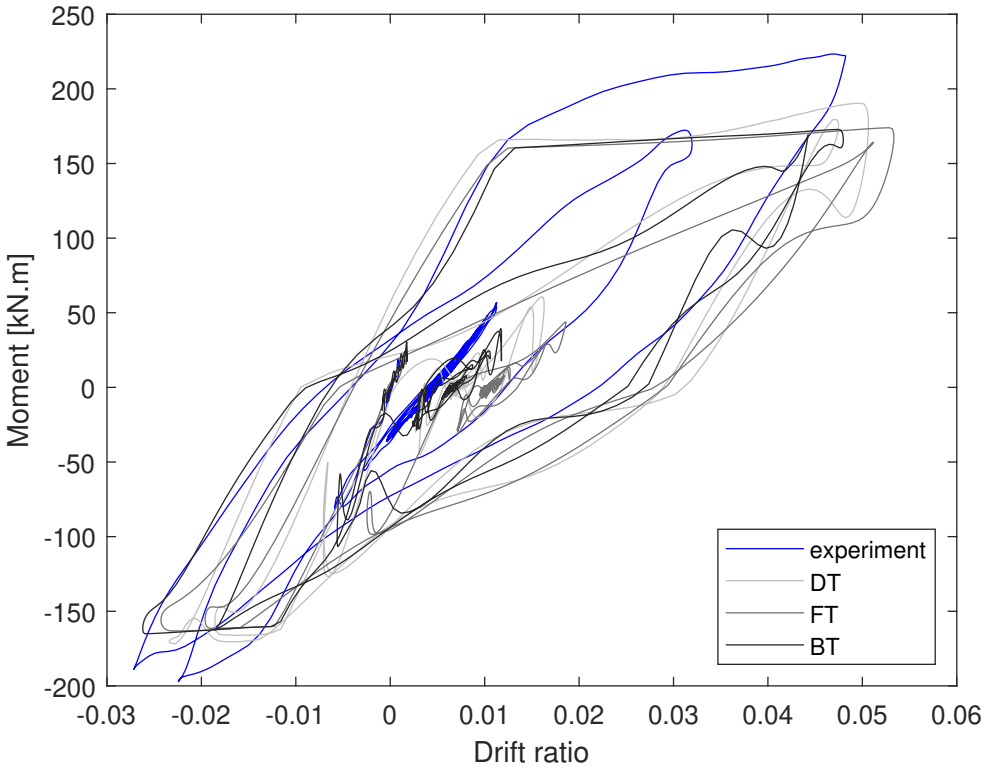

(b)

Figure 4.24 : Comparison of responses simulated using models (DT, FT and BT) with Takeda hysteresis and the actual response: (a) CAMUS3 and (b) A1.

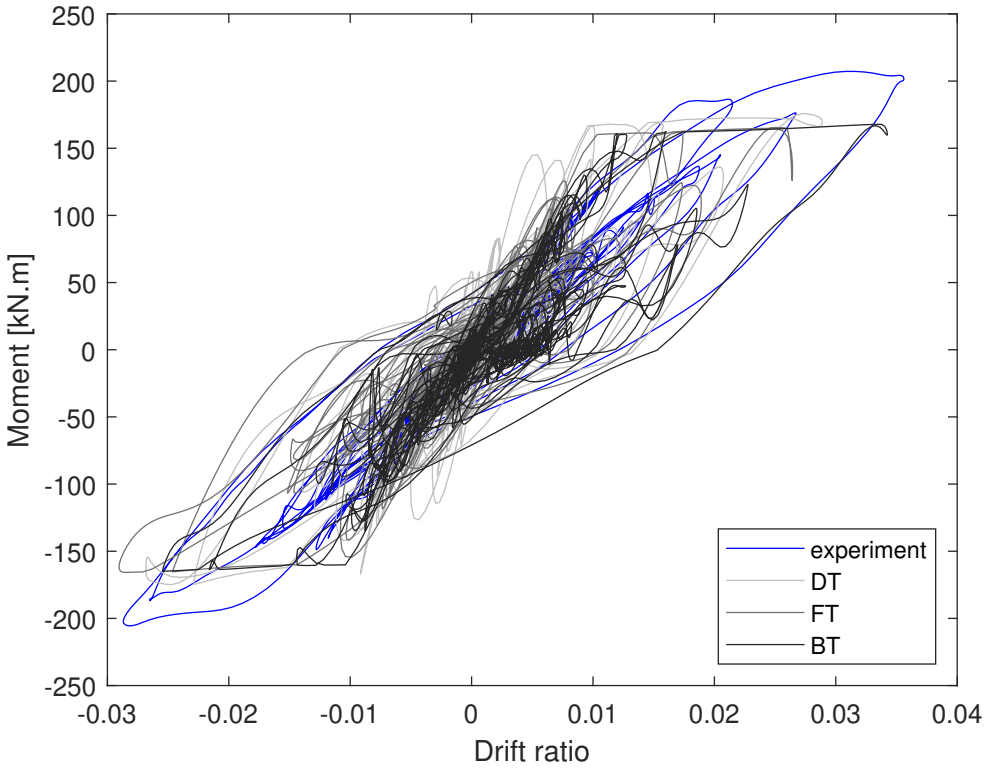

(a)

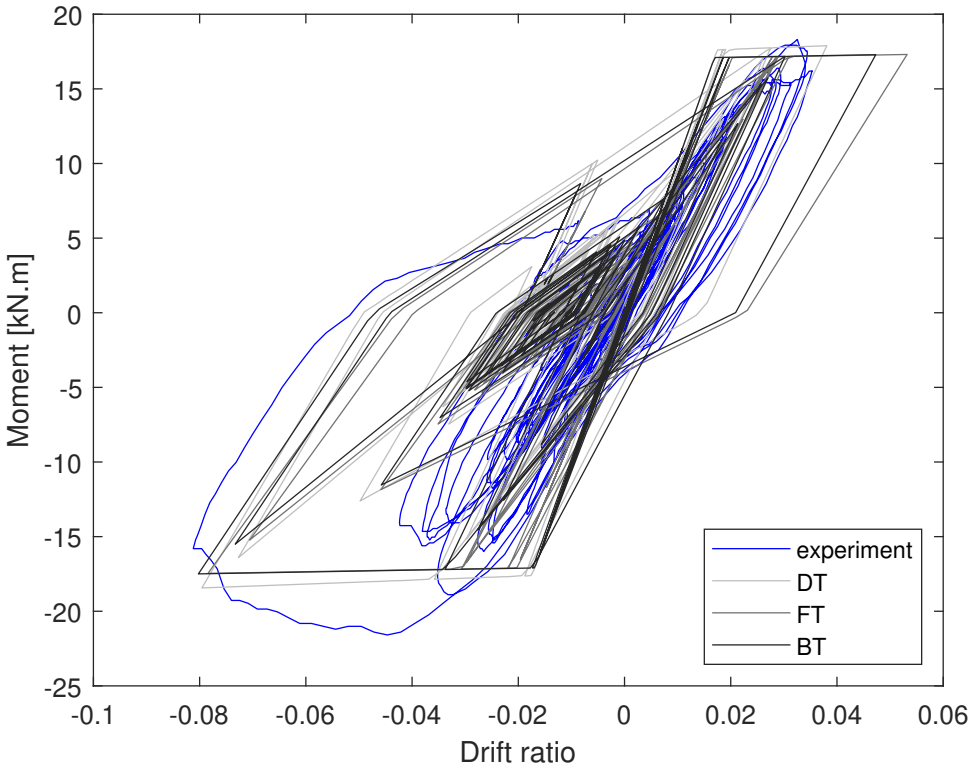

(b)

Figure 4.25 : Comparison of responses simulated using models (DT, FT and BT) with Takeda hysteresis and the actual response: (a) B1 and (b) EBII07.

It can be seen that, the simulated responses show a good agreement with the actual response. Shapes and sizes of the simulated cycles on the whole fit well to the actual response. It is seen that accounting for the stiffness degradation behavior leads to a significant improvement in the performance of the model to capture the actual behavior.

Hysteresis energy dissipation, E_{mod} levels simulated using DT, FT and BT modes and the actual dissipated energies, E_{exp} are listed in Table 4.2. Again and after comparing between the three element formulations, it was found that the type of element formulation model does not have a significant impact on the predicted hysteresis energy dissipation. In general, it is seen that the simulation results are in good agreement with the actual energy dissipation.

Table 4.2 : Simulated hysteresis energy dissipation, E_{mod} obtained using DT, FT and BT models and the actual energy dissipation, E_{exp}.

Test	E_{exp} kJ	E_{mod} DT model kJ	E_{mod} FT model kJ	E_{mod} BT model kJ
WDH3	7.12	5.98	5.71	5.80
WDH4	5.72	4.90	4.56	4.79
WDH5	6.29	4.94	4.88	4.96
WDH6	6.36	6.85	6.93	6.96
CAMUS3	7.81	5.64	5.60	5.75
A1	13.95	15.54	14.50	14.19
B1	15.99	14.20	13.40	14.47
EBII07	5.58	4.07	3.54	3.84

Similar to the investigation undertaken for the bilinear model, correction factor C_E were evaluated for each model and test unit. The results C_Es are plotted in **Figure 4.26**. Even though the errors associated with alternative element formulations are very similar, the results obtained using DT and BT models were observed to be slightly more accurate than those for FT model. However, this difference is very insignificant. It is seen the underestimation that was exhibited for WDH5 for the case of bilinear hystersis model is not exhibited when Takeda hysteresis is utilized. For the Takeda model, response of unit EBII07 seems to be underestimated the most. On the other hand, best accuracy was obtained in the case of WDH6. This is a bit surprising when looking at the moment drift hystersis plot of WDH6 which does not a better agreement between simulation and the test, compared to other units. In general, it is seen that even though the fitting of the hystersis curve plots are much better in the case of Takeda

hysteresis the errors associated with the resulting cumulative energy dissipation levels is not particularly low.

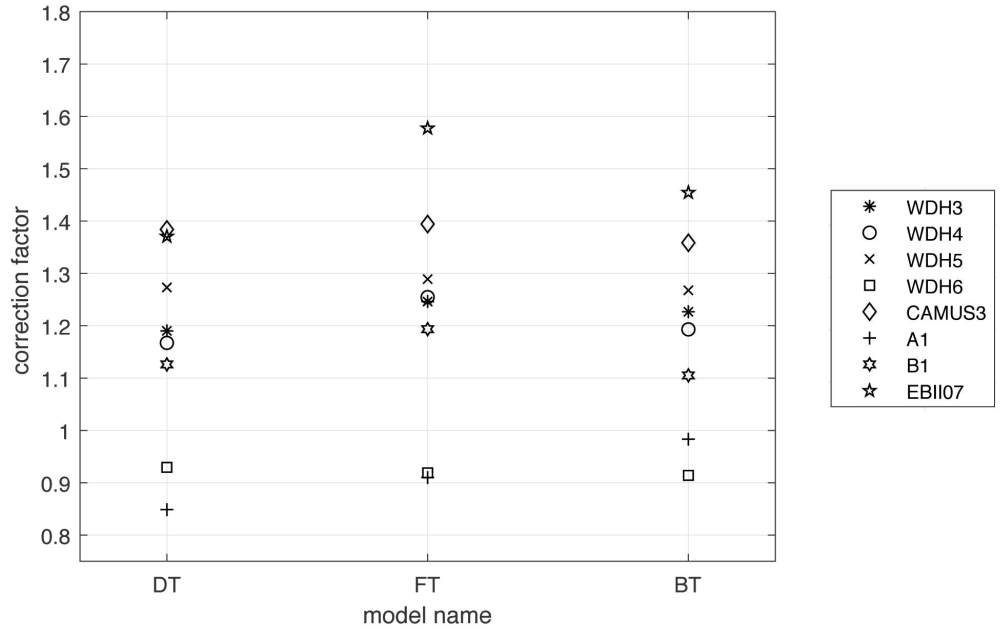

Figure 4.26 : Correction factors, C_E for the energies simulated using Takeda models: DT, FT and BT.

Figure 4.27 shows the median, standard deviation range for the correction factors associated with the models: DT, FT and BT.

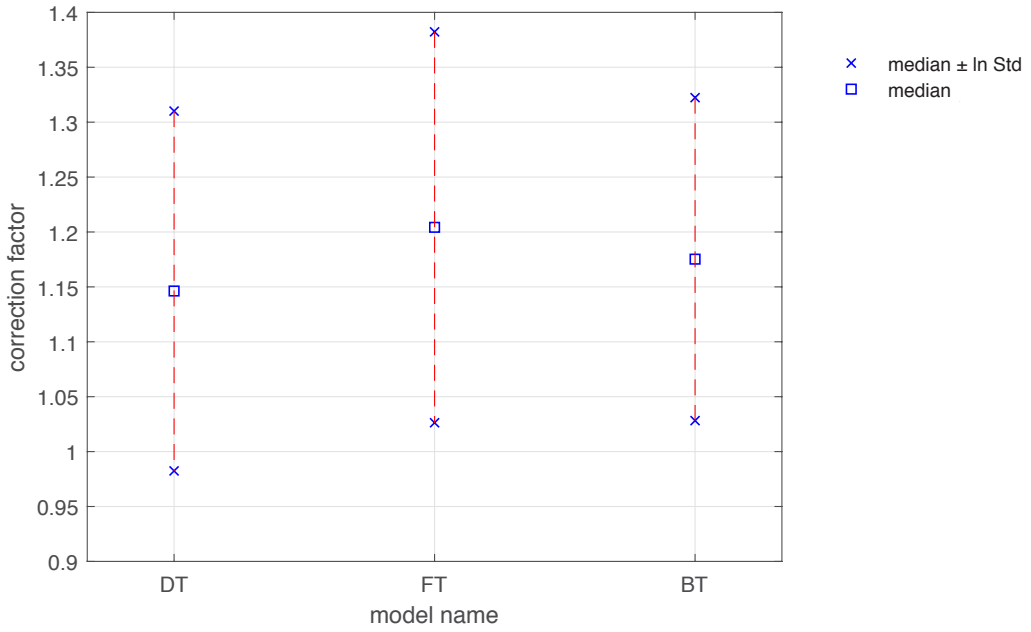

Figure 4.27 : Accuracy and precision for Takeda models (DT, FT and BT).

In principle, Takeda model shares some part of the limitation that is exhibited by the bilinear model since both models do not dissipate any hysteresis energy up until yield limit is exceeded. However once the yield limit is exceeded the Takeda model starts to dissipate energy both in the large and the small cycles -unlike the bilinear model. The specific features of Takeda model results in different levels of energies being dissipated as compared to the bilinear model. For units WDH5, WDH6 and A1 the hysteresis energy dissipation obtained using Takeda model is higher than that simulated using bilinear model. For the other units, opposite effect is observed. On the average, the modeling the hystersis behavior using Takeda model results in slightly (i.e. 2% to 7%) lower levels of energy dissipation being simulated as compared to the bilinear model. This leads to insignificant changes in the overall accuracy of the simulated energy dissipation levels.

Time variation of the total cumulative dissipation was computed. Resulting plots are provided in **figures from 4.28 to 4.32**

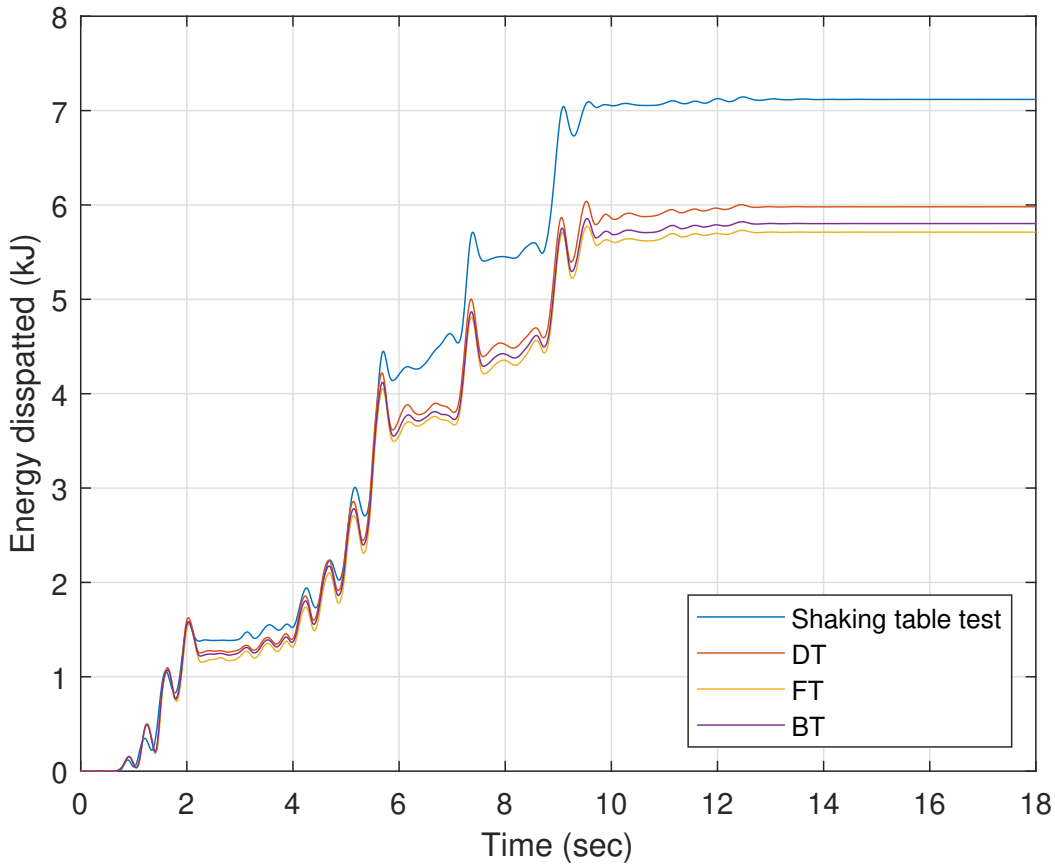

Figure 4.28 : Comparison of the actual hysteretic energy dissipation and the simulated hysteretic energy using Takeda models (DT, FT and BT): WDH3.

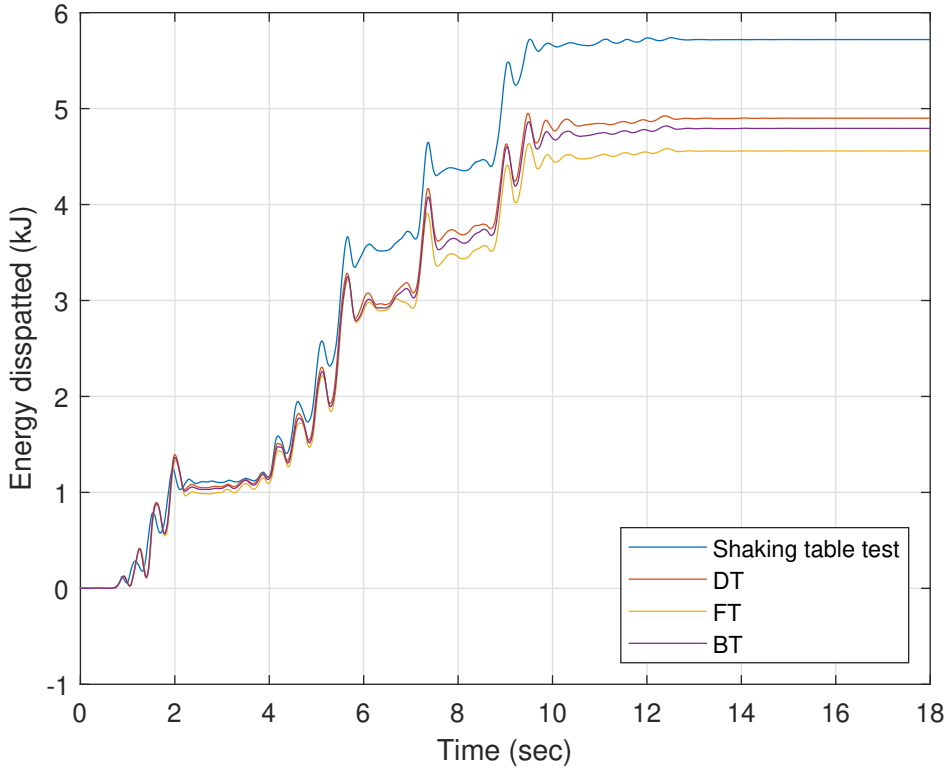

(a)

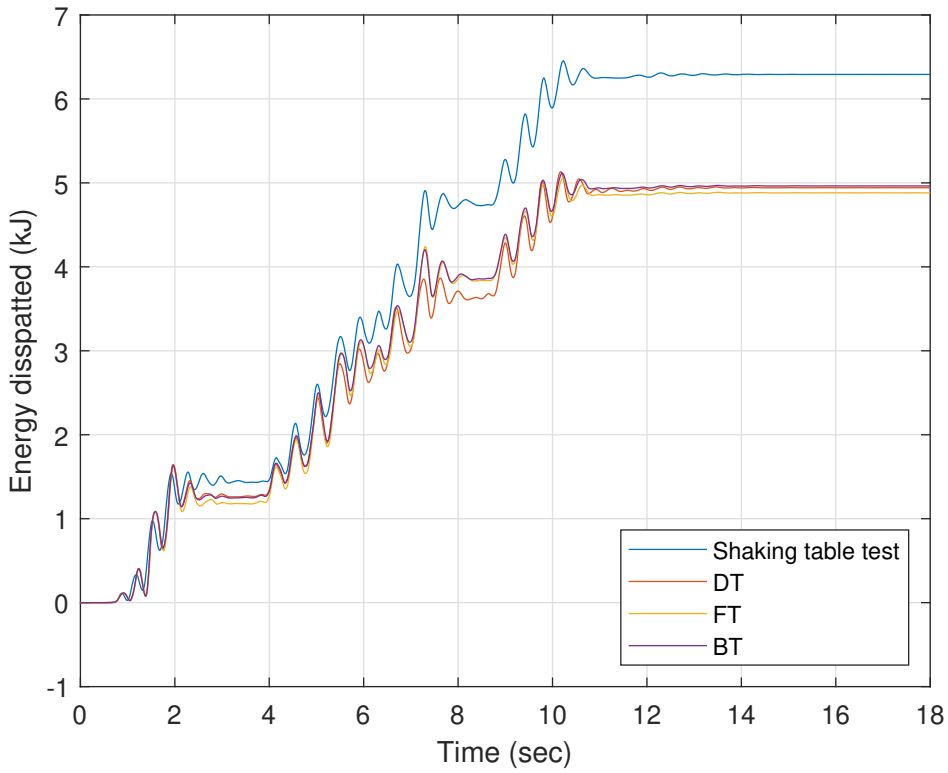

(b)

Figure 4.29 : Comparison of the actual hysteretic energy dissipation and the simulated hysteretic energy using Takeda models (DT, FT and BT): (a) WDH4 and (b) WDH5.

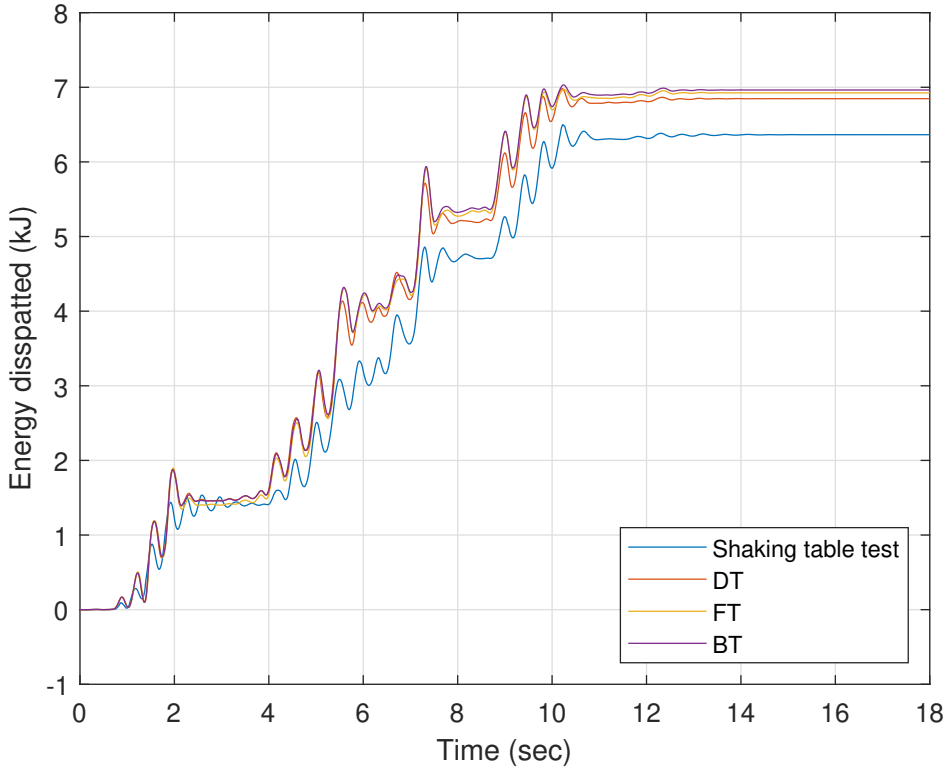

(a)

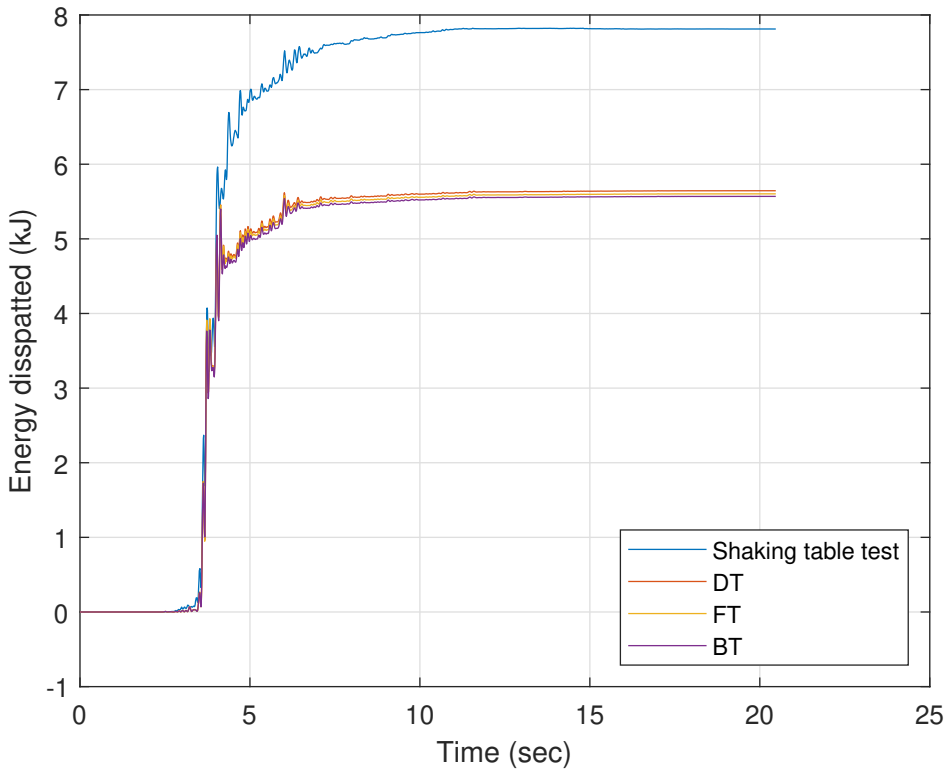

(b)

Figure 4.30 : Comparison of the actual hysteretic energy dissipation and the simulated hysteretic energy using Takeda models (DT, FT and BT): (a) WDH6 and (b) CAMUS3.

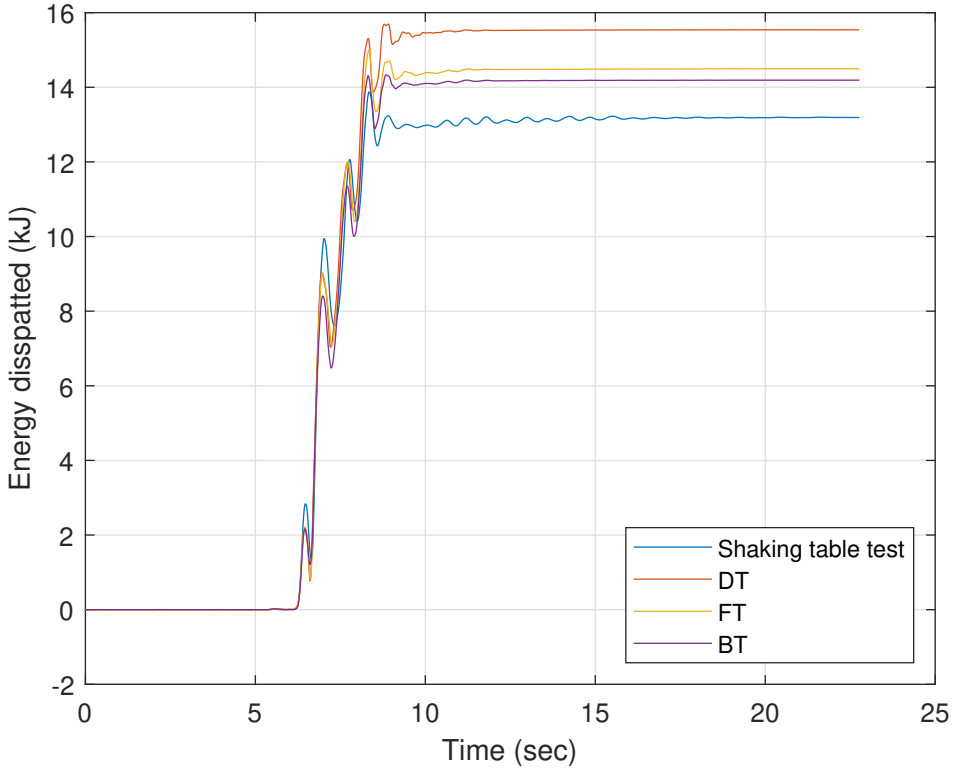

(a)

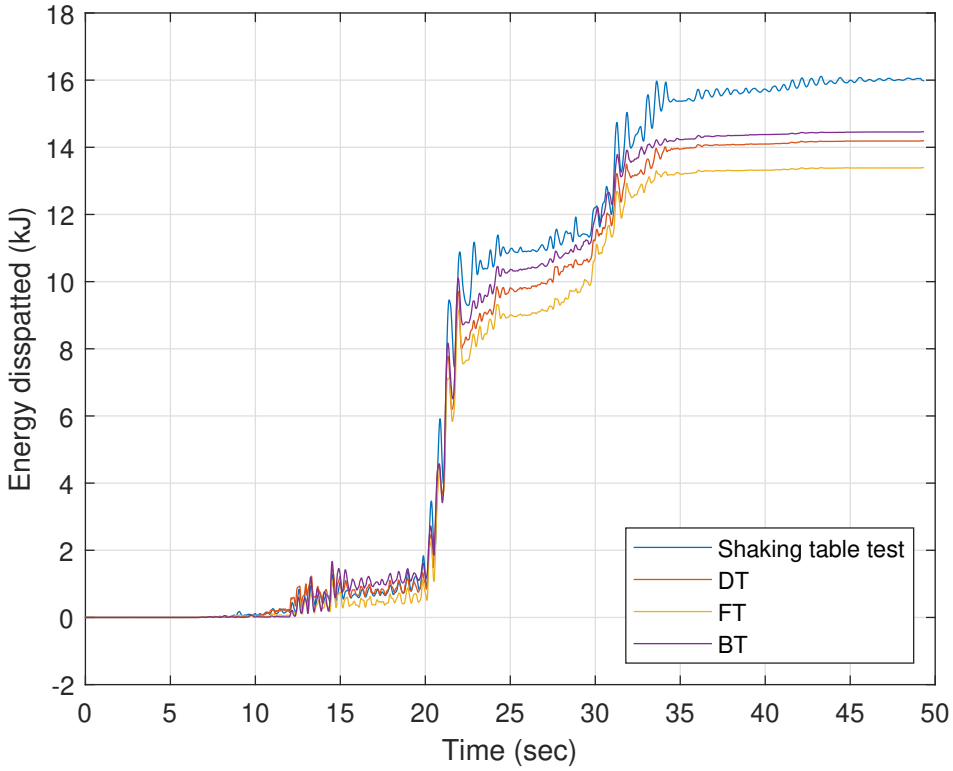

(b)

Figure 4.31 : Comparison of the actual hysteretic energy dissipation and the simulated hysteretic energy using Takeda models (DT, FT and BT): (a) A1 and (b) B1.

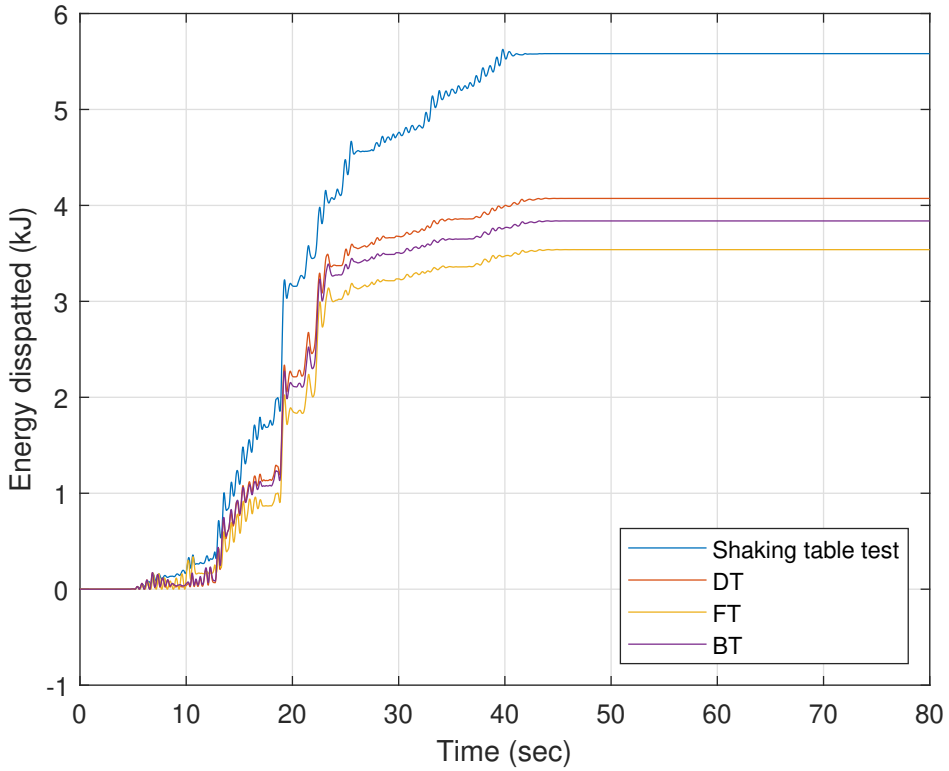

Figure 4.32 : Comparison of the actual hysteretic energy dissipation and the simulated hysteretic energy using Takeda models (DT, FT and BT): EBII07.

Fiber section

Fiber section model is the most complex model among the set of models considered in this investigation. In the fiber section model flexural behavior is not defined by moment-curvature hysteresis rules. Instead, stress-strain responses of the fibers in the cross section are simulated. This results in smoother hysteresis cycles being simulated as compared to Takeda model. It also provides the capability of directly accounting for the axial-flexural behavior interaction. However since for the considered test units dynamic variation of axial load is negligible, this benefit does not play a significant role in the results presented here.

Simulated displacement time histories of the test units are compared with the actual recorded displacement histories of the units in **Figures 4.33-4.36**.

Results indicate that models with fiber section hysteresis are capable of simulating displacement traces with a sufficient level of accuracy which indicates that the created models are acceptable. Peak displacements and the general vibration characteristics exhibited during the excitation are well captured by the model.

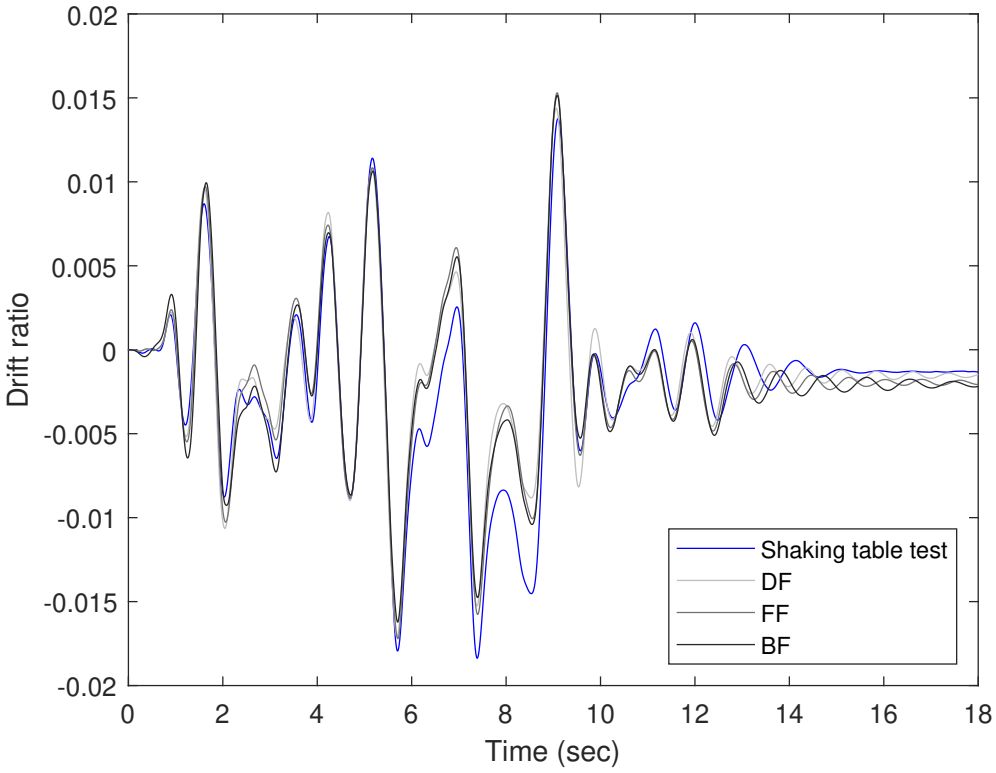

(a)

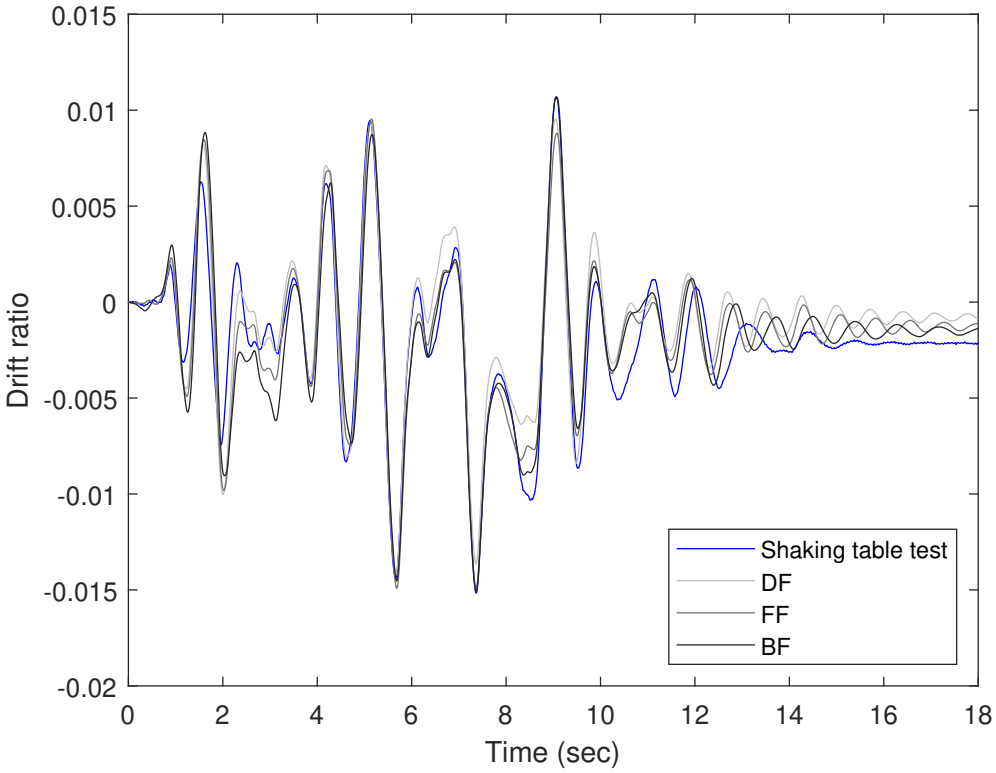

(b)

Figure 4.33 : Comparison of displacement between Fiber models and experiment: (a) WDH3 (b) WDH4.

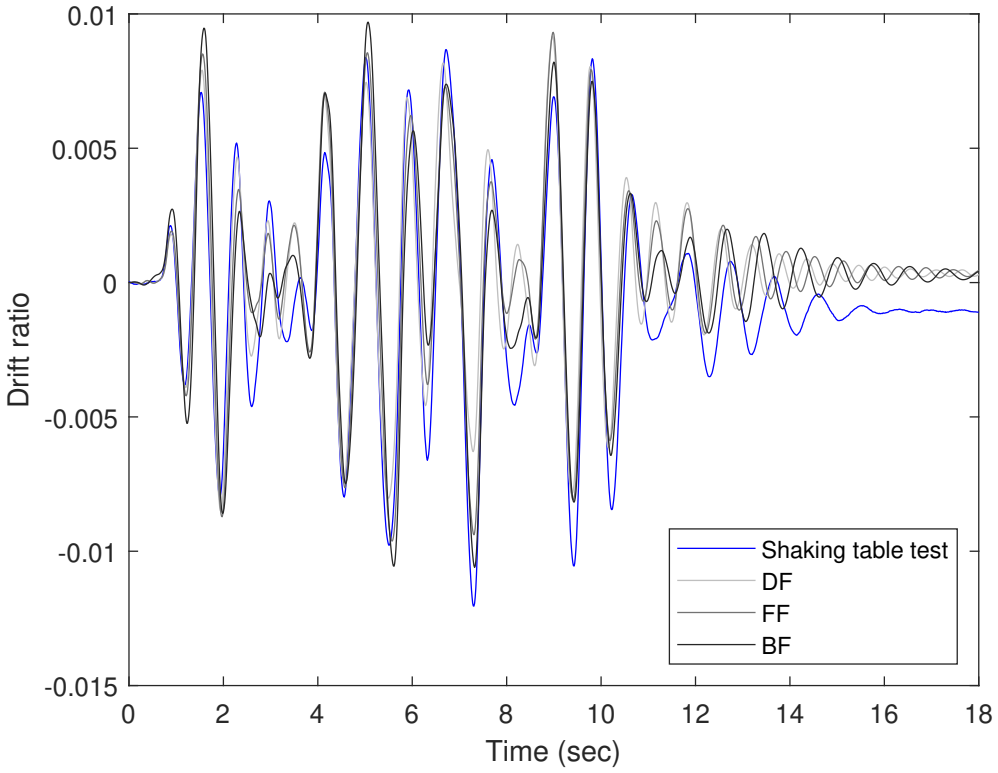

(a)

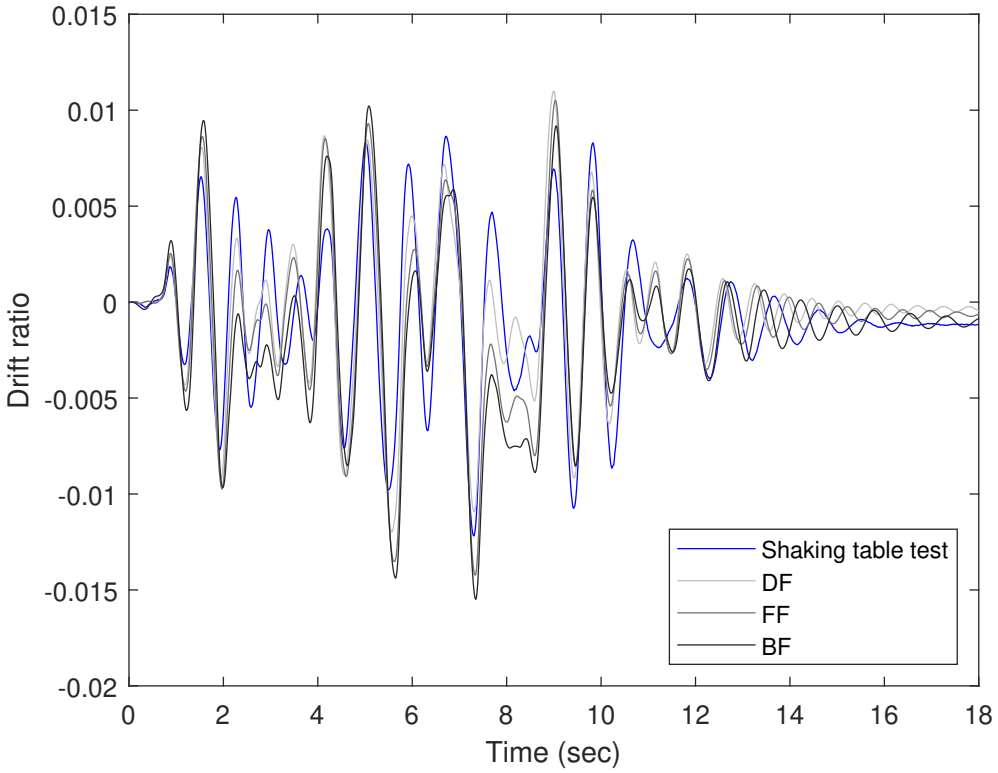

(b)

Figure 4.34 : Comparison of displacement between Fiber models and experiment: (a) WDH5 (b) WDH6.

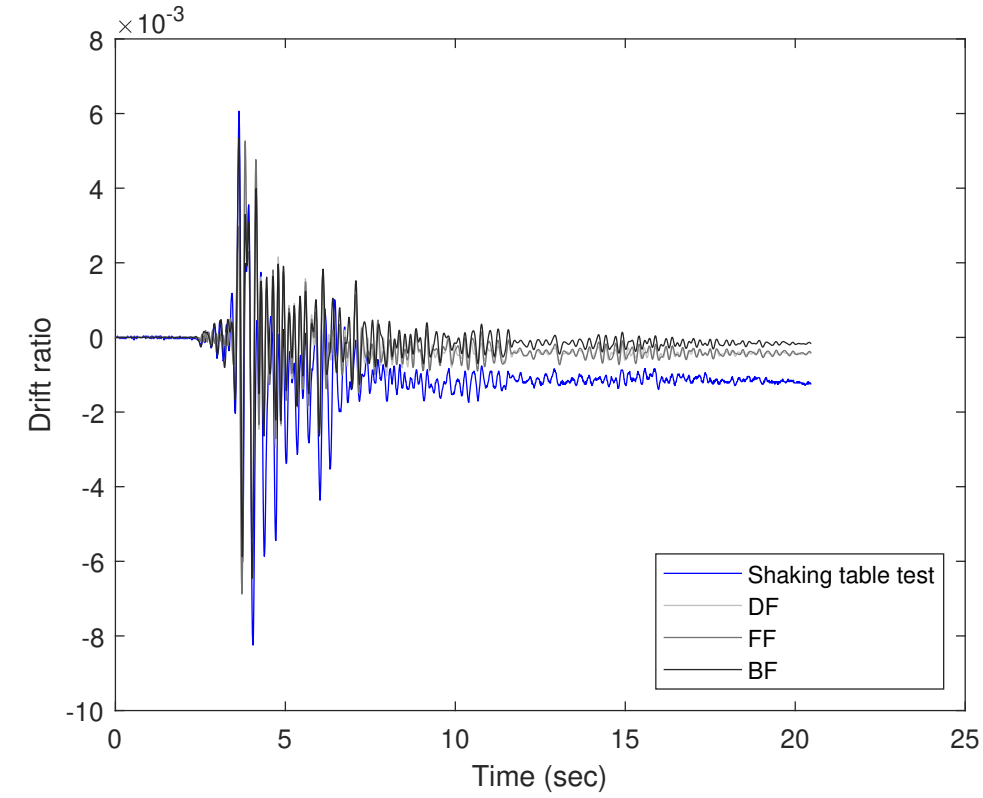

(a)

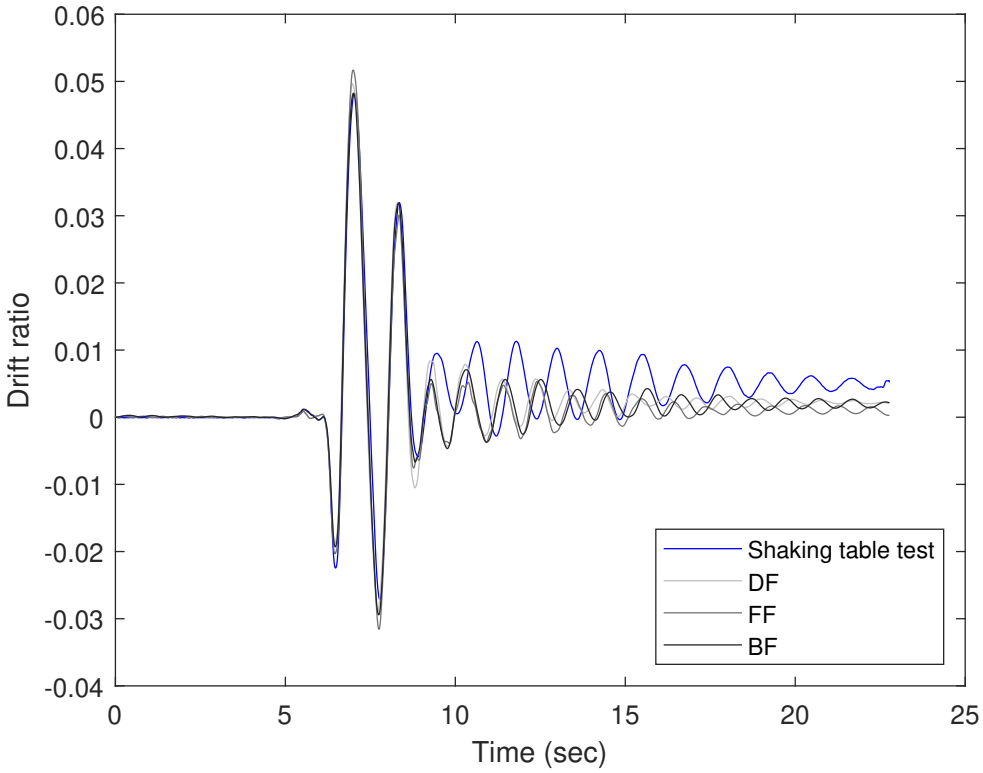

(b)

Figure 4.35 : Comparison of displacement between Fiber models and experiment: (a) CAMUS3 (b) A1.

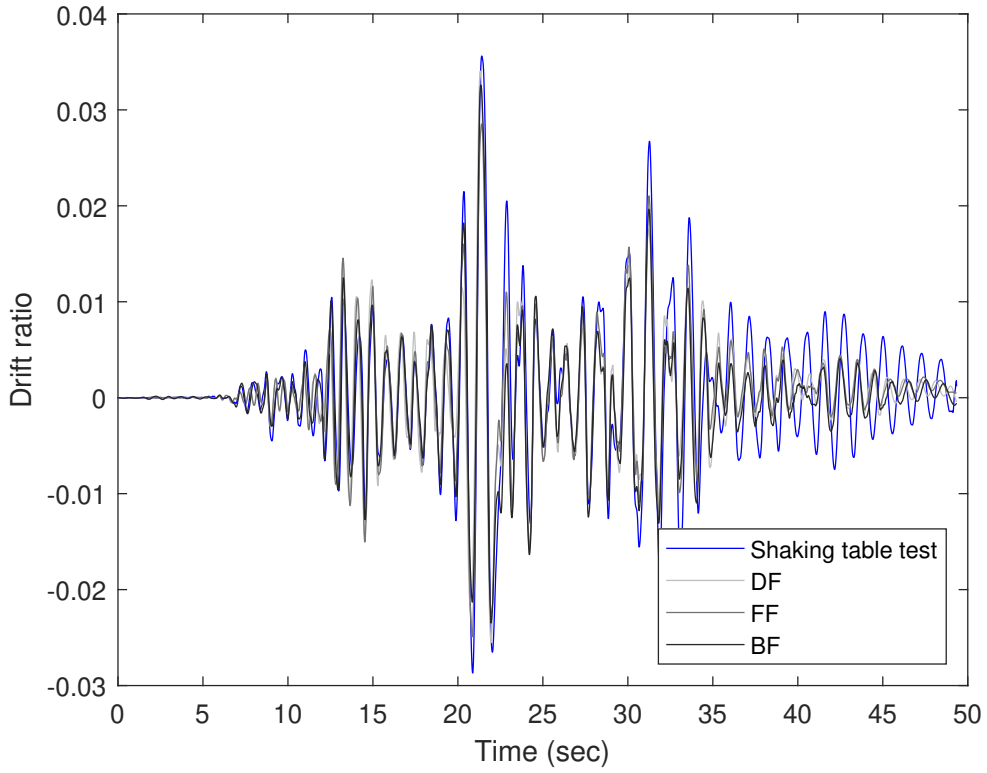

(a)

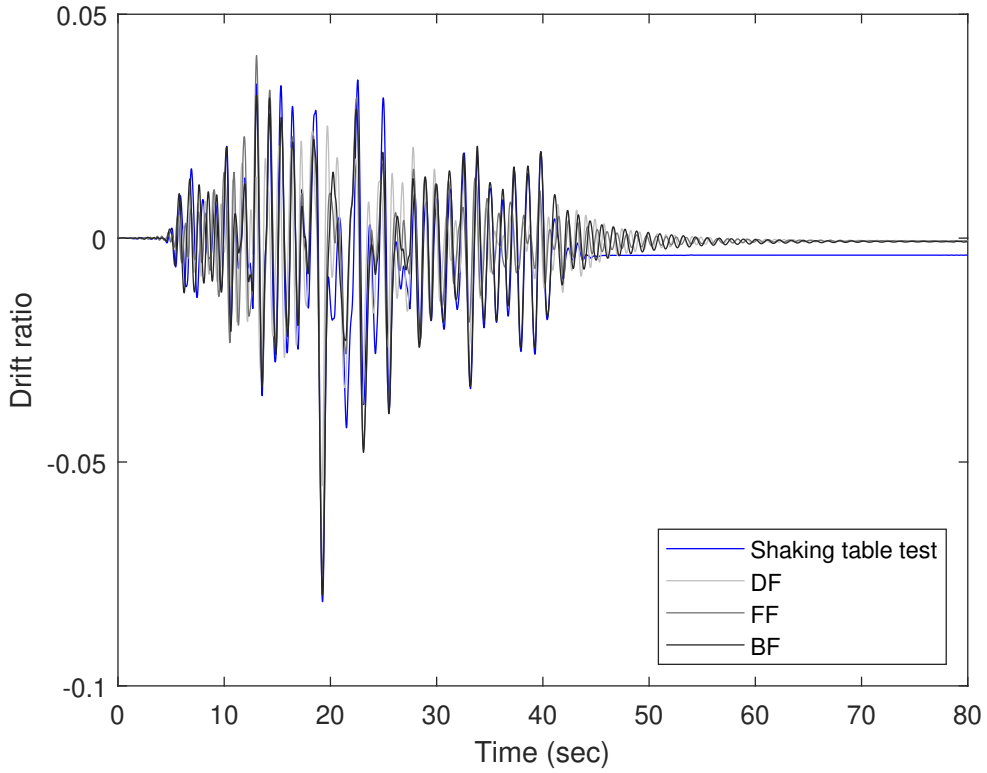

(b)

Figure 4.36 : Comparison of displacement between Fiber models and experiment: (a) B1 (b) EBII07.

The hysteresis cycles simulated using the fiber models are compared to the actual response of the units in **Figures 4.37-4.40**.

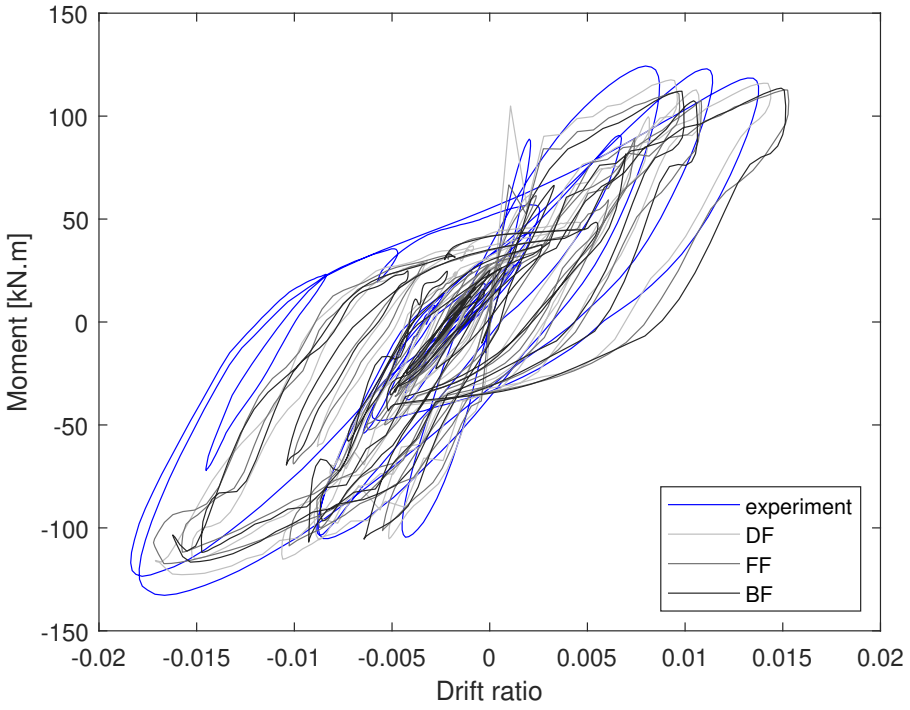

(a)

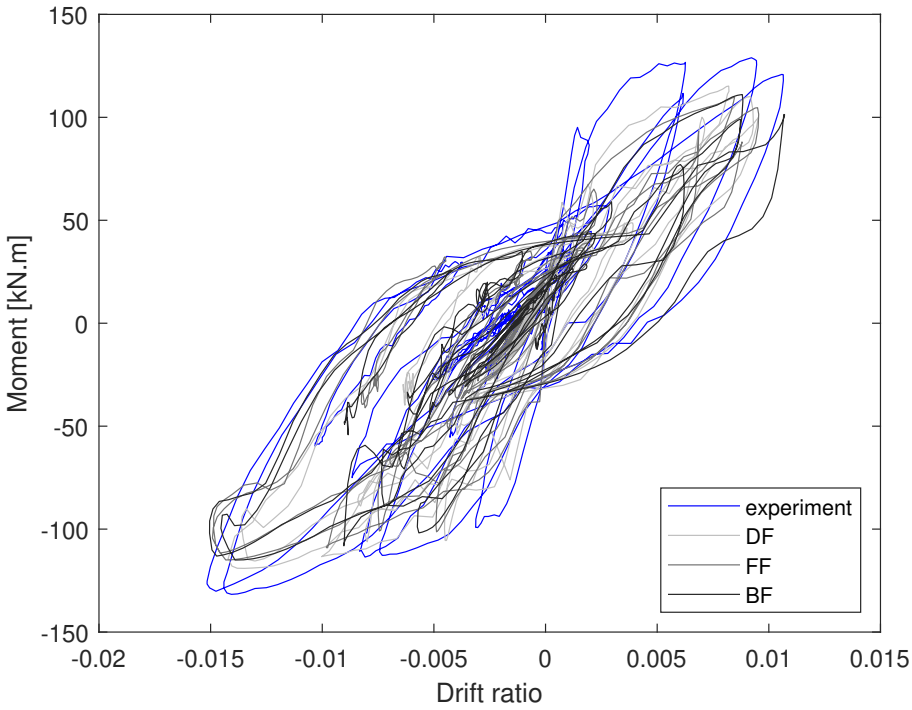

(b)

Figure 4.37 : Comparison of hysteresis behavior between Fiber models and experiment: (a) WDH3 (b) WDH4.

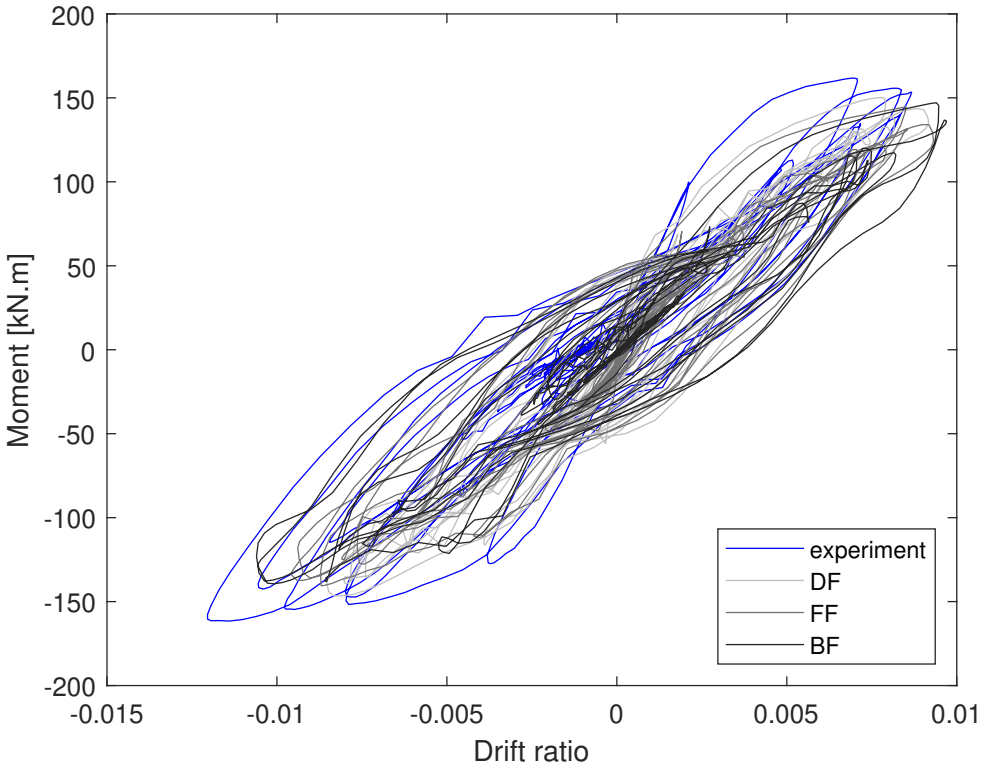

(a)

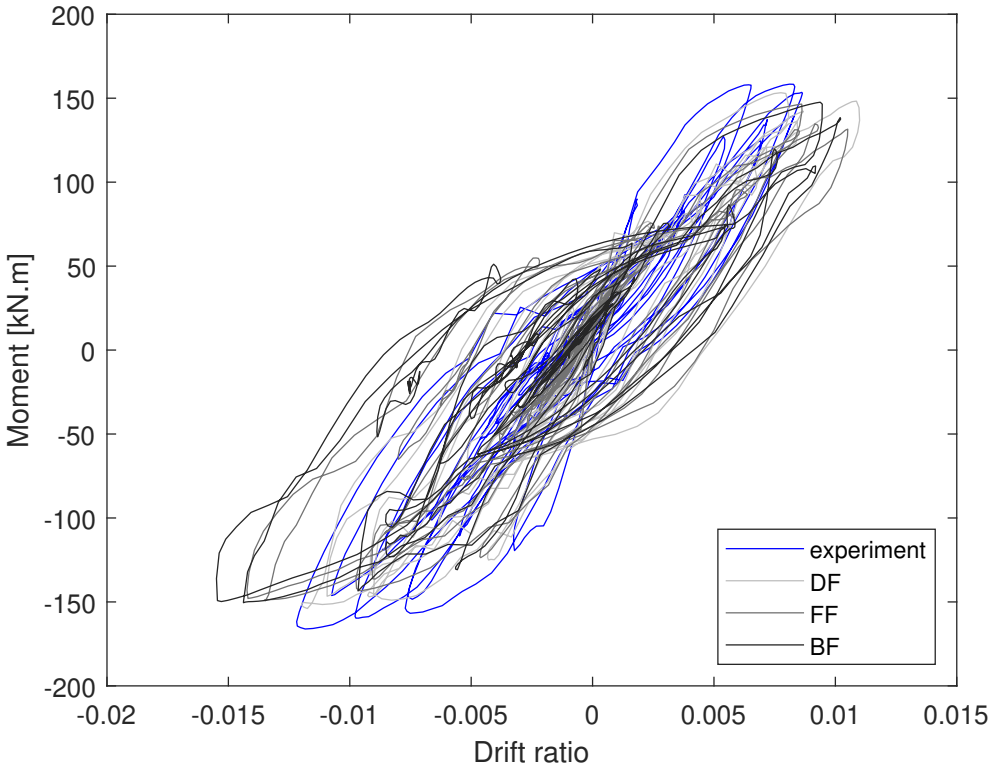

(b)

Figure 4.38 : Comparison of hysteresis behavior between Fiber models and experiment: (a) WDH5 (b) WDH6.

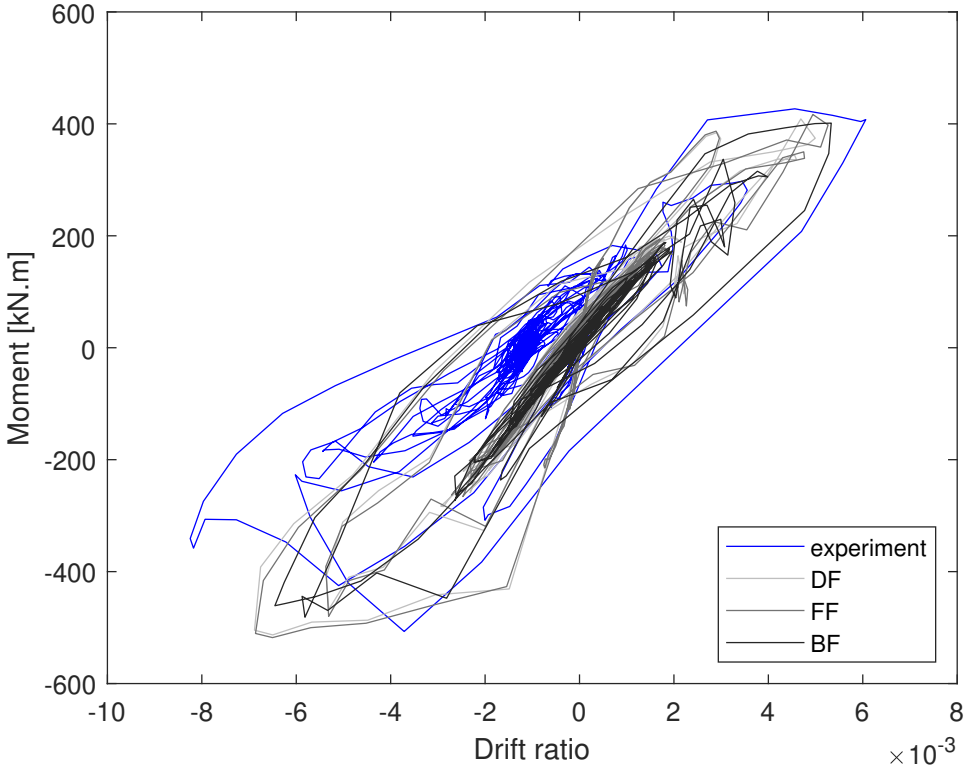

(a)

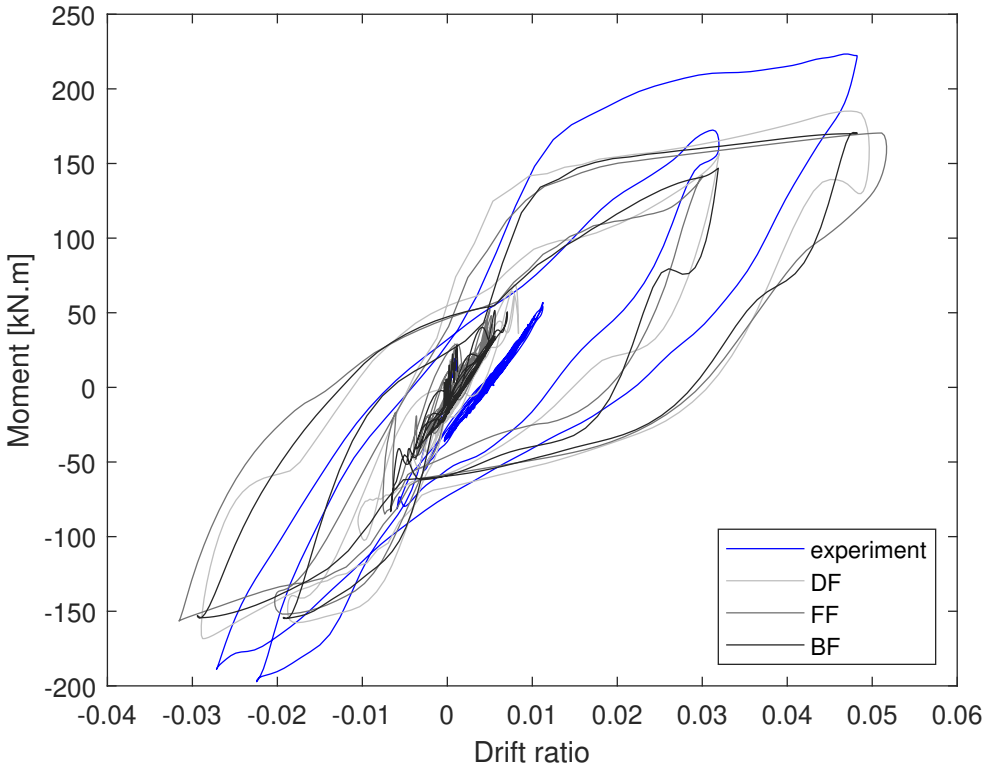

(b)

Figure 4.39 : Comparison of hysteresis behavior between Fiber models and experiment: (a) CAMUS3 (b) A1.

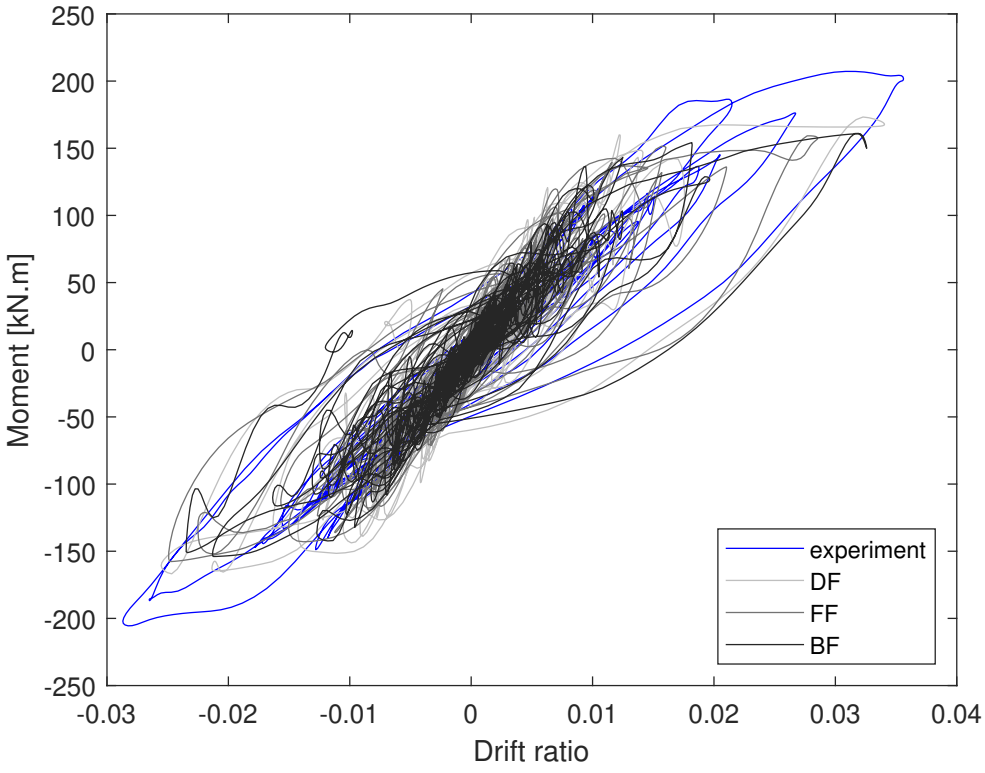

(a)

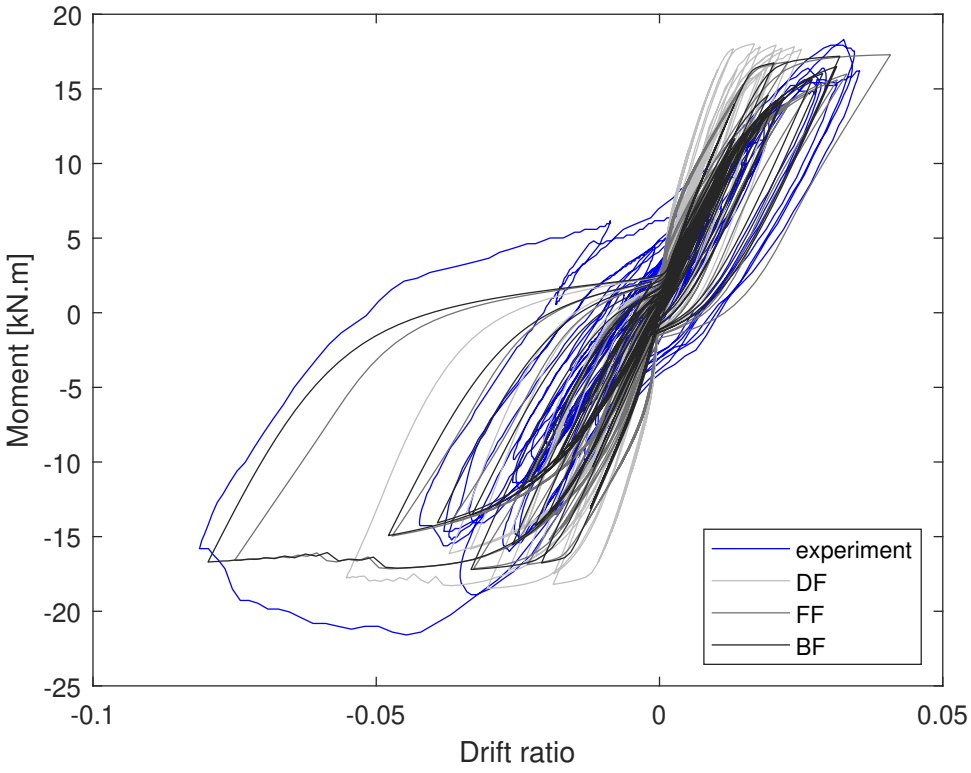

(b)

Figure 4.40 : Comparison of hysteresis behavior between Fiber models and experiment: (a) B1 (b) EBII07.

From the results, it can be seen that smoother hysteresis cycles are obtained as expected. Moreover, it can be observed that for the largest cycles unloading stiffness exhibited in the actual response tends to have a lower stiffness compared to the unloading path followed by fiber section model. However, cyclic response exhibited by EBII07 can be considered as an exception to this case.

Table 4.3 shows the hysteresis energy dissipated of each Fiber test with shaking table tests. In the overall, hysteresis energy dissipation levels simulated using the fiber section model are found to be very close (i.e. difference varies between -10% and +12%) to those simulated using Takeda hysteresis. Similar to the earlier cases, the element formulation was found to have very little impact on predicting hysteresis energy dissipated. It can be considered a bit of a surprise to observe that fiber section model effectively results in a very similar level of energy dissipation to that obtained using the Takeda model. It is also observed that the accuracy of results did not improve significantly when compared to the Takeda model (**Figure 4.41**). This outcome suggests that the additional computational burden associated with fiber section model is not justified by means of any significant improvement in the simulation accuracy -at least for the test units considered here.

Table 4.3 : hysteresis energy dissipated of each Fiber model test with shaking table tests.

Test	E_{exp} kJ	E_{mod} DF model kJ	E_{mod} FF model kJ	E_{mod} BF model kJ
WDH3	7.12	6.08	5.92	5.79
WDH4	5.72	4.66	4.37	4.31
WDH5	6.29	5.20	5.45	5.25
WDH6	6.36	7.19	7.22	7.08
CAMUS3	7.81	5.60	5.35	5.35
A1	13.95	14.88	14.23	13.72
B1	15.99	15.44	13.89	14.63
EBII07	5.58	3.96	3.38	3.71

The hysteresis cycles simulated using the fiber models are compared to the actual response of the units in **Figures 4.42-4.45**.

4.3.1.2 Element formulation models

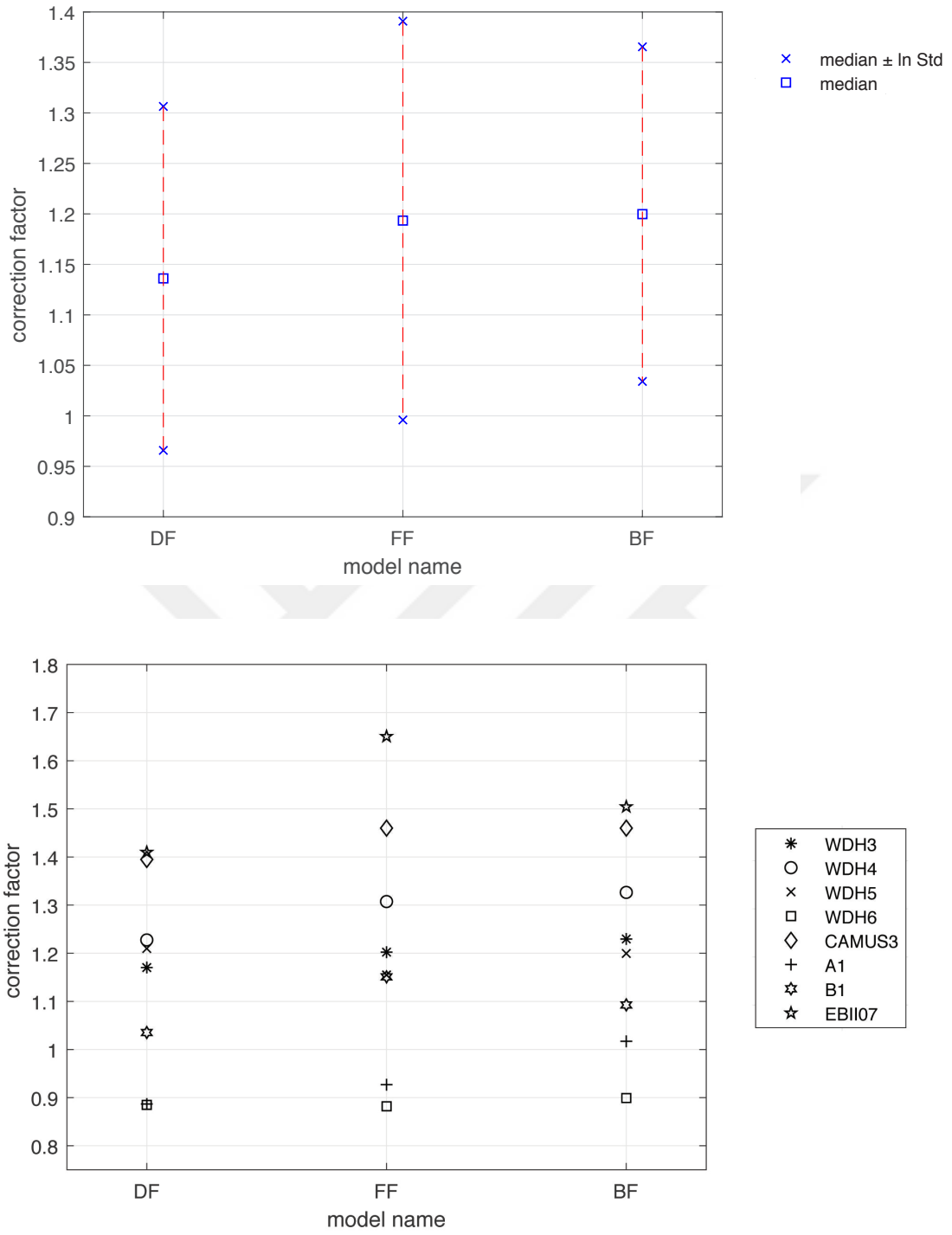

Figure 4.41 : Accuracy and precision for Fiber models (DF, FF and BF).

The impact of finite element formulation (i.e. utilization of displacement-based, force-based or beam-with-hinges elements) on the accuracy of the simulated hysteresis energy dissipation response was observed to be very minor. This was identified as a common results from all section hysteresis models. When the significant scatter of errors and the negligible differences in between the mean errors are considered, it can

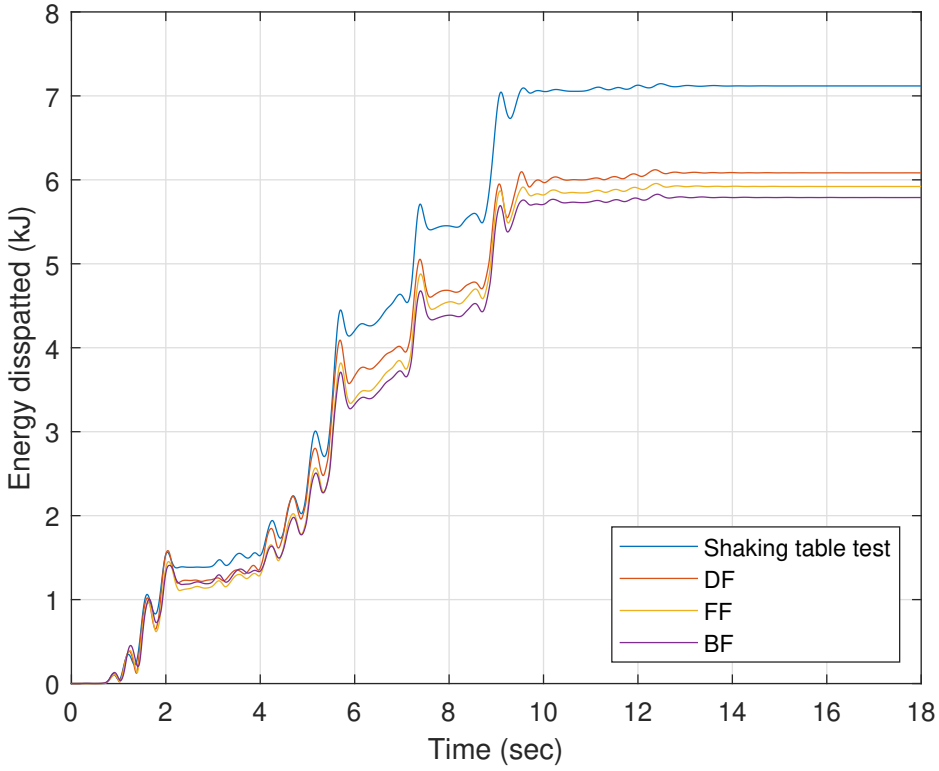

(a)

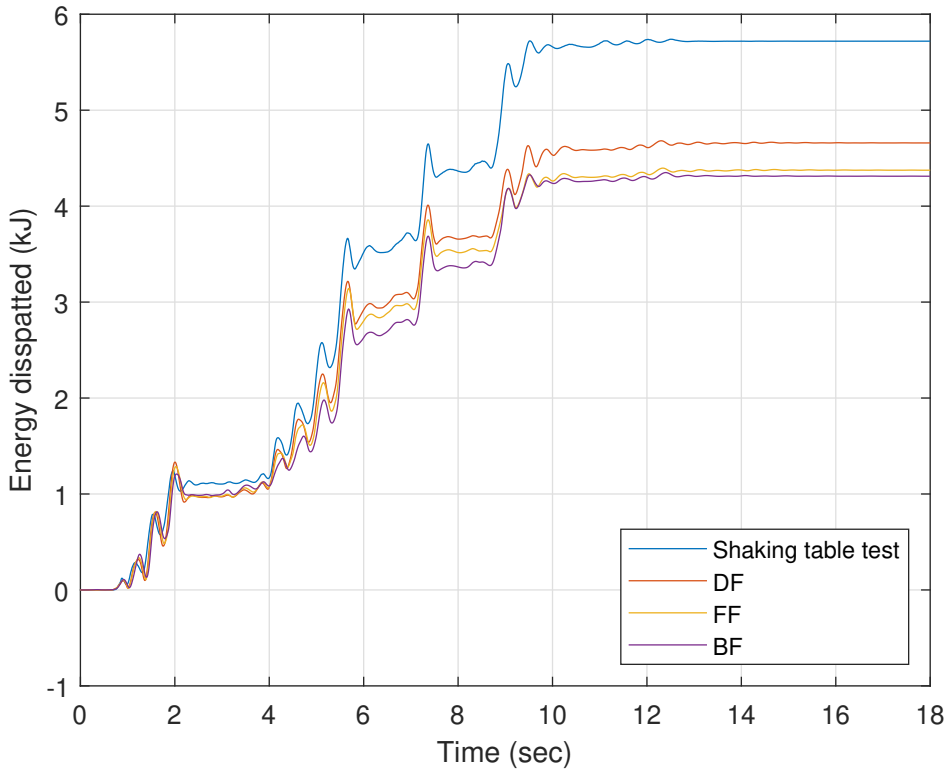

(b)

Figure 4.42 : Comparison of hysteretic energy dissipation between Fiber models and experiment: (a) WDH3 (b) WDH4.

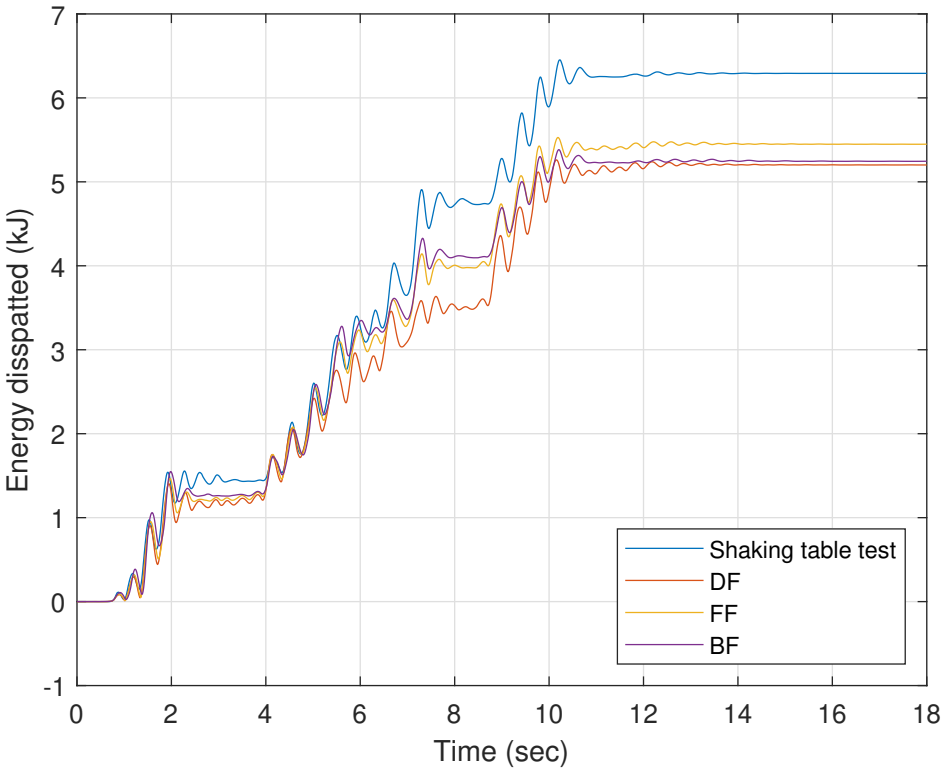

(a)

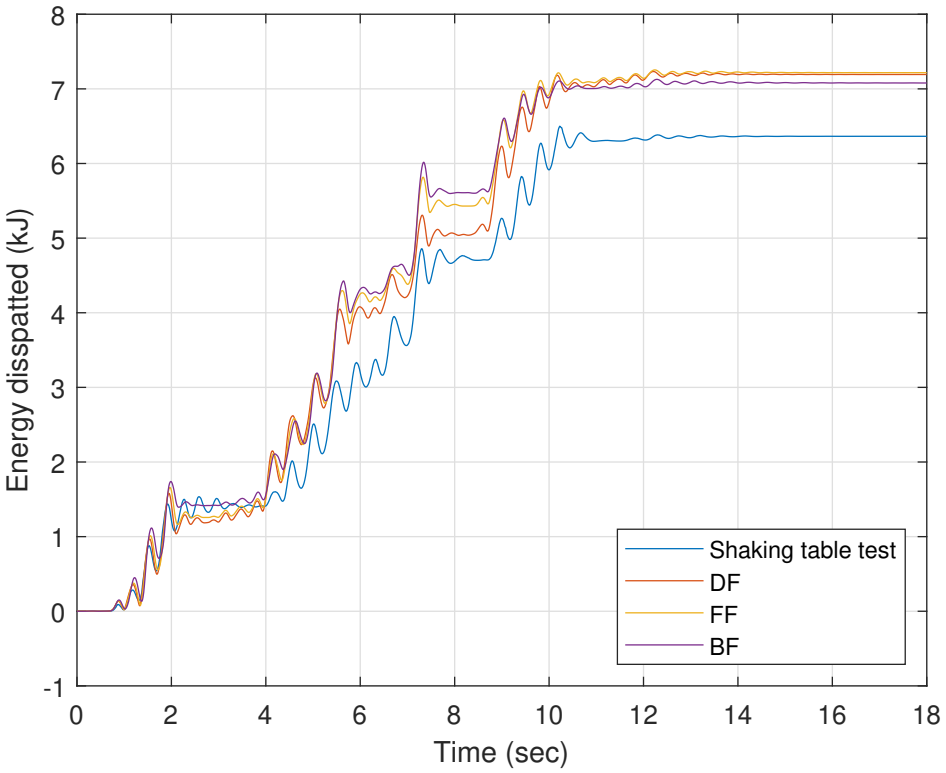

(b)

Figure 4.43 : Comparison of hysteretic energy dissipation between Fiber models and experiment: (a) WDH5 (b) WDH6.

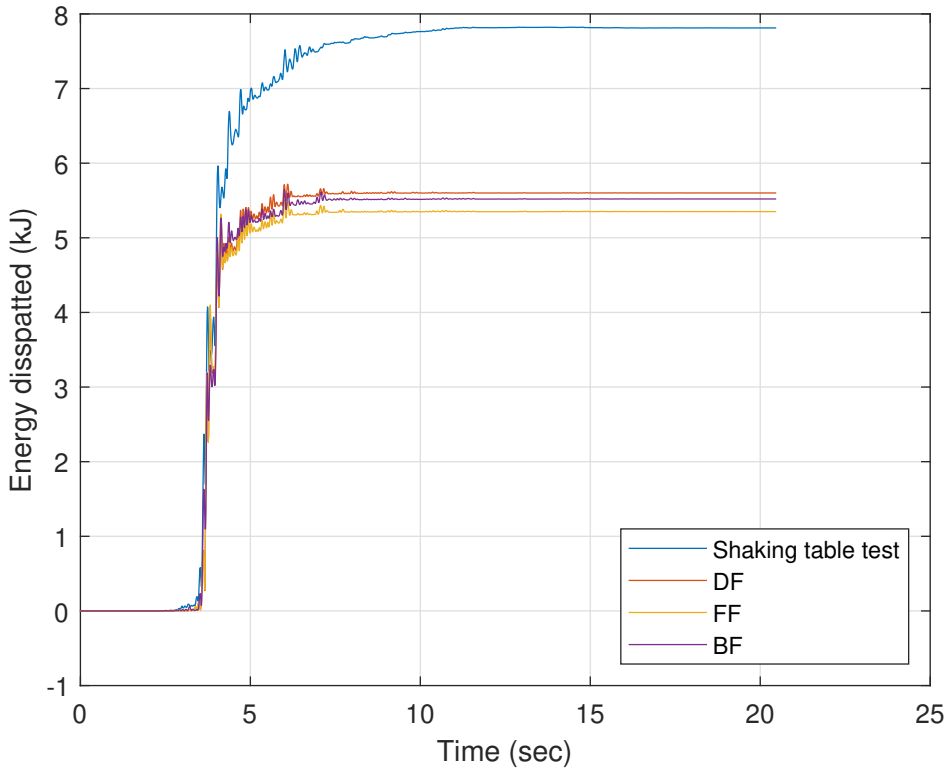

(a)

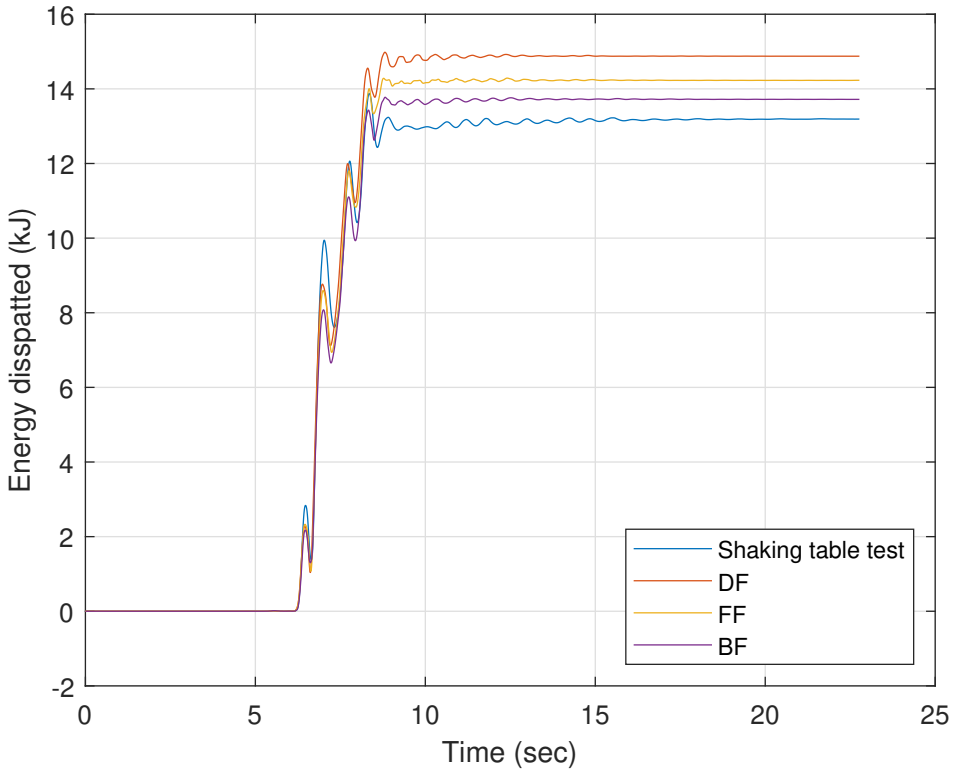

(b)

Figure 4.44 : Comparison of hysteretic energy dissipation between Fiber models and experiment: (a) CAMUS3 (b) A1.

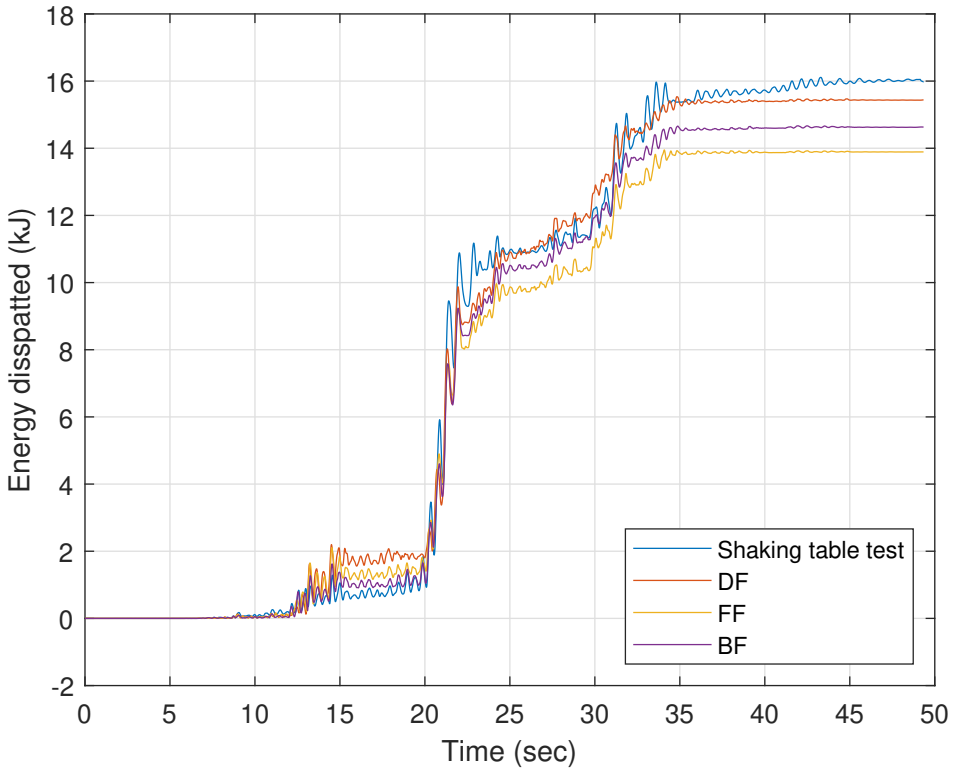

(a)

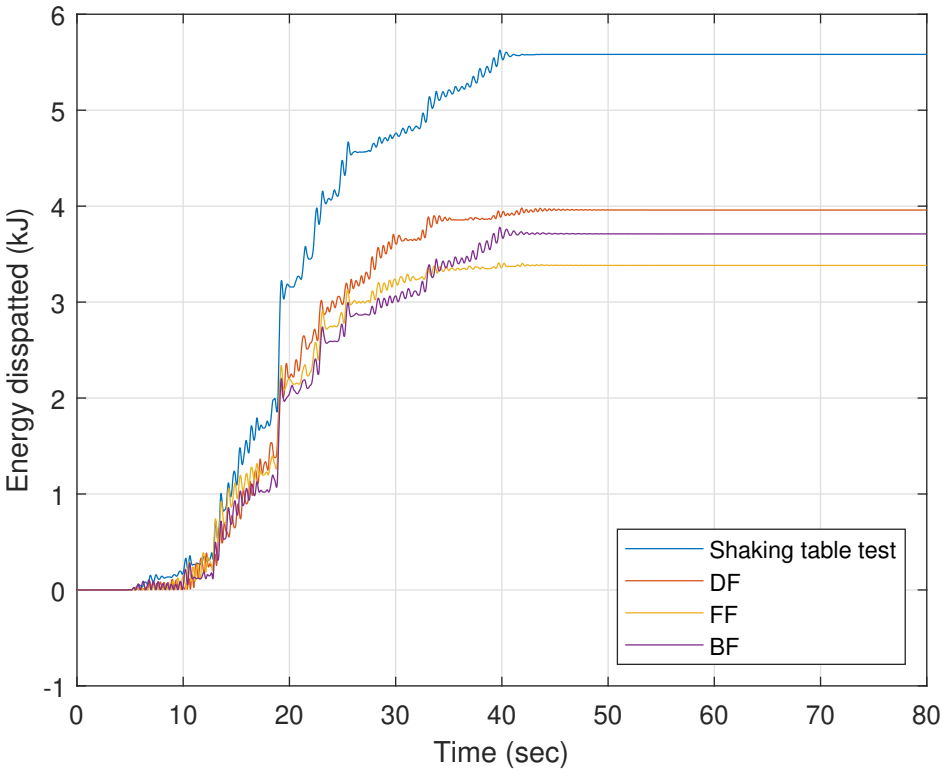

(b)

Figure 4.45 : Comparison of hysteretic energy dissipation between Fiber models and experiment: (a) B1 (b) EBII07.

be said that finite element formulation does not influence the accuracy of the simulated energy dissipation behavior. It should be noted however that this is conditional to the component meshing strategy utilized in this study which aims at achieving a more or less uniform behavior across all element formulations.

4.3.2 Computational time

Computational time has a certain effect in determining the suitable type of model to work with. For this study, the considered components were relatively small and simple, which has lead to computation time factor having a small effect. Still however, in the case when complex models are analyzed necessary computational time would have a significant influence in determining which modeling approach should be used.

Figure 4.46 shows the average computational times for each model to create and analyze the dynamic responses of the models.

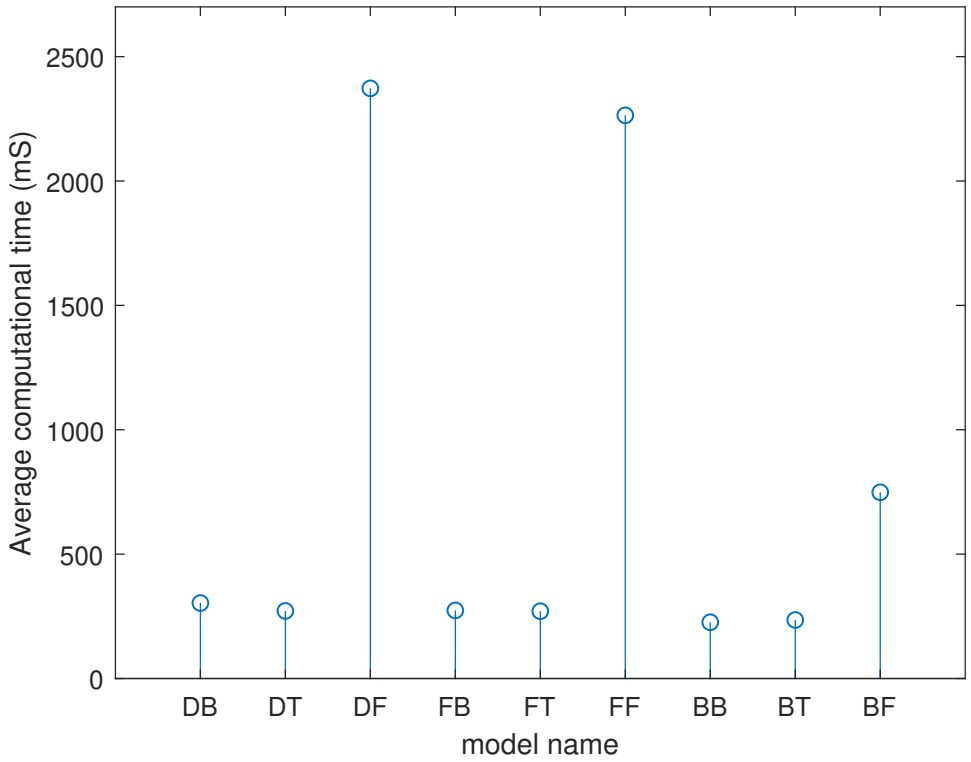

Figure 4.46 : Average computational time.

Comparing the results obtained using different hysteretic models, it is observed that both Bilinear model and Takeda models require very short computation time. This

gives them an advantage over the Fiber model which takes longer to compute. This difference makes fiber model an unfavorable option for analysis of complex models with too many degrees-of-freedom.

When different element formulations are compared, it is seen that the beam with hinges has the shortest computational time. Particularly in the case of fiber section model, computation time required for the beam with hinges element formulation is approximately equal to 30% of the time required for the other element formulations. In between the displacement-based and force-based formulations, there is very little difference in between the required durations for computation. The observed difference between the computation times for alternative formulations may be related to nonlinear flexural section behavior being assigned to integration sections.

4.3.3 Low-level excitation

The amount of total hysteresis energy dissipated by an RC component is non-linearly related to the excitation intensity. When the excitation intensity is lower than or approximately equal to the effective yield limit, accurate simulation of hysteresis energy dissipation is a more complex task. Among the test units considered here, WDH1 is the one that is subjected to a relatively small excitation intensity. The unit had been tested at the seismic action level corresponding to 70% of the design capacity. Analysis performed here showed that the WDH1 correction factor was bigger than any other component's correction factor in an extraordinary way. For this purpose, the results related to WDH1 are excluded from the discussion related "Design-level excitation". Moreover, an alternative intensity level was considered to identify the ranges of errors exhibited in this case. For this excitation level, the following tests were considered for the units other than WDH1: A1 Run1, B1 Run4, and CAMUS3 Nice r2.

As shown in **Table 4.4**, the correction factor of the tests with low excitation was extremely high. This can be explained that when the yield capacity is not exceeded in the model, it does not dissipate energy numerically. However, in the actual shaking table tests the units dissipates some energy below yielding point. As a result, the ratio of the experimental dissipated energy to the modeled dissipated energy ratio turns out to be very high.

Table 4.4 : Low Excitation tests' Correction factor.

Unit	Test Name	excitation to design load	Correction factor
WDH1	Test3	70%	3.3
CAMUS3	Nice r2	33%	8.76
A1	RUN1	31%	10.15
B1	RUN4	38%	3.24

4.4 Maximum Displacement And Energy Dissipation

Maximum displacements of RC elements are known to be highly correlated with the damage sustained by the units during dynamic shaking. In order to develop a comprehensive understanding of the accuracy of simulated response as whole, it is important to identify the errors associated with the simulated maximum displacements. Here, this investigation is made a bit more comprehensively and the relationship between the accuracies of simulated maximum displacements as well as energy dissipation levels are compared for each test unit. These comparisons plots of obtained for the different finite element modeling approaches are presented in **Figures 4.47, 4.48 and 4.49**.

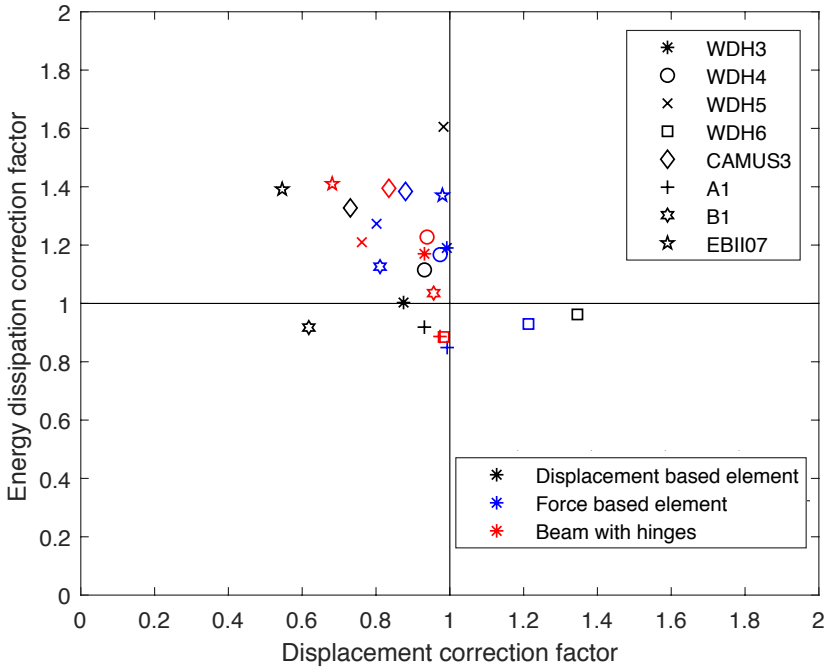

Figure 4.47 : Comparison of the prediction accuracies of alternative modeling approaches, in terms energy dissipation levels and the maximum displacements: Bilinear model.

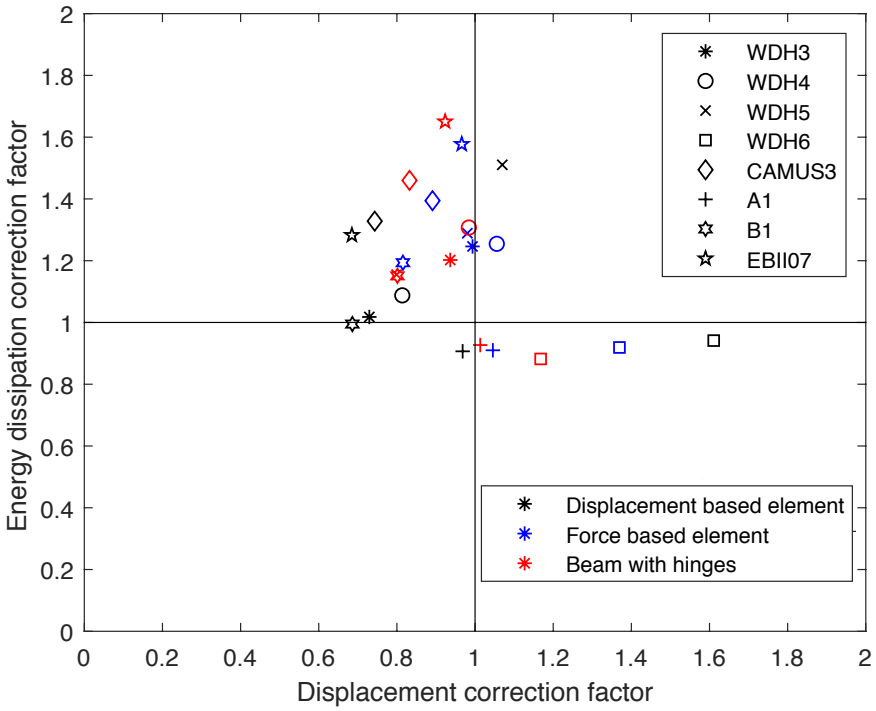

Figure 4.48 : Comparison of the prediction accuracies of alternative modeling approaches, in terms energy dissipation levels and the maximum displacements: Takeda model.

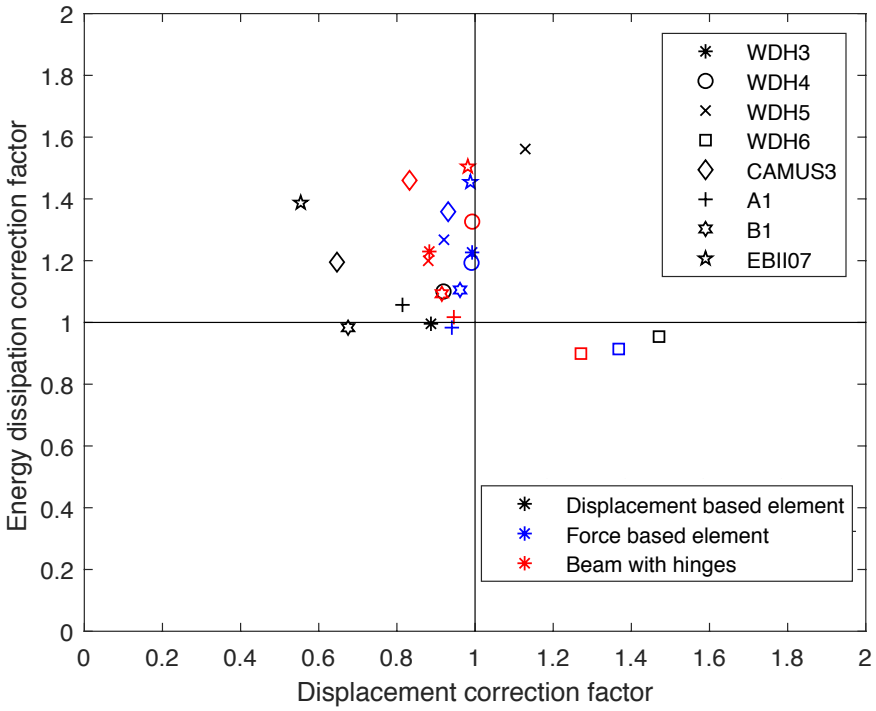

Figure 4.49 : Comparison of the prediction accuracies of alternative modeling approaches, in terms energy dissipation levels and the maximum displacements: Fiber model.

The observed results did not indicate any significant correlation between the errors associated with maximum displacements and energy dissipation levels. Still however, it was observed in general models tended to over estimate the exihibited maximum displacements and underestimate the hsysteesis energy dissipation levels.

4.5 Sensitivity of the Results

4.5.1 Critical damping ratio

During seismic activity, structure does not only dissipate hysteresis energy but also dissipates damping energy as well. This means that damping ratio is a critical parameter that needs to be estimated accurately. In this study and in order to investigate the effects of the assumed critical damping ratio on the amount of hysteretic energy dissipation, the damping ratio ζ is was set equal to ζ =50%, ζ =75%, ζ =125% and ζ =150%. Resulting energy dissipation simulations were compared against the reference model presented in the preceding chapter. In addition, the results were compared with the actual response of the test units to investigate its effects on the final accuracy.

As shown in **Figures 4.50, 4.51 and 4.52** the amount of energy dissipated by the models was found to be increasing as the damping ratio factor decreases. Likewise, the amount of energy dissipated was decreasing when the damping ratio factor increase. This results clearly demonstrates the critical influence of the assumed damping ratio and it is expected. When a high level of critical damping ratio is assumed, major portion of the input energy is dissipated by means of damping and a smaller portion is left to be dissipated by hysteresis response.

It can be seen in **Figure 4.52** that the mean correction factor is becoming closer to one (i.e. the ideal case) as the damping ratio is reduced to 50% of its reference value. This may be interpreted as: decreasing the damping ratio to 50% of its identified level may help preventing any bias. However, one should not directly jump to such conclusions since decreasing the damping ratio may lead to simulated response becoming inaccurate in terms of peak displacement. It is important to note that the reference case (i.e. corresponding to 100%) is the case when damping ratio identified for the test units are utilized directly.

4.5.2 Equivalent plastic hinge length

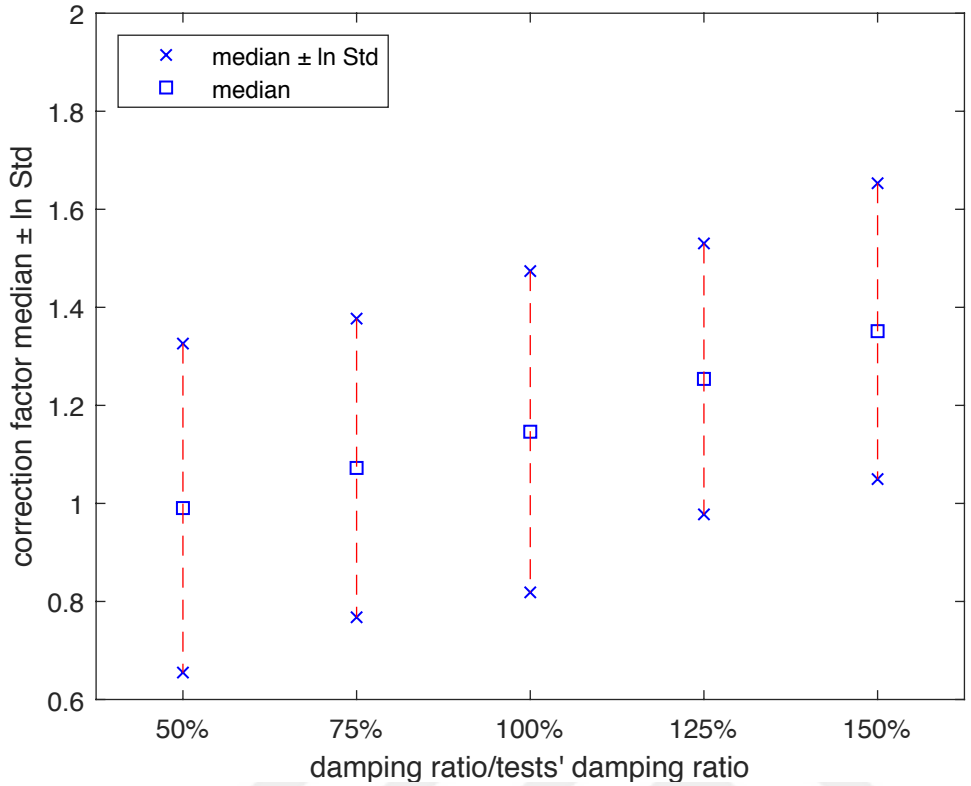

Figure 4.50 : Sensitivity of accuracy and precision for Bilinear models to the adopted Damping ratio.

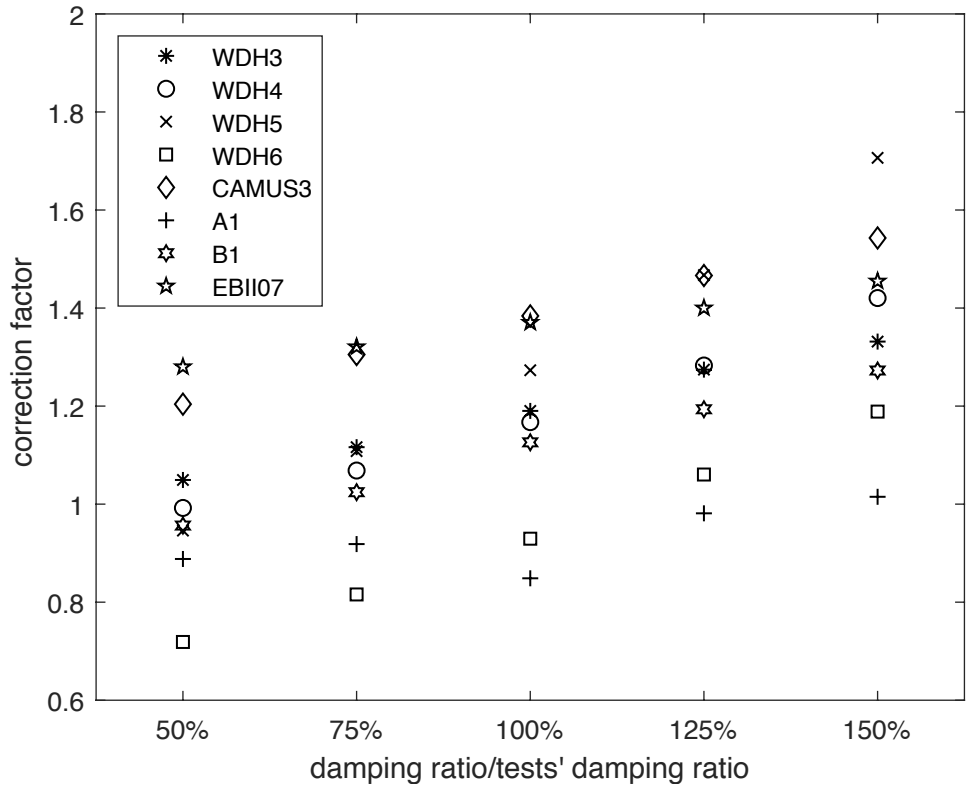

Figure 4.50 : Sensitivity of accuracy and precision for Bilinear models to the adopted Damping ratio.

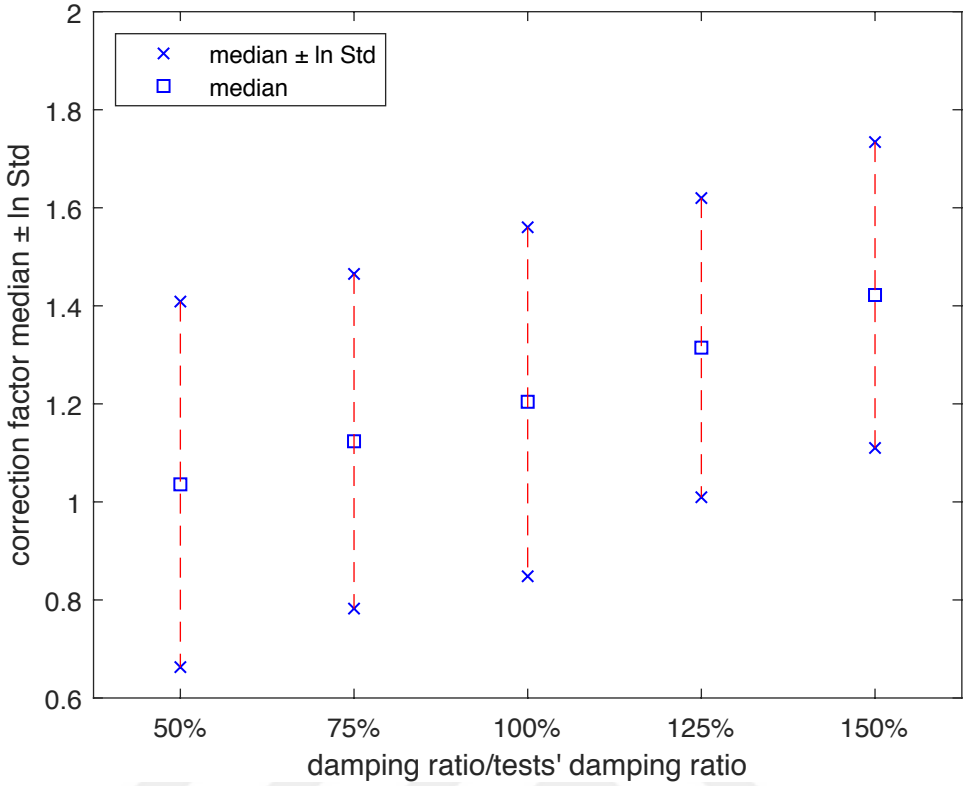

Figure 4.51 : Sensitivity of accuracy and precision for Takeda models to the adopted Damping ratio.

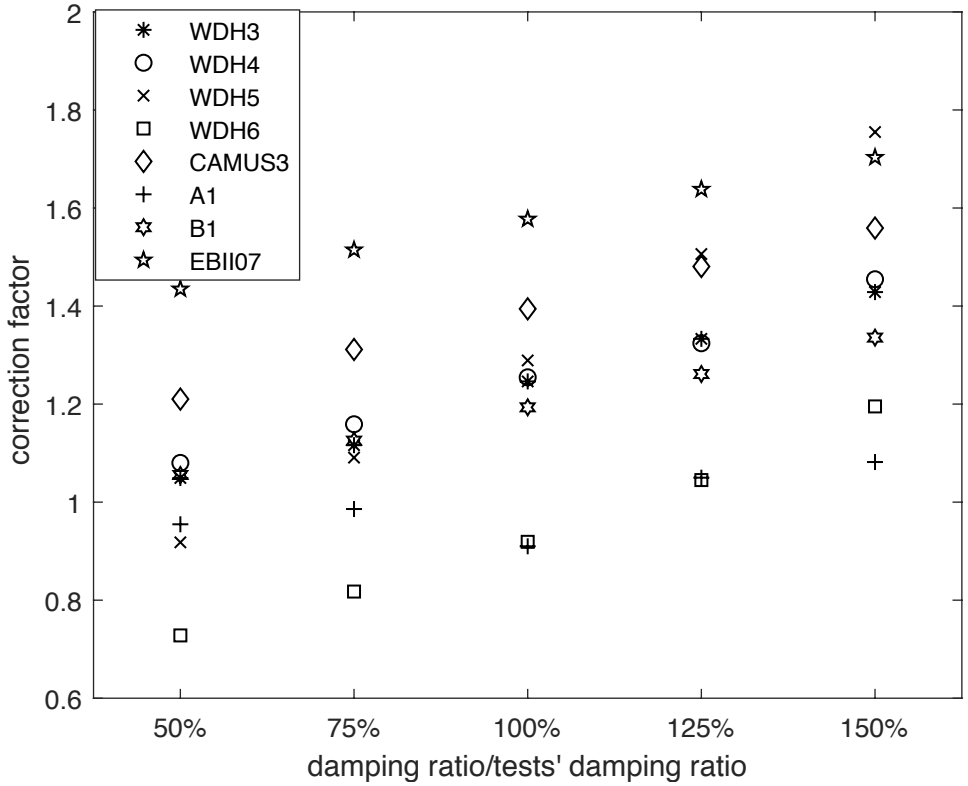

Figure 4.51 : Sensitivity of accuracy and precision for Takeda models to the adopted Damping ratio.

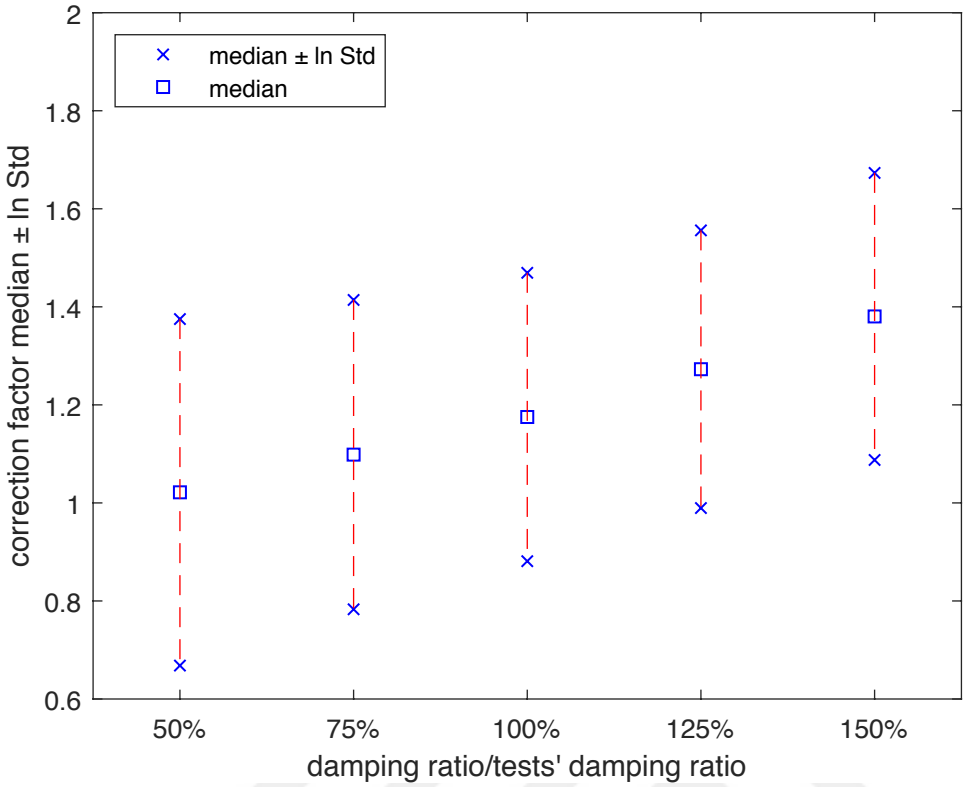

Figure 4.52 : Sensitivity of accuracy and precision for Fiber models to the adopted Damping ratio.

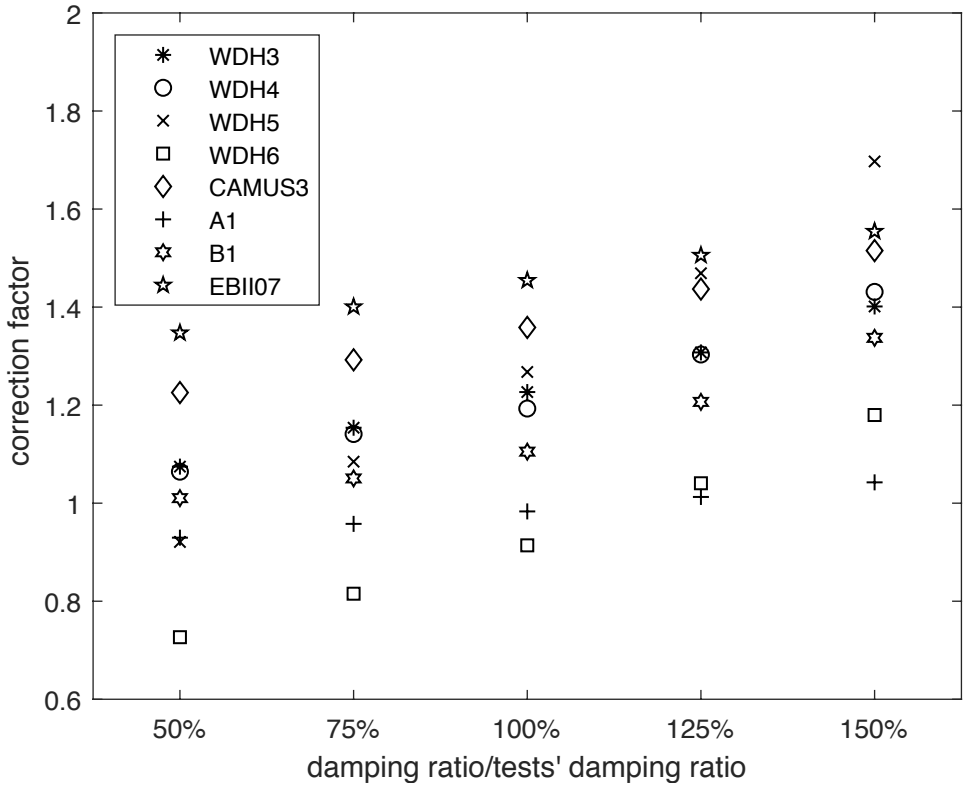

Figure 4.52 : Sensitivity of accuracy and precision for Fiber models to the adopted Damping ratio.

Determining equivalent plastic hinge length is a critical issue in numerical modeling of flexural response of ductile members: A lot of research had been done and still going, on about this subject. In this study, plastic hinge lengths of the units were estimated using the formulation proposed by Priestley et al. [27]. Based on this reference value, the sensitivity of the results to the assumed plastic hinge region was investigated. For this purpose, hinge length L_p was varied by multiplying it with a range of factors that range between 50% and 150%. Resulting energy dissipation levels are then compared with the 100% hinge length to investigate the relative change.

Unlike the damping ratio, changing the hinge length of models does not seem to have a clear relation with the amount of hysteresis energy dissipated **Figures 4.53 to 4.58** whereas clear in changing the hinge length will affect the results in an unsteady way compared to the model results. It was found that the best case for the hinge model is to use the reference value (i.e. 100%) of the hinge length.

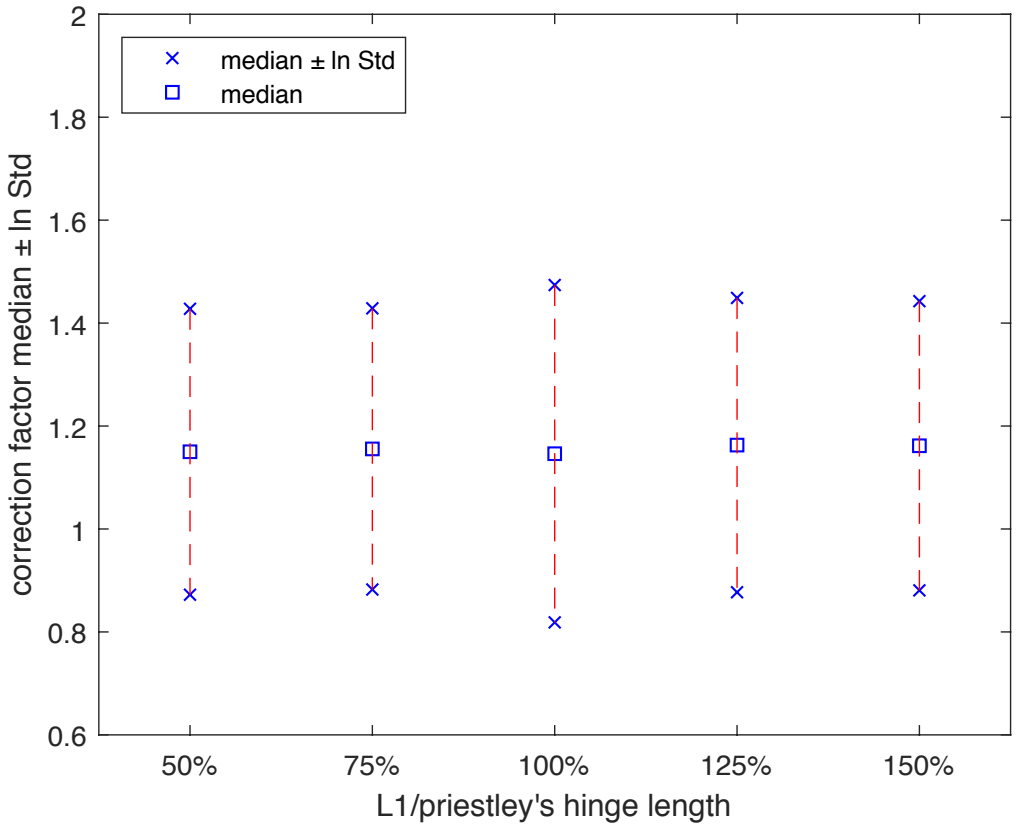

Figure 4.53 : Sensitivity of accuracy and precision for Bilinear models to the adopted hinge length.

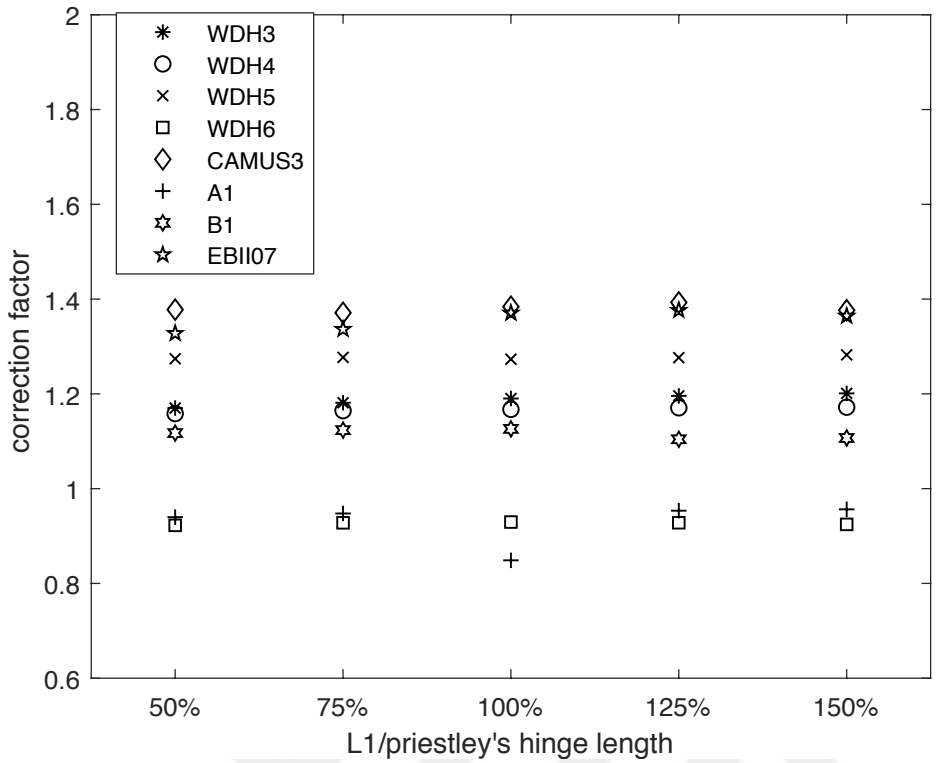

Figure 4.54 : Sensitivity of accuracy and precision for Bilinear models to the adopted hinge length.

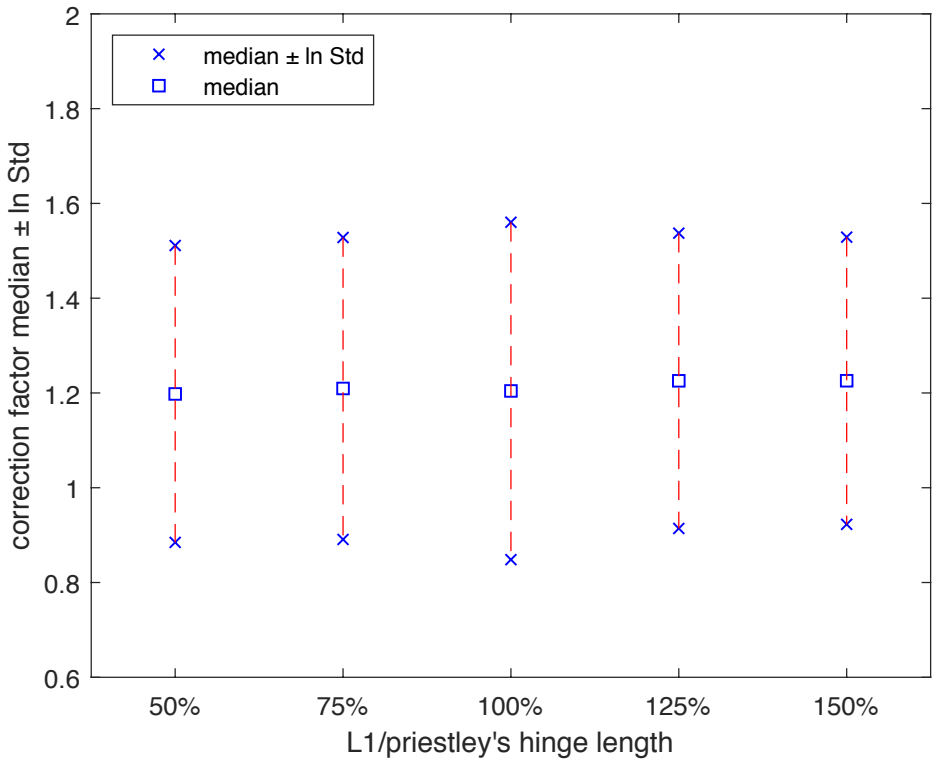

Figure 4.55 : Sensitivity of accuracy and precision for Takeda models to the adopted hinge length.

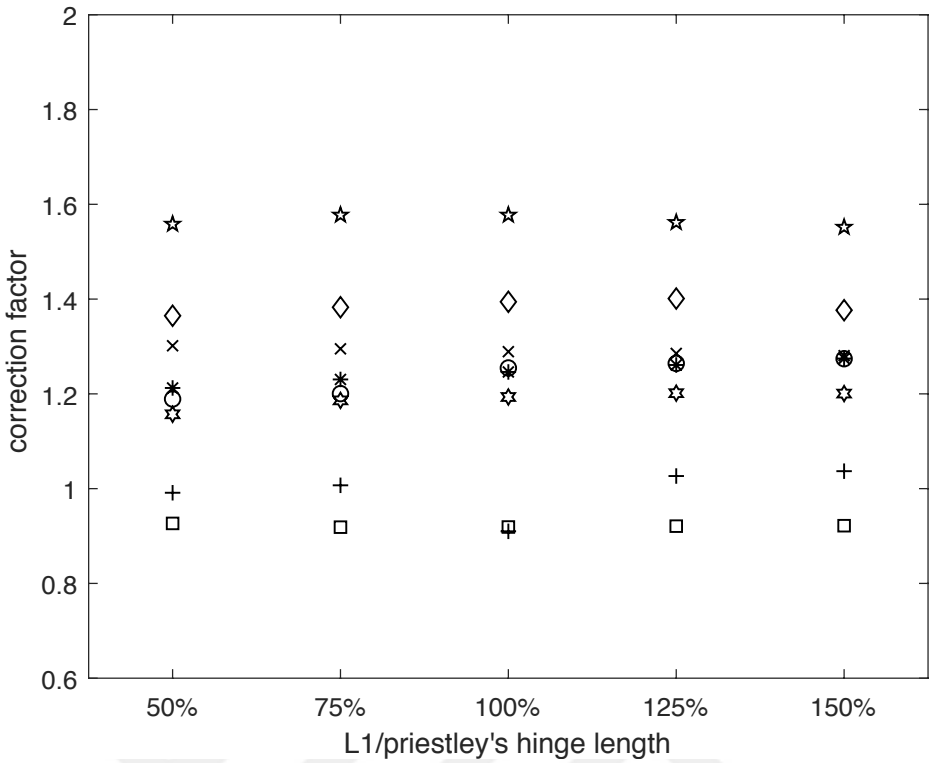

Figure 4.56 : Sensitivity of accuracy and precision for Takeda models to the adopted hinge length.

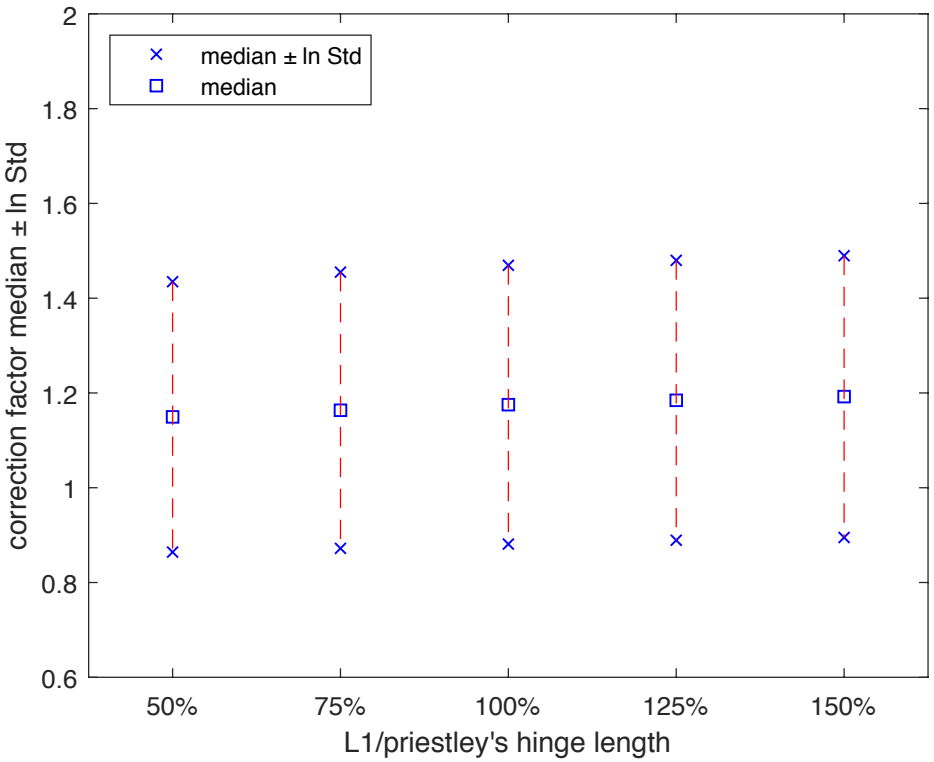

Figure 4.57 : Sensitivity of accuracy and precision for Fiber models to the adopted hinge length.

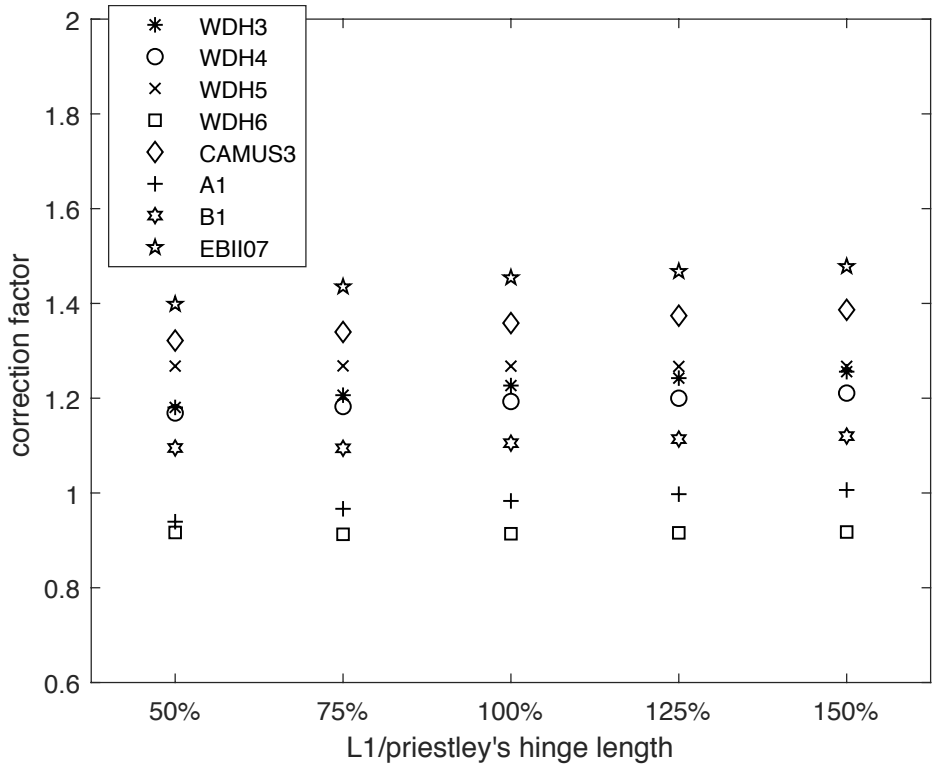

Figure 4.58 : Sensitivity of accuracy and precision for Fiber models to the adopted hinge length.

5. CONCLUSIONS AND RECOMMENDATIONS

5.1 Summary

The main objective of this thesis is to investigate the sensitivity of the estimated hysteretic energy dissipation to major finite element modeling assumptions. For this purpose, shaking table tests for a set of 9 RC components were numerically recreated. Simulated responses were compared against the actual observed behavior. Through the investigation, the imperfections of the numerical models in predicting the hysteretic energy dissipation were highlighted.

The most common hysteretic models (bilinear, Takeda, and fiber section) beside a set of element formulations (displacement based, forced based, and beam with hinges) were considered in this investigation. First, the pushover analysis results simulated using the alternative finite-element modeling approaches are compared against and the actual hysteresis moment versus drift behavior to assess the general characteristics of the simulated quasi-static response. Later, the nonlinear time history analysis were performed and the dissipated energies were computed using the resulting cyclic hysteresis response simulations. Also in this study, the sensitivity of the simulated energy dissipation to some fundamental modeling parameters (i.e. plastic hinge length, the critical viscous damping ratio) were investigated.

5.2 Conclusion

The investigation of hysteretic energy dissipation simulations obtained using conventional finite element modeling approaches for a set of RC members resulted in the following conclusions:

5.2.1 Time history analysis

- It was observed that numerically simulated hystersis energy dissipation behaviors -on average- had an acceptable level of accuracy.

- Even thought the level of error varies among test units and across modeling approaches, the range of this variation is not too wide. Greatest underestimation of energy dissipation was identified to be equal to -38%. It was obtained for the case of WDH5 unit and modeling approach consisting of bilinear section hystersis with displacement based elements. On the other hand, the greatest overestimation (i.e. +13%) was identified in the case of WDH6 unit when the response is simulated using force-based element model with fiber sections. On average, numerical simulation results were observed to underestimate the actual hysteresis energy dissipation by -10%.

- The influence of the assumed flexural hysteresis model (i.e. bilinear, Takeda and fiber section) on the simulated energy dissipation behavior was found to be stronger than the influence of the utilized element formulation (i.e. displacement-based, force-based, and beam with hinges). However, the differences in the observed accuracy was not sufficient to draw and conclusions about the most accurate approach among the alternatives.

- Overall accuracies of the energy dissipation simulations being similar suggests that hysteresis energy dissipation is a robust parameter that is not sensitive to fundamental modeling assumptions.

- Results indicated that excitation intensity being low can drastically increase the relative errors exhibited in the simulation. Yield limit state can be considered as the transition between low-intensity seismic action and the design-level seismic action. Observations reported above are mainly related to the case when units are subjected to design-level seismic action. A brief investigation of the accuracy in the case of low level action revealed that much greater errors were exhibited in that case.

- This investigation is only valuable for tests with a design loading intensity.

- Unlike the expectation, the stiffness degrading Takeda model and the fiber section model exhibits similar levels of accuracy. Additional complexity of the fiber section

model does not lead to a major improvement in the accuracy of the simulated response in terms of energy dissipation level.

- Bilinear model becomes extremely inaccurate in predicting the hysteretic energy dissipation when the excitation force is less than or equal to the yielding moment. Energy dissipation behavior exhibited in the actual responses of the test units during small cycle deformations is not captured by the bilinear model.

- Both forced-based element and displacement-based element and the beam with hinges elements, lead to very close results in terms of energy dissipation response.

- No relation can be found between the simulated maximum displacement prediction and the simulated energy dissipation prediction.

5.2.2 Pushover analysis

- Models consisting of beam with hinges elements with fiber section modeling have lower initial stiffnesses than that of the forced-based and the displacement-based elements.

- The differences observed between the initial stiffness of BF model and those of DF, FF models are found to be related to the stiffness assigned for the elastic element segment. When a cracked stiffness is assigned lower initial sitffness values are simulated.

- Generally, the fiber model shows an acceptably accurate prediction of the hysteretic performance of the shaking table test units.

5.2.3 Sensitivity analysis

- Hysteretic energy dissipation level is found to be inversely proportional to the critical damping ratio assumed in the system. A greater portion of the input energy is dissipated by viscous damping when the damping ratio is increased. This leaves less energy to be dissipated by hystersis behavior.

- Decreasing the damping ratio until 50% , gives the -on the average- best prediction of hysteretic energy dissipation. However, this is not valid for the case of individual test units in the considered set.

- There is no clear relationship between the hysteretic energy dissipation and the equivalent plastic hinges length assumed in the analysis.
- For most of the models, plastic hinge length estimated using the available recommendations was found to be the most accurate in predicting the hysteretic energy dissipation.

REFERENCES

[1] **Yazgan, U. and Dazio, A.** (2011). Simulating maximum and residual displacements of RC structures: I. Accuracy, *Earthquake Spectra*, *27*(4), 1187–1202.

[2] **Bertero, V.V. and Uang, C.M.** (1992). Issues and future directions in the use of an energy approach for seismic resistant design of structures, *Nonlinear seismic analysis and design of reinforced concrete buildings*, 3–22.

[3] **Park, Y.J. and Ang, A.H.S.** (1985). Mechanistic seismic damage model for reinforced concrete, *Journal of structural engineering*, *111*(4), 722–739.

[4] **Zahrah, T.F. and Hall, W.J.** (1984). Earthquake energy absorption in SDOF structures, *Journal of structural Engineering*, *110*(8), 1757–1772.

[5] **Fajfar, P.**, **Vidic, T. and Fischinger, M.** (1992). On energy demand and supply in SDOF systems, *Nonlinear seismic analysis and design of reinforced concrete buildings*, 41–62.

[6] **Akiyama, H.** (1985). *Earthquake-resistant limit-state design for buildings*, University of Tokyo Press.

[7] **Negro, P. and Colombo, A.** (1998). How reliable are global computer models? Correlation with large-scale tests, *Earthquake spectra*, *14*(3), 441–467.

[8] **Code, P.** (2005). Eurocode 8: Design of structures for earthquake resistance-part 1: general rules, seismic actions and rules for buildings, *Brussels: European Committee for Standardization*.

[9] **Kunnath, S.K.**, **Reinhorn, A.M. and Lobo, R.** (1992). *IDARC Version 3.0: A program for the inelastic damage analysis of reinforced concrete structures*, National Center for Earthquake Engineering Research Buffalo, NY.

[10] **LEE, H.S. and KANG, K.Y.** (2000). Correlation of Experimental and Analytical Responses of a 1: 12 Scale 10-Story Reinforced Concrete Frame Having Nonseismic Details.

[11] **Prakash, V.**, **Powell, G.**, **Campbell, S. and Filippou, F.** (1992). DRAIN-2DX user guide, *Department of Civil Engineering, University of California at Berkeley*.

[12] **Mazars, J.**, **Ragueneau, F.**, **Casaux, G.**, **Colombo, A. and Kotronis, P.** (2004). Numerical modelling for earthquake engineering: the case of lightly RC structural walls, *International journal for numerical and analytical methods in geomechanics*, *28*(7-8), 857–874.

[13] **Combescure, D. and Chaudat, T.** (2000). ICONS European program seismic tests on R/C walls with uplift; CAMUS IV specimen, *ICONS project, CEA/DRN/DMT report*, 00–27.

[14] **Tuna, Z.**, **Gavridou, S.**, **Wallace, J.**, **Nagae, T. and Matsumori, T.** (2012). 2010 E-defense four-story reinforced concrete and post-tensioned buildings–preliminary comparative study of experimental and analytical results, *Proceedings*.

[15] **Saiidi, M. and Sozen, M.A.** (1979). Simple and complex models for nonlinear seismic response of reinforced concrete structures, **Technical Report**, University of Illinois Engineering Experiment Station. College of ....

[16] **Neuenhofer, A. and Filippou, F.C.** (1997). Evaluation of nonlinear frame finite-element models, *Journal of structural engineering*, *123*(7), 958–966.

[17] **Mazzoni, S.**, **McKenna, F.**, **Scott, M.H. and Fenves, G.L.** (2006). The open system for earthquake engineering simulation (OpenSEES) user command-language manual.

[18] **Takeda, T.**, **Sozen, M.A. and Nielsen, N.N.** (1970). Reinforced concrete response to simulated earthquakes, *Journal of the Structural Division*, *96*(12), 2557–2573.

[19] **Otani, S.** (1974). Inelastic analysis of R/C frame structures, *Journal of the Structural Division*, *100*(Proc. Paper 10686).

[20] **Riddell, R. and Newmark, N.M.** (1979). Statistical analysis of the response of nonlinear systems subjected to earthquakes, **Technical Report**, University of Illinois Engineering Experiment Station. College of ....

[21] **Spacone, E.**, **Filippou, F.C. and Taucer, F.F.** (1996). Fibre beam–column model for non-linear analysis of R/C frames: Part I. Formulation, *Earthquake Engineering & Structural Dynamics*, *25*(7), 711–725.

[22] **Ghaemian, S.** (2017). Sensitivity Of The Predicted Collapse Capacity Of Rc Buildings To The Utilized Finite Element Modeling Approach, *Ph.D. Dissertation*, Deprem Mühendisliği ve Afet Yönetimi Enstitüsü.

[23] **Mander, J.B.**, **Priestley, M.J. and Park, R.** (1988). Theoretical stress-strain model for confined concrete, *Journal of structural engineering*, *114*(8), 1804–1826.

[24] **Popovics, S.** (1973). A numerical approach to the complete stress-strain curve of concrete, *Cement and concrete research*, *3*(5), 583–599.

[25] **Kent, D.C. and Park, R.** (1971). Flexural members with confined concrete, *Journal of the Structural Division*.

[26] **Menegotto, M.** (1973). Method of analysis for cyclically loaded RC plane frames including changes in geometry and non-elastic behavior of elements under combined normal force and bending, *Proc. of IABSE symposium*

on resistance and ultimate deformability of structures acted on by well defined repeated loads, pp.15–22.

[27] **Calvi, G.**, **Priestley, M. and Kowalsky, M.** (2007). Displacement–based seismic design of structures, *Earthquake spectra*, *24*(2), 1–24.

[28] **Scott, M.H. and Fenves, G.L.** (2006). Plastic hinge integration methods for force-based beam–column elements, *Journal of Structural Engineering*, *132*(2), 244–252.

[29] **Yazgan, U.** (2009). The use of post-earthquake residual displacements as a performance indicator in seismic assessment, *Ph.D. Dissertation*, ETH Zurich.

[30] **Kaba, S.A. and Mahin, S.A.** (1984). *Refined modelling of reinforced concrete columns for seismic analysis*, University of California, Earthquake Engineering Research Center.

[31] **Newmark, N.M.** (1959). A method of computation for structural dynamics, *Journal of the engineering mechanics division*, *85*(3), 67–94.

[32] **Hachem, M.M.**, **Moehle, J.P. and Mahin, S.A.** (2003). *Performance of circular reinforced concrete bridge columns under bidirectional earthquake loading*, Pacific Earthquake Engineering Research Center Berkeley, CA.

[33] **Stone, W.C. and Taylor, A.W.** (1993). Seismic performance of circular bridge columns designed in accordance with AASHTO/CALTRANS standards.

[34] **Lestuzzi, P.**, **Wenk, T. and Bachmann, H.** (1999). *Dynamische Versuche an Stahlbetontragwänden auf dem ETH-Erdbebensimulator*, volume240, ETH Zurich.

[35] **Lestuzzi, P. and Bachmann, H.** (2007). Displacement ductility and energy assessment from shaking table tests on RC structural walls, *Engineering Structures*, *29*(8), 1708–1721.

[36] **Priestley, M.N.**, **Seible, F. and Calvi, G.M.** (1996). *Seismic design and retrofit of bridges*, John Wiley & Sons.

APPENDICES

APPENDIX A.1 : Bilinear idealizations for the test units.

APPENDIX A.1

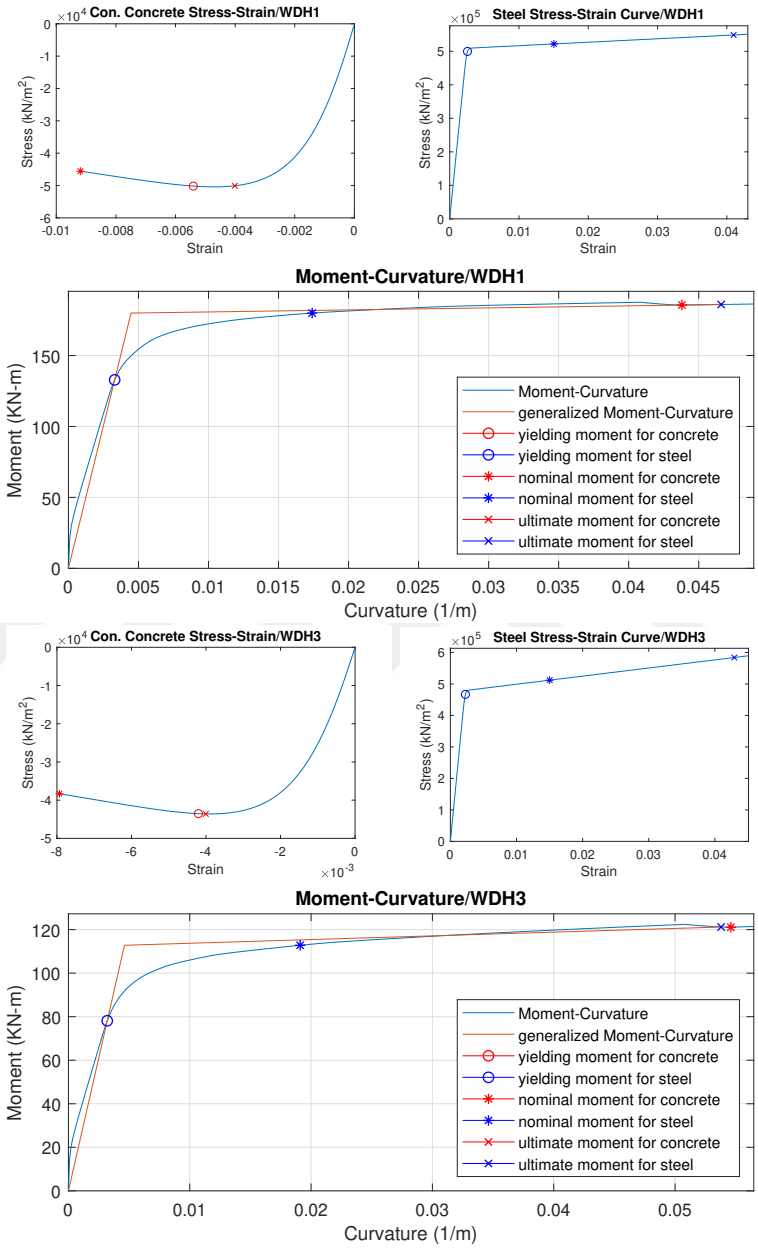

Figure A.1 : Bilinear idealizations established for WDH1 and WDH3 test units.

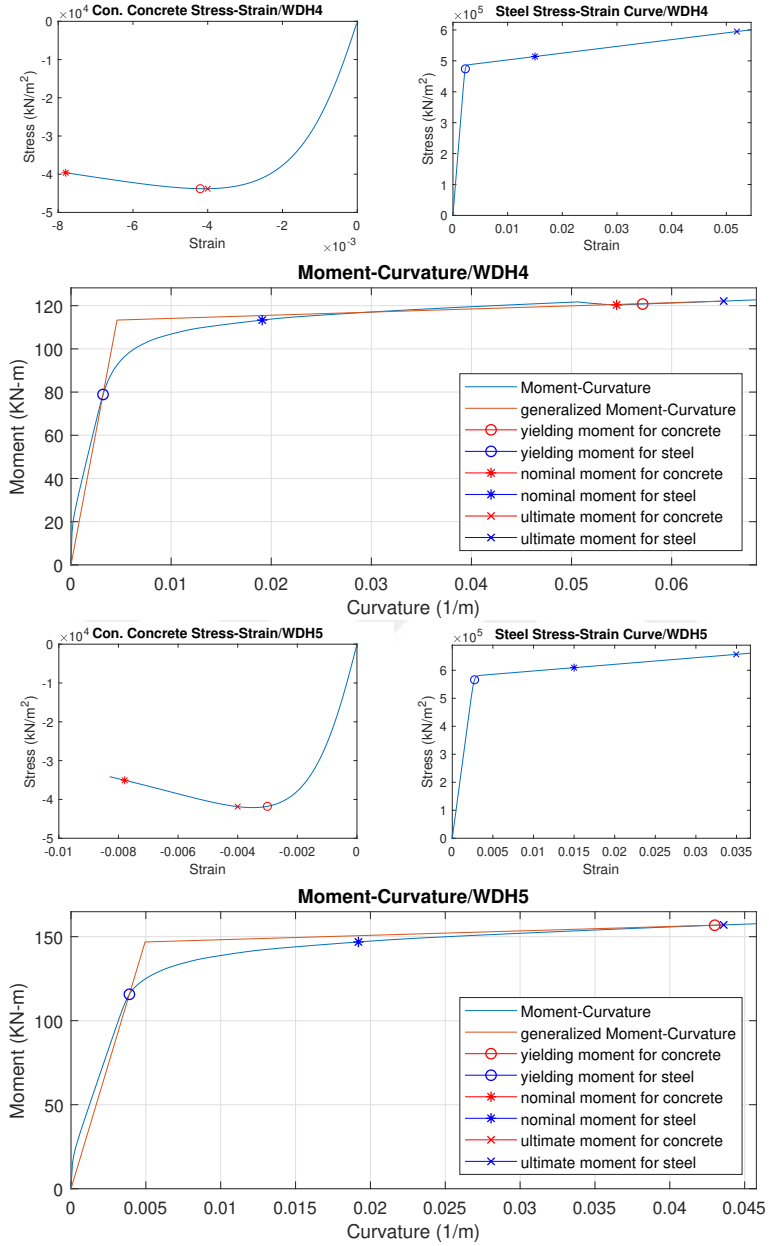

Figure A.1 : Bilinear idealizations established for WDH4 and WDH5 test units.

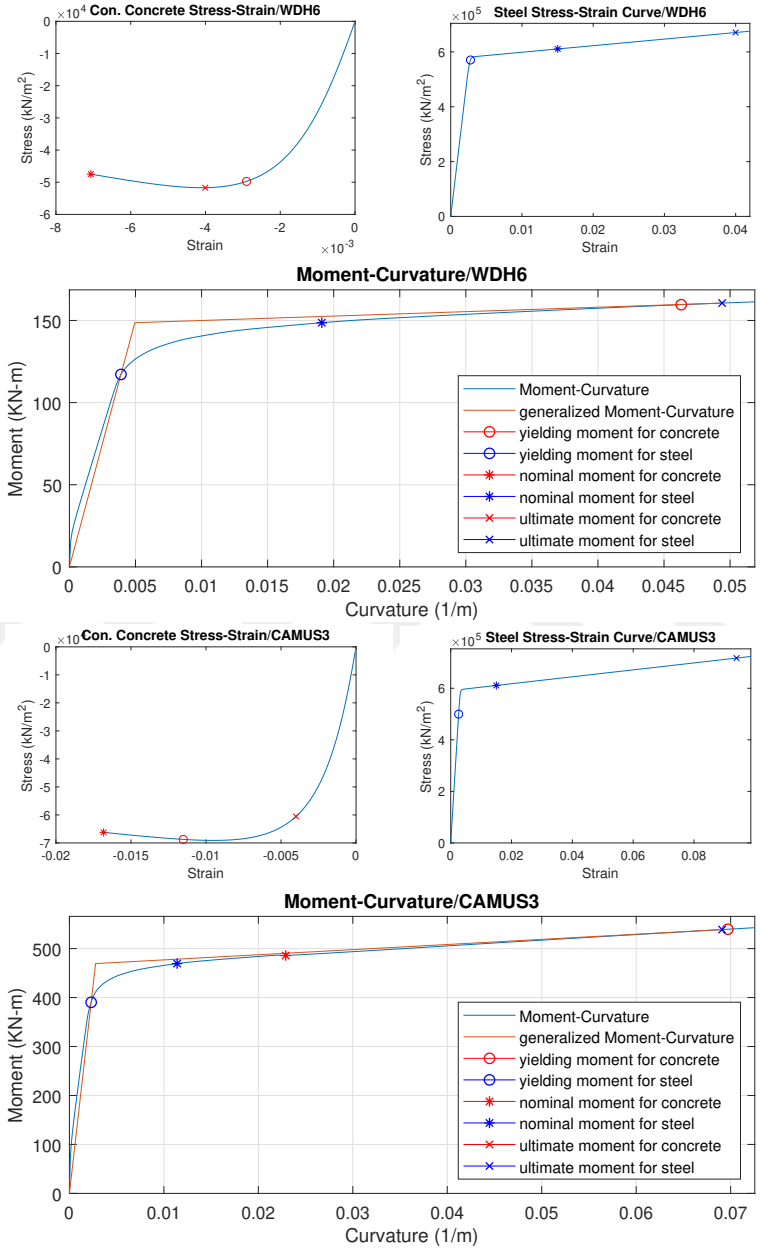

Figure A.1 : Bilinear idealizations established for WDH6 and CAMUS3 test units.

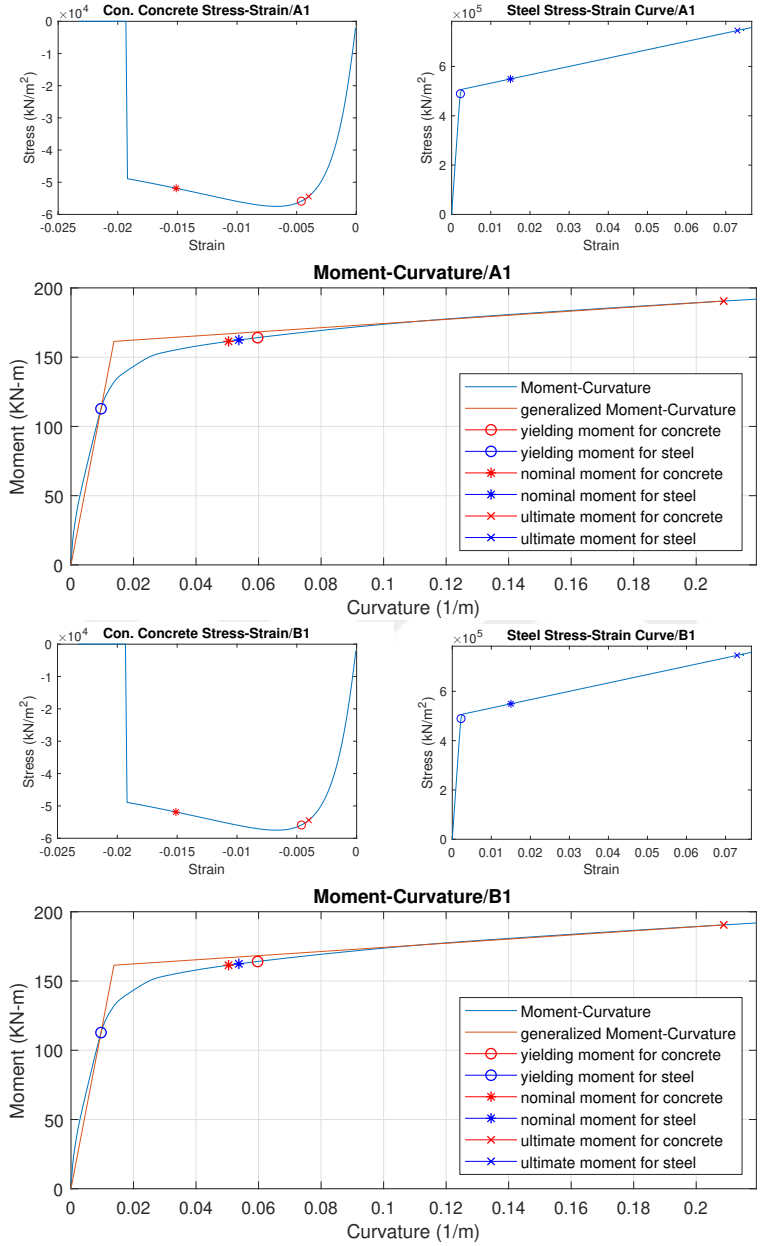

Figure A.1 : Bilinear idealizations established for A1 and B1 test units.

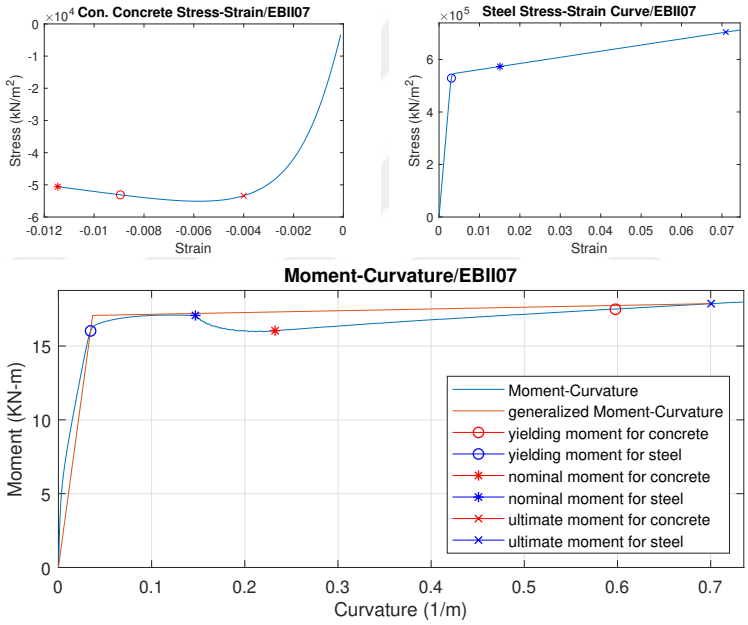

Figure A.1 : Bilinear idealizations established for A1 and B1 test units.

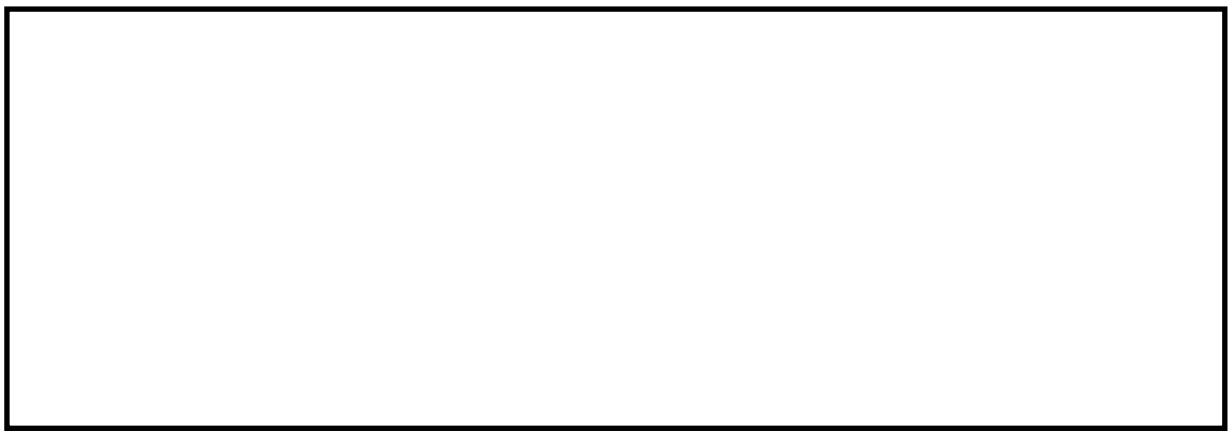

Name Surname **:Ahmed AbuAisheh**

EDUCATION **:**

- **B.Sc.** **:** Graduation year, Bahçeşehir University, Faculty of Engineering, Department of Civil Engineering
- **M.Sc.** **:** Graduation year, Istanbul Technical University, Faculty of Earthquake Engineering and Disaster Management, Earthquake Engineering

A. B. ABUAISHEH	ACCURACY OF SIMULATED HYSTERESIS ENERGY DISSIPATION BEHAVIOR OF DUCTILE RC COMPONENTS	2021